AD NUMBER

AD008892

LIMITATION CHANGES

TO:

Approved for public release; distribution is unlimited.

FROM:

Distribution authorized to DoD only; Administrative/Operational Use; 01 FEB 1953. Other requests shall be referred to Office of Naval Research, Arlington, VA 22203. Pre-dates formal DoD distribution statements. Treat as DoD only.

AUTHORITY

ONR ltr dtd 26 Oct 1977

AD _____

KINETICS OF FAST REACTIONS (II)
Rates of the NO_2-N_2O_4 Reaction
Project NR 051-242
A Thesis by M. R. Gustafson

KINETICS OF FAST REACTIONS
RATES OF THE NO_2-N_2O_4 REACTION
FROM HEAT CAPACITY LAG DATA

A TECHNICAL REPORT (Part II)

Project NR 051-242: Contract number N6 onr-264 (17)

Period covered: September 1, 1949 to November 1, 1952

being essentially

A THESIS SUBMITTED TO THE GRADUATE SCHOOL

OF CORNELL UNIVERSITY

by

M. R. GUSTAVSON, Research Assistant

in partial fulfillment of the requirements

of the Ph.D. degree

This work was done under the supervision of

S. H. Bauer, Professor of Chemistry

in

The Department of Chemistry

at

Cornell University

Ithaca, New York

February 1, 1953

TABLE OF CONTENTS

I. Introduction

All chemical reactions take place at definite rates, and the determination and interpretation of these rates has long been one of the central problems of chemical research. Fundamental to the complete treatment of this problem is an understanding of the mechanism of energy transfer between molecules on collision, for only by learning the details of this process will it be possible to obtain an understanding of how molecules go from their normal states to activated states, and then to form products.

This thesis is concerned with the study of very rapid reactions wherein the slowest step, and hence the factor which limits the rate of approach to equilibrium, may well be the rate of energy transfer between molecules on collision. For this purpose the isentropic flow experiment of Kantrowitz[1] has been extended for the case of carbon dioxide, and applied to the study of the pressure dependent chemical reaction ($N_2O_4 \rightleftharpoons 2NO_2$).

A. A Review of the General Theory of Energy Transfer During Molecular Collision

Early studies of the rate of energy equilibration between the internal and external degrees of freedom of molecules were the outgrowth of attempts to explain the absorption of sound by gases. In 1870 Boltzmann[2] suggested that it was within the realm of possibility that the transfer of energy between molecular motion (translation) and the motion of the atoms within a molecule with respect to one another (vibration) might take a rather long time. This notion was expressed in a much more definite form by H. A. Lorentz[3] in a paper published initially in 1881, and entitled, "Les Équations du mouvement des gaz, et la propagation du son suivant la theorie cinétique des gas". This paper contains the first detailed application of the then new kinetic theory of gases to the problem of sound propagation through a gas. Application of the law of conservation of energy to the system gave rise to a new term which Lorentz interpreted as being due to a temporary displacement on rapid compression and rarefaction of the equilibrium between the translational energy of the molecules and their intramolecular energy. The existence of such a delay in establishing equilibrium between the external and internal degrees of freedom of a molecule is equivalent to a reduction of the effective heat capacities of the gas. Since this increases the effective γ, the net

result is an increase both in the velocity and absorption of sound in the gas.

The question in its general form was raised by Hertz[4] in 1882, and in 1903 Jeans[5] pointed out that the general solution of this problem is not obvious even for a highly simplified model utilizing classical mechanics. Jeans investigated the effect of having a portion of the internal energy lagging behind the translational energy, and showed that both the velocity and absorption would be increased; and further, that the new absorption would be proportional to the square of the frequency. Then, using as a model a sphere with its center of mass displaced from its geometrical center, he attempted to calculate the magnitude of the effects for the case in which the rotational energy lagged. Jeans concluded that the effect would be small, especially for the velocity, but that the observed high absorption in air could be accounted for in this fashion. This work was undertaken by Jeans in an attempt to reconcile the values of γ found by sound velocity measurements (the Kundt-tube method) with those calculated from the principle of equipartition of energy. However, the quantum theory had already removed the major discrepancy between the measured heat capacities and those computed from equipartition, and therefore this calculation was dropped from Jeans' "Dynamical Theory of Gases" (Cambridge) in editions subsequent to the first, in 1904.

No new theoretical work was done for some time, but in 1914 J. G. Stewart[6] published a paper entitled "The Inapplicability of Boltzmann's Equipartition Hypothesis to Gases in a State of Change of Internal Energy; and its bearing on the experimental determination of the Specific Heat of Gases". He pointed out that in experiments on the expansion of gases through nozzles measurement of pressure or temperature after a specified expansion gave values lower than those calculated from the adiabatic theorem using the equilibrium values of γ, and that the measurements of amounts of material discharged give values greater than is possible with reversible expansion. Also, he noted that values of γ taken by the explosion method, wherein the change of translational energy is even more rapid, are greater than those obtained by static methods. To explain these discrepancies he invoked the hypothesis of slow energy exchange between external and internal modes.

The next great impetus to the discussion of this problem was the invention of the acoustic interferometer by G. W. Pierce[7] in 1925. For the first time, it became possible to measure the velocity of sound in gases with an accuracy of 0.1%. For carbon dioxide Pierce found a velocity increase of several per cent with increasing frequency; a value far in excess of the immeasurably small increase predicted by the classical theories of Stokes and

Kirchoff. He, himself, attributed the large value to the effect of thermal conductivity, and it remained for Herzfeld and Rice[8] to give the correct explanation based on the slow rate of exchange of energy between the vibrational and translational degrees of freedom.

From then on a wealth of sonic data became available, and coupled with this advance has gone an ever growing understanding of the process of energy transfer between molecules on collision. We shall not attempt here to make a complete survey of this field. Rather we refer those interested in the utilization of sonic phenomena to the admirable and thorough thesis of E. H. Freedman[9], and those interested in the theoretical aspects of relaxation phenomena to the complete discussion presented in the thesis of B. Widom.[10] We shall site, however, some of the major papers which are landmarks along the way to our present understanding of the process of energy transfer, and outline briefly the conclusions drawn therein.

The first lengthy analysis of inelastic molecular collision processes in the language of quantum mechanics was published by C. Zener[11] in 1935. As a first approximation his model pictured each molecular system of atoms as bound together by elastic forces, while atoms of different molecules interacted as hard elastic spheres. Considering the one dimensional case, he then calculated the energy interchange for a single head on impact from the

principles of energy and momentum conservation. It is clear that the finite time required to establish contact between the two systems acts as a severe restraint upon the exchange of internal energy. The interaction between colliding molecules is actually so gentle that in general many vibrations occur during the effective time of a collision, and theory shows that the energy transfer dies off exponentially with the number of these vibrations which can take place during such an interval. Zener then improved the rigid sphere model by assuming that the atoms of separate systems repel one another according to the simple law $V = ce^{-r/d}$. Classical mechanics applied to this model shows that for d not too small there is but a small tendency for the energy of a rapid oscillator to be transferred to a less rapid oscillator or to translational degrees of freedom. This treatment points up the fact that a specified amount of internal energy will be dissipated much more rapidly if it can be given up to translational energy as several small quanta rather than as one large quantum. Hence for polyatomic molecules we would expect, all other things being equal, that those vibrations with lower frequencies will tend to have shorter relaxation times. An interesting sidelight is Zener's conclusion that the comparatively large quanta which H_2 can absorb as energy of rotation, which are still small compared to vibrational quanta, makes it unique in deactivating efficiency.

In principle the calculation of the extent of energy transfer on collision requires the use of a complete quantum mechanical picture. However, Zener[12] and, independently, Landau and Teller[13] have proposed an approximate semi-classical theory of these inelastic molecular collision processes which glosses over a number of the difficulties encountered in the quantum mechanical problem. In this semi-classical approach the vector which gives the separation of the centers of mass of the two particles is taken to be an explicit function of the time as given by classical dynamics. The interaction potential is then a known function of the time, and its effect on the internal states of the system can be found by application of the first order time-dependent perturbation theory. Using this approach Landau and Teller[13] have published a general theory for the relaxation time of a real non-dissociating polyatomic gas wherein several modes of vibration may contribute to the energy absorbing process. They established that large velocities play a dominating role and predicted that the logarithm of the relaxation time of a gas expressed in molecular collisions should be proportional to $T^{-1/3}$.* Recently a thorough discussion of the relationship between the completely quantum mechanical and semi-classical

---

* See section I. B.; cf. ref. 1(a)iii, figure 6.

theories has been presented by Widom.[10]

A rather complete summary of work on the problem of molecular energy transfer up until 1949 is provided by H. S. W. Massey's[14] survey article entitled "Collisions Between Atoms and Molecules at Ordinary Temperatures". He sums up the present status of the problem as follows:

"A considerable volume of evidence is available concerning the ease with which energy exchange may occur between that of relative translation and various degrees of internal freedom of the colliding systems. Nevertheless, although it is possible to give general rules concerning these energy transformations, we are still far from possessing an interpretation so complete as to make possible the prediction of the rates of a particular reaction except in a very few cases."

In a recent paper Curtis and Adler[15] have applied group theoretical arguments to the treatment of three-dimensional collisions following Zener's work for the one dimensional case.[11] The scattering coefficients were obtained by an analysis of the solutions of the internal wave equations involving the three coordinates specifying the internal configuration. The angular transition probabilities were obtained for the case in which transitions are relatively infrequent (weak coupling) in terms of integrals of the interaction potential and a set of phase shifts. This treatment is applicable to normal low energy thermal collisions, but not to the high energy collisions which

occur in hot atom chemistry. Since they consider the question of energy transfer, molecular dissociation or rearrangements are not directly part of this problem and hence were not considered. The essential difference is that in the energy transfer process only weak coupling is postulated between colliding units.

In a brief recent paper Herzfeld[16] has succeeded in calculating directly the rate of energy exchange between internal and external degrees of freedom for liquid benzene. The Lennard-Jones interaction potential and model of the liquid are used; the fourth-order terms in the interaction provide the coupling between internal vibrations and Debye waves. This results in a value three times too rapid, which is in astonishingly good agreement with the experiment, in view of the approximations made.

Yet more recently Schwartz, Slawsky, and Herzfeld[17] have attempted a quantitative calculation of the relaxation time in pure gases and in chemically nonreactive gas mixtures. They followed the wholly quantum mechanical method of Zener[11], using an exponential repulsion in a one-dimensional model, and concluded that in some cases the great effect which impurities have may be accounted for either by their low masses and resultant high velocity, or by "near resonance" transfers in which the vibrational quantum of the substratum is used partly to excite the vibration of the impurity, only the difference being transferred to trans-

lation. However, there are a number of interesting cases for which neither of these explanations apply. The theoretical values here obtained for the relaxation times are 10 to 30 times shorter than the experimental values, but the authors express the opinion that this difference may have arisen because of the use of a one-dimensional model.

Widom[10] has extended Zener's original proposal for symmetrizing the theory in the case of head-on collisions to cover the more general case of non-zero impact parameter and has provided proof for the assertions of Rosen and Zener[18] and of Landau and Teller,[13] to the effect that the semi-classical theory is an adequate approximation to the quantum mechanical theory whenever the relative translational energies which are involved are much greater than the amount of energy exchanged. He discussed the statistics of semi-classical collisions in order to derive expressions for temperature-dependent probabilities of inelastic encounters and presented a detailed discussion of classical motion in a spherically symmetric inter-molecular potential. The system CO_2-H_2O was treated semi-classically, assuming that the interaction potential was spherically symmetric, and corresponded to that interaction between the CO_2 and H_2O molecules which would occur were they to approach in a certain most favorable orientation. The resulting probabilities were then corrected by multiplying by a suitable orientation factor. The relevant potentials were based on considerations of the chemistry of the acid-base inter-

action between CO_2 and H_2O. A potential of the type (a) was used rather than type (b), which is that for the inter-

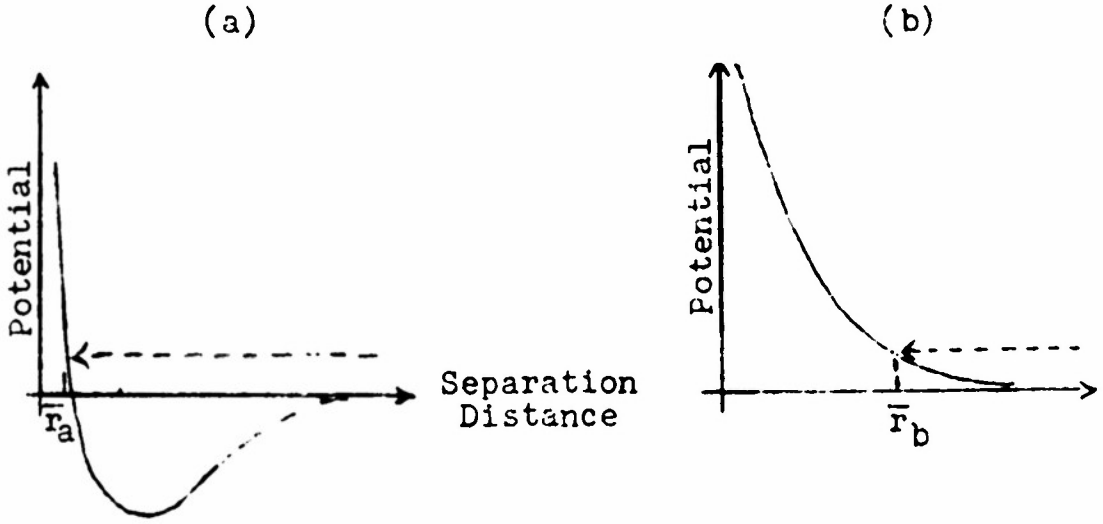

action of molecules between which there can be no chemical interaction. For a molecule with a given collisional energy (dotted arrow) it is clear that for (a) the minimum distance of approach is of the order of a bonding distance ($\bar{r}_a$), and that this interaction occurs more sharply (greater slope) than for (b). Thus in (a) the effective time of collision is less, and hence there is an increased probability of energy transfer. On the basis of the semi-classical treatment, and the statistics of generalized impact parameters, Widom found that the effective collision diameter is a monotonically decreasing function of the temperature. He then showed that when corrected for the low energy failure of the semi-classical theory, the collision diameter also decreases at low temperatures, and therefore, in agreement with experiment, it passes through

a maximum. This theory quantitatively accounts for the observation of Eucken and Becker[19] that the probability of transfer of energy on collision is larger the greater the chemical reactivity of the two colliding molecules, even though no chemical change actually takes place.

The transition state approach of Laidler and Eyring[20] has been of some use in correlating qualitatively certain general observations. The above mentioned observation of Eucken and Becker[19] was qualitatively explained as follows. Consider a potential energy surface which represents a collision between X and Y which could react chemically. However, in an energy transfer process we are concerned not with major transitions between valleys in the potential energy surface, which occur when a chemical change takes place, but rather with transitions between the vibrational levels within one valley. For proper presentation of the potential, the surface should be constructed with skewed axes[21,22], and the degree of dissymmetry of the valley will depend on the tendency for chemical reaction. When a chemical reaction is possible the valley is definitely not symmetrical but distorted, particularly at positions corresponding to close approach of the particles, and when the system enters this distorted region the probability of transfer to another vibrational level becomes appreciable, and may be high. Thus the transference of energy will be associated in an approximate manner with chemical reactivity.

It is clear, however, that the number of possible initial and final states may be very large and that even between two given states the number of likely reaction paths may be very great. It is this complexity which makes any detailed microscopic treatment quite difficult, and predictions nearly impossible.

As an extension of the potential energy surface approach, Castellan and Hulbert[23] have calculated reflection coefficients for a matter wave in a parabolic channel and in a square channel, each channel closed at one end by a vertical plane tilted slightly from the normal to the axis of the channel. This enabled them to find theoretically the number of collisions necessary to dissipate one quantum of vibrational energy and comparison with the data from measurements on sound dispersion shows good agreement for N_2O and CO_2. They also arrived at some tentative conclusions regarding the temperature dependence of the average probability of transition per collision.

The correlation of the probability of collisional energy transfer with chemical reactivity is not strong in the dispersion of sound experiments, since, owing to the low temperatures, the vibrational levels are far down the potential-energy valleys, in which region the distortion due to reactivity is very small. Hence the number of collisions required to effect a change of level is very large. In the spectroscopic work on energy level transitions,[24]

on the other hand, the vibrational levels involved are higher, their spacing is much smaller, and the number of collisions required is therefore less; the correlation with chemical reactivity is much more pronounced.

With respect to unimolecular reaction, it seems clear from the experimental observation that no amount of added gas can increase the specific rate to a value greater than its limiting value at high pressures, that the added molecules do not interfere with the over-all chemical reaction, and that their function is to maintain the equilibrium concentration of activated molecules. If the property possessed by foreign gases of maintaining the equilibrium concentration of activated complexes, and thus preventing the falling off in rate of a unimolecular reaction at low pressures, is to be attributed to their ability to transfer some of their energy to vibrational energy of the reacting molecule, then some parallelism is to be expected between their efficiency in this respect and the removal of excess vibrational energy in association reactions. This parallelism is borne out by the experimental evidence.

Rosen[25] discussed the case of collision between a molecule and an atom or another molecule where some vibrations are excited in the former and a binding to the latter is produced. A stable system may form after collision only if the potential energy of the particles as a function of the distance between them has a minimum and if

the sum of this potential energy and the energy of relative motion is less than the top of either side of the potential valley. Clearly the free particles have energy above the outer wall of the potential valley, and Rosen shows, by means of an approximate solution of the wave equation, that in some cases a portion of this energy of relative motion may flow to other parts of the system.

For the purpose of determining the order of magnitude of the lifetime of a molecule having an excess of energy Rosen supposed that there are three atoms in a line, the two outside atoms each being connected to the inside atom by a potential of the Morse type. He then considered the case where one vibrator in a relatively low state, with vibrational quantum number m, is supposed to drop back to the lowest state (vibrational quantum number zero), the energy being taken up in the transition into the continuum representing dissociation of the other vibrator. Rosen concluded that if $m > 4$ there is very little chance of the molecule decomposing before it exchanges energy at collision.

Rice[26] pointed out, however, that it is not necessary that the exchange of energy should take place in one step, but that it can take place through a series of exchanges of smaller amounts of energy between the vibrators without dissociation taking place, until one of them is in a state where its probability of dissociation is great. The probability of dissociation ultimately taking place will then not fall

off as rapidly with increasing m as Rosen has predicted.

Amongst the most recent papers are two by E. Bauer[27] in which he discussed the recombination of two atoms in the presence of a third body by considering the probability coefficient of the reverse process, the dissociation of a molecule by collision. Various mechanisms for dissociation were briefly discussed, and an attempt was made to estimate the general order of magnitude of the cross section for the excitation of a molecule into the vibrational continuum of its electronic ground state. This cross section, which was calculated by a method depending upon correcting the Born approximation by means of the exact one dimensional problem, was computed for the recombination of two hydrogen atoms in the presence of a third during a collision. The three-body coefficient, obtained from the cross section of the reverse dissociation process by the principle of detailed balance, is much smaller than the empirical values. An estimate of the number of thermal collisions required to de-excite the first vibrational state of hydrogen by collisions with protons is more nearly in line with empirical values.

Messiah[28] has extended a mass tensor approximation to the computation of the scattering of slow neutrons by molecules taking into account the molecular vibrations. The calculations were made for the case of H_2 and CH_4 at room temperature for neutron energies below the threshold

of excitation of higher vibrational states. The agreement with experiment is very satisfactory in the expected range of validity. The asymptotic form of the total cross section for large values of the incident energy was derived, and numerical calculations show that the asymptotic behavior is quickly reached.

B. Measurements on Carbon Dioxide

a. Sonic Method

As was noted in the preceding section, Pierce was the first investigator to make precision measurements of the velocity of sound in various gases, and the increase of velocity with increasing frequency which he observed was correctly interpreted shortly thereafter by Herzfeld and Rice as resulting from the finite time required for the equilibration of energy between vibrational and translational degrees of freedom.

Since then very many measurements have been made and a diversity of methods for taking sound velocity and absorption data invented. We will make no attempt to summarize these investigations, but rather refer the reader to three papers which together admirably cover the period from the investigations of Pierce up until relatively recent times.

The first of these papers is a review published by Richards[29] in 1939 and entitled "Supersonic Phenomena". This paper opens with a complete derivation from first principles of the equations governing the propagation of plane sound waves, and then proceeds to review experimental methods and observations. The coverage of this paper is quite remarkable as may be suggested by the fact that its bibliography lists, with at least a short comment on each, no less than three-hundred forty-eight entries.

The second paper is by Kittel[30] and is entitled "Ultrasonic Research and the Properties of Matter". This excellent review paper covers propagation in gases, liquids, and solids, experimental methods, applications to other fields, and unusual phenomena associated with liquid helium. The bibliography concentrates on papers since 1942, and thus forms with that of Richards a very nearly complete listing of the pertinent studies of ultrasonic phenomena published prior to 1946.

The third review is by Markham, Beyer, and Lindsay[31] and was published in 1951. This paper is entitled "Absorption of Sound in Fluids", a broad field which it covers quite well. Emphasis was placed on a discussion of basic principles and concepts rather than on detailed calculations. A listing of the more reliable experimental data was included. The excellent bibliography covers important work in the field published prior to 1951.

In 1950 Lambert and Rowlinson[32] published a very interesting study in which they reported measurements of ultrasonic dispersion in a series of organic vapors over a range of frequencies, temperatures, and pressures. They concluded that, for polyatomic molecules in general, there is little hindrance to the interconversion of translational and vibrational energy, especially at high temperatures. Slow interconversion, leading to ultrasonic dispersion, was found only for small or rigid molecules, where internal

rotations or vibrations of low frequency are absent.

Recently Zartman[33] has been able to improve the ultrasonic interferometer so as to attain greater sensitivity and reproducibility. These improvements, coupled with scrupulous care in preparing samples, should go far towards increasing the consistency of measured values. It seems, however, that this technique has very nearly reached the upper limit of its precision.

Out of this wealth of work the following basic conclusions fundamental to this thesis have been reached with respect to dispersion and absorption of sound in pure gases:

i) Dispersion and absorption of sound are to be expected in any polyatomic gas in which there is an appreciable vibrational excitation, due to the inevitable inefficiency of the conversion of translational energy into quanta of vibrational energy by collision.

ii) The effect of pressure variations is in accord with the kinetic theory of heat; an increase of pressure increases the number of collisions and displaces the dispersive region to higher frequencies. Double collisions appear to be the usual mechanism by which vibrational energy is excited[34]; all of the measurements with carbon dioxide have indicated that the relaxation time is proportional to the pressure of the gas indicating a bimolecular relaxation process.

iii) Generally the effect of increasing the temperature is to increase the transition probability (note exception, H_2O with CO_2).

iv) Very small traces of foreign gases may have an enormous effect on the efficiency of the collision process, and consequently on the location of the dispersive region (see later data on carbon dioxide). The effect of the presence of these traces is always to shift the dispersive region to higher frequencies; any other result would necessitate a revision of the collision theory.

v) In nearly all cases sonic measurements show several energy states adjusting with a common frequency over the range measured. That is, experimentally one obtains only one dispersive region. It has long been considered unlikely that the several states have equal relaxation times in these cases[35], but rather it has seemed more probable that they fall out together because of rapid redistribution of energy within the molecule. This point has now, however, been resolved by a new method discussed later.

Over three score studies on the velocity and absorption of sound in carbon dioxide are reported in the literature[36]; those of Eucken[37] and co-workers on carefully purified carbon dioxide cover the widest ranges of temperatures,

frequencies, and pressures and show the greatest over all precision and consistency. They have also made detailed studies of the effects produced by known amounts of foreign gases. We shall use their data[38] for comparison purposes, and refer the reader to the paper by Kantrowitz[39] for a comparison with the data of other workers. Following the formula of Landau and Teller we here plotted in figure 1 the log of the relaxation time (in molecular collisions) versus $T^{-1/3}$.

At 293°K. the "collision number" for pure carbon dioxide is 57,000, while between water and carbon dioxide it is 105.[38] Hence collisions between carbon dioxide and water molecules are over 500 times as effective in de-exciting the carbon dioxide as are collisions between carbon dioxide molecules. For details on the effect of changing the temperature see work by Widom.[40]

b. Shock Tube Method

Recently Smiley, Winkler, and Slawsky[40] have reported the results of shock tube investigations on carbon dioxide. They recorded by means of interferograms the relaxation region behind plane shock waves in a shock tube containing carbon dioxide. In these interferograms the fringe displacement is a direct measure of the density change. The peak temperature in the carbon dioxide shock is about 900°K., at which temperature the lowest vibrational modes of carbon dioxide make a large contribution to the enthalpy. They

Figure 1

Plot of the logarithm of the Relaxation Time (in molecular collisions) vs $T^{-1/3}$ for Carbon Dioxide[37c]

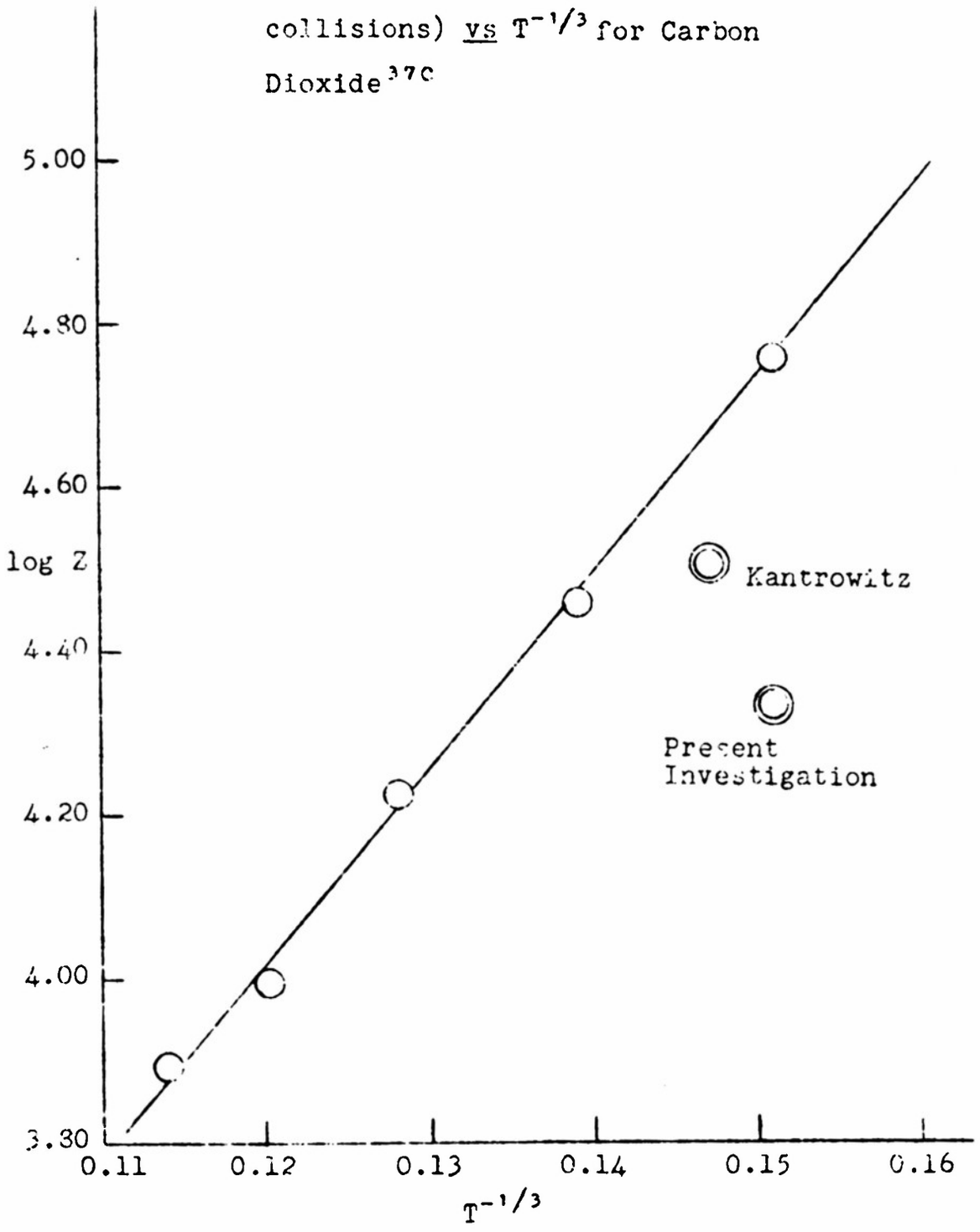

obtained a value of approximately 0.1μsec. at normal pressures, whereas a value of 6μsec. would be expected for bone dry carbon dioxide. They claim, however, that the observed value is in rough agreement with that expected for the known water vapor content of about 3%. The brief note published indicates that this work will be extended; it is hoped that attendant upon this extension greater accuracy in specifying the experimental conditions will be forthcoming. Specifically, more definite information with respect to purity of reagents and precision of the readings would be desirable, as well as studies to determine whether the relaxation rate is really proportional to the displacement for such a large disturbance from equilibrium.

c. Infrared Method

The newest method to be applied to the study of relaxation phenomena in pure and mixed gases involves a process which may be looked upon as the reciprocal of the sound dispersion method. In this new method, modulated radiation of such a spectral composition as to be absorbed by one or several degrees of freedom is passed through the gas. This energy is absorbed through vibrational excitation, and if there were immediate equilibration between all degrees of freedom it would appear instantly as a rise in translational temperature, and hence in pressure. However, if there is a lag in the establishment of equilibrium there will be a lag between irradiation and rise in translational temperature.

The pressure variations in the gas are followed by a microphone, and by studying the phase relation between the microphone output and the impinging modulated beam one can determine the energy transfer lag between those modes which absorb the radiation and those of translation, responsible for the pressure. This method was suggested independently by Gorelik[41] and Slobodskaya[42] in Russia and Cottrell[43] in England.

The most interesting feature of this method is that it enables one to determine the relaxation time of individual vibrational, or even rotational, modes.* Slobodskaya applied this method to the much disputed case of carbon dioxide, and has measured the lifetimes of vibrational quanta corresponding to the three absorption bands 2.7μ, 4.3μ, and 14.8μ.

$\lambda(\mu)$	τ(sec.)	Probability of Inelastic Collisions
4.3	7×10^{-6}	1.6×10^{-5}
2.7	4×10^{-6}	2.8×10^{-5}
14.8	1.6×10^{-6}	6.9×10^{-5}

In the case of sound dispersion measurements, which give only a single relaxation time, we would expect to get a value equal to or slightly larger than that of the lowest vibrational frequency. The value of 1.6×10^{-6} sec. for the 14.8μ band obtained in this work agrees well with that

---

* See comment in section I.B.a.

of Kneser who obtained 1×10^{-6} sec. from sonic measurements under the same conditions.

Another great advantage of this method is the very small sample required and the ease of isolating it from contamination. While Slobodskaya reports a precision of 10% within a series of measurements, it is probable that the accuracy can be increased with further work. To date not enough is known about this method to indicate its ultimate possibilities, but it is clear that they must certainly be quite great.

d. Impact Tube Method

Since this method is the one utilized in this thesis it will be described in detail elsewhere. We here quote, however, the results obtained by two previous investigators who have applied this method to the measurement of the relaxation time of carbon dioxide. Kantrowitz[1(a)iii] obtained as a final average collision number 32,600 at 105°F. At a temperature of 65°F. and one atm. Griffith[44] obtained a value of 2.02μ sec. for the relaxation time of carbon dioxide containing an unknown concentration of H_2O.

C. Measurements on Nitrogen Tetroxide

a. Sonic Method

In 1910 Nernst and Keutel[45] first suggested that it might be possible to determine the velocity of a chemical reaction by measuring the velocity of sound through an equilibrium mixture. Using high enough frequencies, one should obtain the velocity corresponding to the passage of the sound wave through the mixture without reaction, but at sufficiently low frequencies one should expect the equilibrium to adjust itself by reaction to the periodic compression and rarefaction, and hence decrease the velocity of sound. At intermediate frequencies one would then expect a "critical region" with intermediate velocities.

In his Berlin Inaugural-Dissertation Keutel reported the results of applying the Kundt-tube method of measuring sound velocities to the NO_2-N_2O_4 system, which he studied at various pressures. He concluded that the gas does not behave as a mixture of two non-reacting ases, but that the reaction between them was not so fast as to maintain complete chemical equilibrium during the passage of the sound wave. He also concluded that the specific heat cannot be measured by this method because of the displacement of the equilibrium is unknown, but surmised that with improved technique and more accurate thermodynamic data it would prove possible to determine the rate. He did not, however, derive the relationship between the sound velocity and the

rate constant.

Einstein,[46] in 1920, developed the theory of the effect of frequency on the velocity and absorption of sound in a mixture of chemically reacting ideal gases of negligible absorption.

The dissociation of the colorless gas nitrogen tetroxide to form the highly colored red nitrogen dioxide provided one of the earliest examples for the application of thermodynamics to the calculation of the effect of temperature on equilibrium.[47] It was also, as we have noted, the first chemical reaction to which the sonic method of rate determination was applied. There have been many subsequent attempts to utilize the sonic method to determine the rate of this reaction, both because the reaction is itself of intrinsic interest due to the wealth of information about its other parameters, and because the low heat capacity of the reactants and products compared to the high heat of reaction make the chances of success particularly favorable.[48] The maximum decrease in sound velocity has been calculated for this case to be approximately 3.8% at 25°C. and 1 atm.[49] This theoretical calculation is for the low frequency limit where the chemical reaction follows completely. We shall now review briefly the sonic measurements which have been reported on this system.

The first measurements made on this system were those of E. and L. Natanson,[50] who measured the velocity of sound for only a single frequency, and hence could make no esti-

mate as to the position of the critical range of frequencies where the velocity would be affected by the reaction. Keutel, and later Selle,[51] concluded that the "critical region" lay within the audible range; a conclusion not borne out by later work. The early experiments of Argo[52], and later those of Grüneisen and Goens[49], demonstrated that the critical range lies above the audible range of frequency. Einstein's equations were first employed by Richards and Reid,[53] who applied them to their velocity measurements on the NO_2-N_2O_4 system, and calculated that the rate constant for the dissociation reaction $N_2O_4 = 2NO_2$ is $4.8 \times 10^4 \pm 0.5 \times 10^4$ sec.$^{-1}$ at 25°C. and 260 mm., with an activation energy for dissociation of 13.9 ± 0.9 kg.cal./mole.

Using frequencies in the ultrasonic range measurements have also been made by Olson and Teeter,[54] Teeter,[55] Kistiakowsky and Richards,[56], and Kneser and Gauler.[57] Olson and Teeter concluded that the critical range had actually been passed at a frequency of 51,570 cycles per second in the gas at 565 mm. pressure and 25°C. In later investigations on this system Teeter concluded that, due to the interference of vibrational heat capacity relaxation, it was not possible to determine the rate constant in this way. Kistiakowsky and Richards have carefully studied a wider range of conditions and have found that to within 0.5% there is no systematic change of velocity with frequency between 10 and 80kc. For the highest frequency the

measurements were carried down to a pressure of 300 mm. of Hg. These investigators found that the greatest source of error was evidently small, almost undetectable traces of impurities. The problem was restudied by Kneser and Gauler who agreed with Teeter on the perturbing effect of the vibrational relaxation, and also noted the fact that the ideal gas law could not be applied to a gaseous system that condensed near room temperature.

This problem of ideality had already been considered by Luck,[58] who extended Einstein's treatment to the case of mixtures of real absorbing gases. He concluded: "The departure of a reacting gas mixture from ideal properties cannot change the type of sound velocity dependence upon frequency in the mixture, but can affect numerical values, and so can probably explain the discrepancies between experiment and the earlier theory.

"The practical effect of absorption on the precise measurement of sound velocity in the dispersive frequency region is to render such measurement impossible. Precise velocity measurements in the dispersive region are essential for reaction rate determination since very small velocity differences are involved, but the absorption maximum should be sufficient in actual gases to reduce sound intensity to less than 2% of its initial value in 14 wave-lengths, making the usual interferometric velocity measurements both very difficult and very inaccurate.

"On the other hand, it may be seen from the graph that absorption measurements offer a promising means of determining the reaction rate. The curve of absorption versus frequency shows a reasonably sharp maximum."

Unfortunately, absorption coefficients as a function of frequency are difficult to determine with accuracy.

The whole problem has been considerably clarified by a long paper by Damköhler,[59] who considered the propagation of a sound wave in a gaseous system in which any number of reactions are taking place. In this paper all other loss factors such as thermal conductivity, thermal relaxation, and viscosity were taken into account. He concluded that for the case of NO_2-N_2O_4 there may well be interference between the relaxation effects due to reaction and those due to the vibrational heat capacity.

The conclusion with which most of the above investigators concur is that the available sonic data can at best give a minimum value for the velocity constant for the N_2O_4 dissociation reaction, viz., 5×10^4 sec.$^{-1}$.

b. Dissociation under a Temperature Gradient

Dirac[60] suggested in 1924 that if a gas such as nitrogen dioxide-tetroxide was subjected to a temperature gradient, the concentrations necessary for equilibrium would be different at different points so that there would be diffusion between the two kinds of molecules, a steady state being attained when the rate of diffusion of double molecules

into any region is equal to their excess rate of decomposition over their rate of formation within that region. He develops equations which would enable one to compute the reaction rate in terms of other physical constants of the gas from a detailed knowledge of the concentration or temperature gradient under steady state for a fixed overall temperature gradient. However, for any practical case the quantities to be measured fall off so rapidly over the region of interest that this method would be of no value in determining rates of the order of 1×10^{1} sec.$^{-1}$, or faster.

c. Method of Brass and Tolman

This method has been succinctly described by Brass and Tolman[61] as follows:

"The general nature of the method was to cause an equilibrium mixture of the two gases to flow with a sudden drop in pressure through a perforated diaphragm, and take measurements of the temperature of the gas both before passage through the diaphragm and at successive positions in the path of flow beyond. The sudden drop in pressure and concentration on passage through the diaphragm should be followed by an increase in the degree of dissociation of the tetroxide and, since the reaction is endothermal, this should be accompanied by a drop in the temperature of the gas. Hence, knowing the velocity of flow and the temperature at different distances beyond the diaphragm, it was hoped that conclusions as to the rate of dissociation

could be drawn."

This method has some advantages over the acoustic method since the equipment required is much less complicated and yields information as to the rate more directly. Unfortunately there is a great deal of uncertainty due to lack of knowledge about the behavior of jets issuing from the fine holes in the diaphragm and difficulty in making precision temperature measurements on the flowing gas since the thermocouples not only drain heat from the system but also provide local regions where friction, compression, and possibly catalytic effects may disturb the postulated uniform gradient in reaction.

The best estimate of the unimolecular dissociation rate constant based on this experiment is 8.2×10^{4} sec.$^{-1}$ at 1 atm. and 25°C., but this value the authors state may be in error "even as to order of magnitude". There is, however, a definite positive effect which the authors feel can only be explained by a high rate of dissocation of nitrogen tetroxide.

d. Shock Tube Method

Using the conventional shock tube method Carrington and Davidson[62] have passed a shock wave through an equilibrium mixture of NO_2 and N_2O_4. Passage of the shock wave provides a rapid adiabatic non-isentropic compression, and the subsequent dissociation of N_2O_4 is followed photoelectrically with light of such wavelengths as to be ab-

sorbed preferentially by either NO_2 or N_2O_4. Using this method they studied the dissociation of N_2O_4 in the presence of a large excess of nitrogen over the temperature range -20° to 28° and over the nitrogen pressure range 0.5 to 4 atm. Around 1 atm., the rate law is $\frac{-d(N_2O_4)}{dt} = k(N_2O_4)(N_2)$; $k = 2.0 \times 10^{14} \exp(-11000/RT)$ liter mole^{-1} sec.$^{-1}$. At higher nitrogen pressures, the rates are less than the values predicted by the above equation and it is estimated that the limiting first-order rate constant for the dissociation of N_2O_4 is $k = 10^{16} \exp(-12900/RT)$ sec.$^{-1}$

This method is analogous to one limit of the method applied in this thesis, and will be discussed extensively in this light in sections II and V. It has the advantages of requiring simpler equipment and only small amounts of gas. There may be some disadvantage involved in not being able to vary the rate of energy input as this means that displacements from equilibrium will be large for measurable shocks.

II. Theoretical Analysis of Impact Tube Experiments

A. General Nature of this Experiment

Impact tube experiments are based upon the sudden change in energy distribution experienced by a rapidly flowing fluid when it impinges upon a stationary object of such small dimensions as not to alter greatly the general flow pattern. In this case the object is an impact tube at the face of which the gas flow is stopped and the energy of mass motion is rapidly converted into random molecular motion, which is then redistributed among the various other degrees of freedom. Knowledge of the steady state pressure at the face of the impact tube can be made to yield information about the nature of the energy exchange processes taking place. As additional information one must have the pressure, temperature, and velocity of the gas before impact and the size of the impact tube.

The production of the gas stream by flow through a nozzle and its subsequent compression are shown diagrammatically in figure 2. Figure 3 shows the velocity profile with respect to distance and time along the central streamline approaching a source shaped impact tube.* Initially

---

* The streamlines around the impact tube may be computed according to the method outlined on p. 212, of ref. 1.

Figure 2

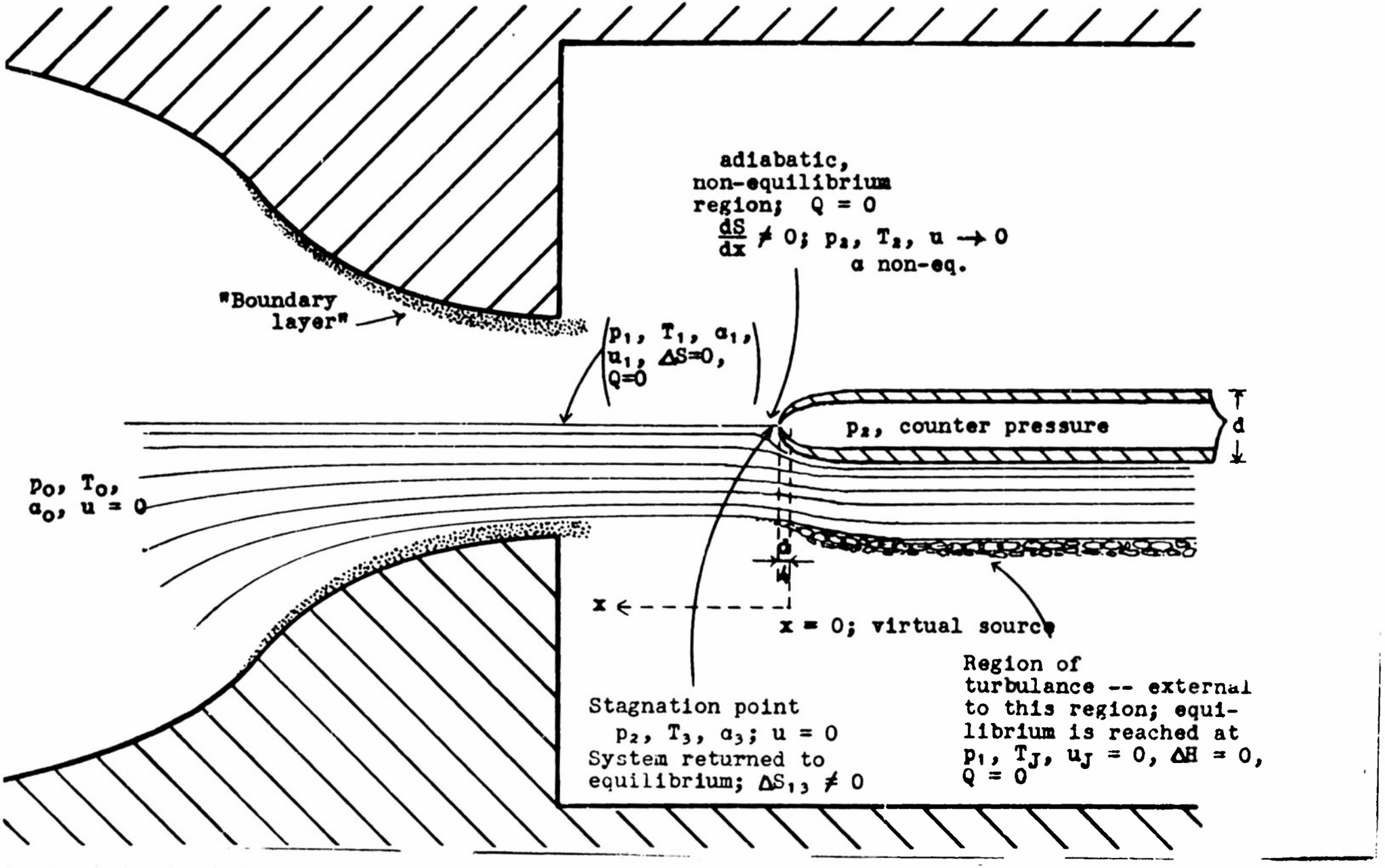
adiabatic,
non-equilibrium
region; Q = 0
$\frac{dS}{dx} \neq 0$; p_2, T_2, $u \rightarrow 0$
a non-eq.
"Boundary layer"
p_1, T_1, a_1,
u_1, $\Delta S=0$,
$Q=0$
p_2, counter pressure
d
p_o, T_o,
a_o, $u = 0$
δ
x
x = 0; virtual source
Stagnation point
p_2, T_3, a_3; u = 0
System returned to
equilibrium; $\Delta S_{1,3} \neq 0$
Region of
turbulance -- external
to this region; equi-
librium is reached at
p_1, T_J, $u_J = 0$, $\Delta H = 0$,
$Q = 0$

Fig. 3

Velocity of gas along central stream line approaching source shaped impact tube: $u(x) = u_1[1 - d^2/16x^2]$

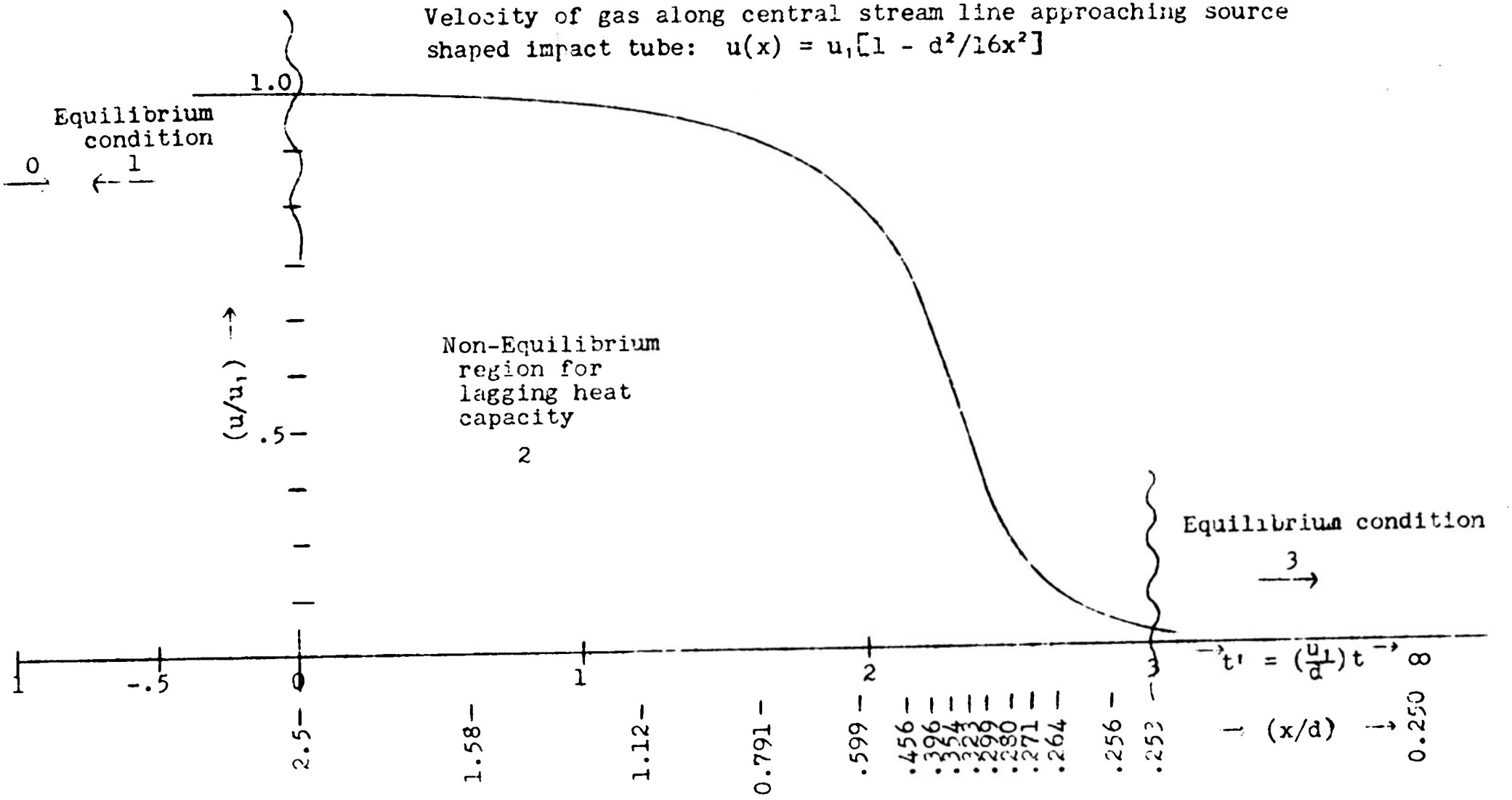

the gas is in equilibrium at a pressure, p_o, and temperature, T_o, and has a negligible flow velocity, u_o. Since the pressure in the expansion chamber is maintained at less than p_o, the gas flows through the nozzle, and under certain conditions (design and operating details are in following section) one obtains over a region around the center of the orifice a non-turbulent stream of gas at a pressure, p_1, temperature, T_1, and flow velocity, u_1. Upon approaching the impact tube the gas along these streamlines is slowed and brought to stagnation at the face of the impact tube. If one imagines that the energy of mass motion is converted instantaneously into random molecular motion, the pressure and temperature change as a consequence to new instantaneous values p_2, T_2, which relax eventually to equilibrium at p_3, T_3, $u=0$. Under steady state conditions there is no net gas flow across the face of the impact tube and hence one may imagine the face of the impact tube to be covered by a thin diaphragm balanced for equal pressures inside and outside. Thus the pressure measured by a manometric device attached to the impact tube is the stagnation pressure at the face of the tube.

If the time over which pressure changes occur in flow through the nozzle is large compared to the equilibration time of the gas then the adiabatic expansion through the nozzle may be considered to occur by a series of infinitesimal equilibrium steps and the entropy change will be zero.

The enthalpy of the gas will be lessened by an amount equal to the kinetic energy of mass motion of the gas.

On encountering the face of the impact tube the kinetic energy of mass motion is returned to the gas as random molecular motion. For an experiment of this type the compression time depends upon the ratio of the size of the impact tube face to the streaming velocity of the gas, the gas flow not being effected by the presence of the impact tube until it is within a distance equal to a few times the breadth of the impact tube face (see figure 3). With gas flow velocities amounting to several tenths of a Mach number and impact tubes having a circular cross section of approximately 0.03 cm. diameter compression times of the order of 1×10^{-6} sec. can readily be attained.

If this compression time is long compared to the equilibration time of the gas, equilibrium will be maintained during compression and the latter will be isentropic; the final temperature and pressure will clearly equal those of the reservoir. If, on the other hand, this compression time is <u>very</u> short compared to the equilibration time of the gas, the energy input will occur instantaneously compared to the equilibration time of the processes involved, and the maximum entropy increase will occur. In order to obtain information about the rate of the equilibration processes it is necessary to have the compression time and equilibration time of the same order of magnitude, for then the fraction of the maximum entropy increase which is produced may be used

to determine the equilibration time in terms of the known compression time. After a very rapid compression the temperature which corresponds to the translational energy of the molecules rises to a peak value, T_2, and the pressure becomes p_2. In general this pressure will not equal p_o, and Griffith has shown that for a non-reacting ideal gas $p_2 < p_o$. That this is also true for a reacting mixture of ideal gases will be shown in part C of this section. During the subsequent adjustment period the temperature corresponding to the translational modes decays to some equilibrium value, T_3, while the other modes (i.e. vibration, reaction) gain energy and follow a different path with energy distributions corresponding to a special "temperature" T_*. Under the conditions of this experiment this adjustment occurs at a constant pressure, p_2, and the temperature change is compensated for by an increase in the density, or by an appropriate shift in the degree of dissociation for a chemically reacting mixture.

Figure 4 is a schematic drawing* showing these changes. In this figure τ represents a characteristic reaction time of the proper order of magnitude to make this experiment yield significant results and $\bar{c}$ is the average velocity of random molecular motion.

---

* This figure based in part on figure 1 of ref. 44b.

Figure 4

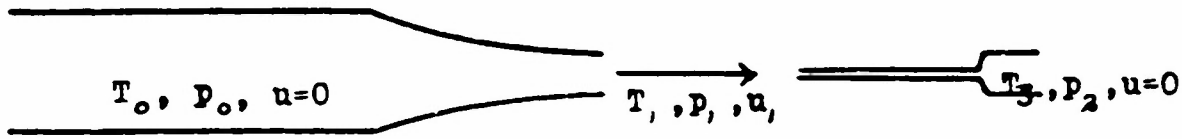

State: 0 1 2 3

TEMPERATURE HISTORY

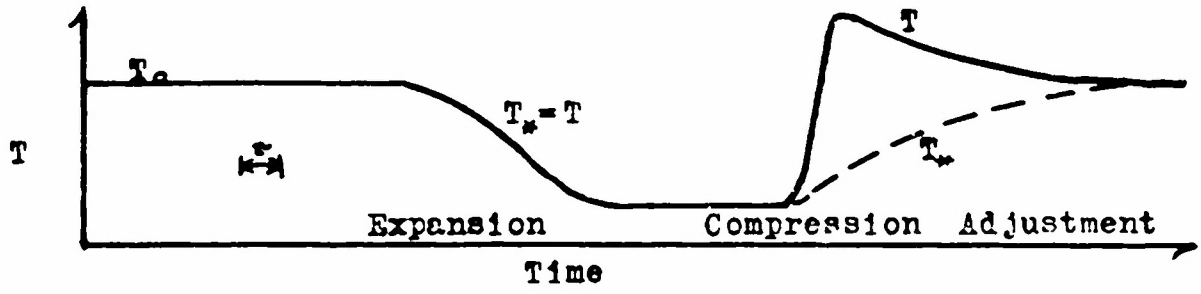

PRESSURE HISTORY

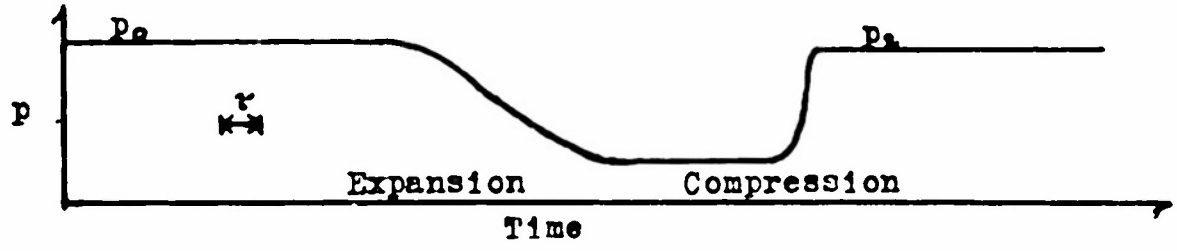

KINETIC THEORY PICTURE

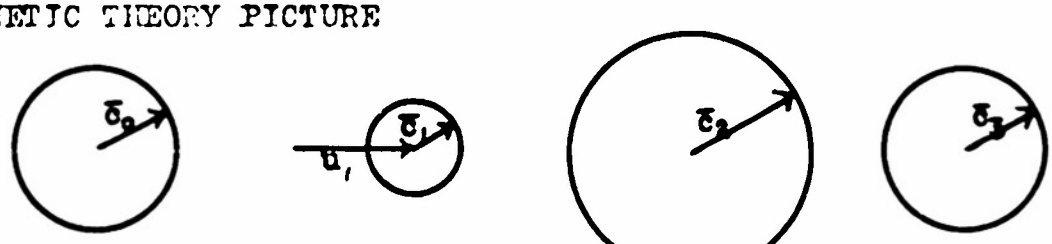

State: 0 1 2 3

B. Theory for a Nonreacting Ideal Gas

In this subsection the theoretical equations governing the impact tube experiment as applied to a nonreacting ideal gas are developed. To a large extent this development is based on the work of Kantrowitz[1] and Griffith.[44] The general case of a real non-dissociating gas has been discussed in some detail by Bauer.[63] The important equations (7), (15), and (19) are, however, developed by an independent method, which the author feels is at once clearer and less intuitive than earlier approaches. An inaccuracy in the earlier work is also pointed out. The guiding principle in formulating this section has been to develop the equations in such a fashion that their extension to the case of a reacting mixture of gases in the following section could be easily followed.

In order to specify completely the state of a typical non-dissociating gas like carbon dioxide, the pressure and a single temperature suffice provided the system is in equilibrium. The nature of this experiment is such that at the face of the impact tube the translational energy is increased so rapidly that the system does not remain in thermodynamic equilibrium. The rotational modes follow this change in translational energy within a comparatively short time, and on the time scale of this experiment[64] one may assume that they are in equilibrium with the translational modes. The vibrational modes are not directly coupled with the trans-

lational modes and, although in general there is coupling between the vibrational and rotational modes, it is usually very weak so that whereas the latter follow rapid changes in translational energy, the former do so only after an appreciable (of the order of microseconds) time lag. However, the vibrational modes of a molecule are rather strongly coupled to each other and maintain an equilibrium energy distribution even under these conditions. Accordingly, one may define two temperatures: T as the temperature in the Boltzmann formula corresponding to the population distribution among translational and rotational states, and T_{vib} as the temperature in the Boltzmann formula corresponding to the population distribution among vibrational states. The specific heat may then be regarded as arising from two sources, vibrational motion, and all the rest. The vibrational contribution is $C_{vib} \equiv dE_{vib}/dT_{vib}$, where E_{vib} is the energy of vibrational motion. C_p' refers to the specific heat at constant pressure not including vibrational degrees of freedom. For $T_{vib} = T$ one has the usual total specific heat, $C_p = C_p' + C_{vib}$. The ideal gas equation of state will be assumed throughout.

The entropy change involved in each step of the impact tube method for the idealized case of instantaneous compression will now be discussed. This will clearly give the maximum possible entropy gain. The enthalpy changes will also be followed.

The expansion through the nozzle is sufficiently slow compared to the rate of equilibration so that the process proceeds reversibly. The expansion is also adiabatic ($Q = 0$).

$$\Delta S_{01} = 0 \quad \text{and} \quad \Delta H_{01} = -Mu_1^2/2 \ . \qquad (1)$$

Here M is the molecular weight of the gas and u_1 is the unit mass velocity of the stream in state 1.

For a truly instantaneous compression the entropy change is equal to zero since the non-lagging modes follow reversibly and the lagging modes are in nowise effected. The energy of mass motion is returned to the gas' non-lagging modes.

$$\Delta S_{12} = 0 \quad \text{and} \quad \Delta H_{12} = Mu_1^2/2 \ . \qquad (2)$$

During the equilibration period following such a compression, the experiment is so arranged (see figure 2) that the pressure remains at p_2 while the non-lagging degrees of freedom go from T_2 to T_3 and the lagging degrees of freedom go from T_1 to T_3. The entropy increases, but there is no change in the enthalpy.

$$\Delta S_{23} = \left\{ C_{vib} \ln \frac{T_3}{T_1} + C_p' \ln \frac{T_3}{T_2} \right\} > 0, \text{ and } \Delta H_{23} = 0. \qquad (3)$$

Now consider going directly from the initial state (0) to the final state (3). The pressure changes from p_0 to p_2, while the temperature of all modes goes from T_0 to T_3; hence

$$\Delta S_{03} = \left\{ C_p \ln \frac{T_3}{T_0} + R \ln \frac{p_0}{p_2} \right\} , \text{ and } \Delta H_{03} = 0. \qquad (4)$$

Since any reversible path may be used to evaluate the entropy change,

$\Delta S_{03} = \Delta S_{01} + \Delta S_{12} + \Delta S_{23}$, and substituting from equations (1), (2), (3), and (4) one gets

$$R \ln \frac{p_0}{p_2} = C_{vib} \ln \frac{T_0}{T_1} + C_p' \ln \frac{T_0}{T_2} . \qquad (5)$$

Note that T_3 cancels out since $C_p = C_p' + C_{vib}$. Since all of these steps occur adiabatically the total energy of the system is conserved and hence considering states 0 and 2

$$C_p'(T_2 - T_0) + C_{vib}(T_1 - T_0) = 0. \qquad (6)$$

Solving (6) for T_2 and substituting into (5) gives

$$\frac{p_0}{p_2} = \left\{ \frac{\frac{C_p}{C_{vib}} - 1}{\frac{C_p}{C_{vib}} - \frac{T_1}{T_0}} \right\}^{C_p'/R} \left(\frac{T_0}{T_1}\right)^{C_{vib}/R} . \qquad (7)$$

From $\Delta S_{01} = 0$ one may deduce the familiar adiabatic relation for an ideal gas:

$$R \ln \frac{p_0}{p_1} = C_p \ln \frac{T_0}{T_1} . \qquad (8)$$

Combining equations (6), (7), and (8) then allows one to compute the maximum (instantaneous compression) pressure defect $(p_0 - p_2)_{i.c.}$. Equation (6) is needed to give T_2.

For any nonreacting gas with lagging and non-lagging degrees of freedom the time rate of entropy change may be written as

$$\frac{dS}{dt} = \left(\frac{\partial S}{\partial p}\right)_{T,T_{vib}} \frac{dp}{dt} + \left(\frac{\partial S}{\partial T}\right)_{p,T_{vib}} \frac{dT}{dt} + \left(\frac{\partial S}{\partial T_{vib}}\right)_{p,T} \frac{dT_{vib}}{dt} . \qquad (9)$$

The coefficients to be used here are:

$$\left(\frac{\partial S}{\partial p}\right)_{T,T_{vib}} = -\left(\frac{\partial V}{\partial T}\right)_{p,T_{vib}} = -\frac{R}{p}$$

$$\left(\frac{\partial S}{\partial T}\right)_{p,T_{vib}} = \frac{1}{T} C_p' \qquad (10)$$

$$\left(\frac{\partial S}{\partial T_{vib}}\right)_{p,T} = \frac{1}{T_{vib}} C_{vib} \ .$$

The hydrodynamical momentum conservation equation yields $\frac{dp}{dt} = -\frac{\varrho}{2}\frac{du^2}{dt}$, which may be rewritten for an ideal gas as

$$\frac{dp}{dt} = \frac{p}{RT}\left(-\frac{M}{2}\frac{du^2}{dt}\right) \ . \qquad (11)$$

Substitution of (10) and (11) into (9) yields

$$\frac{dS}{dt} = \frac{1}{T}\frac{M}{2}\frac{du^2}{dt} + \frac{C_p'}{T}\frac{dT}{dt} + \frac{C_{vib}}{T_{vib}}\frac{dT_{vib}}{dt} \ . \qquad (12)$$

Treating the time rate of enthalpy change in a similar manner:

$$\frac{dH}{dt} = \left(\frac{\partial H}{\partial p}\right)_{T,T_{vib}}\frac{dp}{dt} + \left(\frac{\partial H}{\partial T}\right)_{p,T_{vib}}\frac{dT}{dt}$$

$$+ \left(\frac{\partial H}{\partial T_{vib}}\right)_{p,T}\frac{dT_{vib}}{dt} = -\frac{M}{2}\frac{du^2}{dt} \ . \qquad (13)$$

For an ideal gas $(\partial H/\partial p)_{T,T_{vib}} = 0$, and substituting the appropriate values for the other coefficients gives

$$\frac{dH}{dt} = C_p'\frac{dT}{dt} + C_{vib}\frac{dT_{vib}}{dt} = -\frac{M}{2}\frac{du^2}{dt} \ . \qquad (14)$$

Using (14) to eliminate the derivatives of u^2 and T from (12) then yields the important relationship

$$\frac{dS}{dt} = C_{vib} \left\{ \frac{1}{T_{vib}} - \frac{1}{T} \right\} \frac{dT_{vib}}{dt} \quad . \tag{15}$$

One may now find quite simply the entropy gain for instantaneous compression. After such a compression $du^2/dt = 0$ and equation (14) yields

$$C_p' \frac{dT}{dt} + C_{vib} \frac{dT_{vib}}{dt} = 0 \ . \tag{16}$$

This may be integrated using as the boundary condition $T = T_{vib} = T_3$ to give

$$T = - \frac{C_{vib}}{C_p'} T_{vib} + \frac{C_p}{C_p'} T_3 \ . \tag{17}$$

Combining (17) with (15) and integrating over the equilibration period following the instantaneous compression one gets

$$\Delta S_{i.c.} = \int_{T_{vib} = T_1}^{T_{vib} = T_3} \frac{C_{vib}}{\bar{T}^2} \left\{ - \frac{C_{vib}}{C_p'} T_{vib} + \frac{C_p}{C_p'} T_3 - T_{vib} \right\} dT_{vib}$$

$$= \frac{C_{vib}}{\bar{T}^2} \frac{C_p}{C_p'} \left\{ \frac{T_3^2}{2} + \frac{T_1^2}{2} - T_3 T_1 \right\} \ . \tag{18}$$

$\bar{T}^2$ is taken as the average of (TT_{vib}) over the whole process, and from figure 4 a good value is seen to be $\bar{T} = \frac{1}{2}(T_0 + T_1)$. The specific heats and equilibration times will be taken at this temperature as well. Since the process is adiabatic

$$C_p(T_1 - T_0) + \frac{v_1^2}{2} = C_p(T_3 - T_0) \ , \qquad \text{and}$$

(18) becomes

$$\Delta S_{i.c.} = \frac{1}{2} \frac{C_{vib}}{\bar{T}^2} \frac{C_p}{C_p'} \left(\frac{M}{2} u_i^2\right)^2 . \qquad (19)$$

This formula is identical to that found by Kantrowitz and Griffith following a kinetic formulation. The kinetic analysis applies to the case of non-instantaneous compression as well, and will now be discussed.

As was noted in Section I., the details of the collision process must be examined in order to find an expression for the rate at which energy exchange will occur between the various modes. An assumption is introduced; namely, that after a small perturbation from equilibrium the time rate of adjustment of the vibrational energy is proportional to its displacement from equilibrium.[59,65a]

$$\frac{d\, C_{vib}\ T_{vib}}{dt} = C_{vib}\,(T_3 - T_{vib})/\tau . \qquad (20)$$

Semi-classical treatments of this problem[10,13,66,67] have shown τ to have the following functional dependence:

$$\tau \approx p^{-1} (\nu s)^{-2/3} \left(\frac{m}{T}\right)^{-1/3} \exp\left\{(\nu s)^{2/3} \left(\frac{m}{T}\right)^{1/3}\right\} . \qquad (21)$$

Here ν is the vibrational frequency, s the molecular radius, and m the molecular mass. When changes in the temperature are small τ may be considered constant, and after a time τ the temperature difference diminishes to 1/e, or 0.368, of its original value. For a first order process this time is clearly independent of the magnitude of the

starting temperature difference, and is frequently referred to as the "relaxation" time.

Kantrowitz, and Griffith as well, used a somewhat different assumption instead of (20), writing

$$\frac{d\, C_{vib}\, T_{vib}}{dt} = C_{vib}\,(T-T_{vib})/\tau_K \qquad . \qquad (22)$$

That is, they postulated that the time rate of adjustment of vibrational energy is proportional to the difference between the actual vibrational energy and the vibrational energy for equilibrium partition at the translational temperature T. The difference between these two assumptions, (20) and (22), clearly depends on the ratio of (T_3-T_{vib}) to $(T-T_{vib})$. Since the relaxation process is adiabatic $C_p'(T-T_3) + C_{vib}(T_{vib}-T_3) = 0$, and it follows that $\frac{T_3-T_{vib}}{T-T_{vib}} = \frac{C_p'}{C_p}$. Hence relaxation times calculated according to the two different assumptions will be related as follows:

$$\tau/\tau_K = C_p'/C_p \qquad . \qquad (23)$$

The work of Damköhler,[59] Manes,[65a] and others indicates clearly that the assumption (20) is to be preferred. However, since the various formulas and earlier treatments have been developed according to assumption (22), we shall for purposes of comparison continue with the latter except where otherwise stated.

Following Kantrowitz, the variable ϵ, which represents the excess energy in the lagging modes over the energy at

equilibrium partition at the temperature T, is now introduced as a measure of the disequilibrium.

$$\epsilon \equiv C_{vib} (T_{vib}-T) \quad . \tag{24}$$

In experiments wherein changes in T are small compared to T itself, (15) may be rewritten using (22) and (24) as

$$dS = - \frac{\epsilon dt}{\tau_K} \cdot \frac{T-T_{vib}}{TT_{vib}} \cong \frac{\epsilon^2 \, dt}{\tau_K \, C_{vib} \, \bar{T}^2} \quad . \tag{25}$$

$\bar{T}^2$ is here defined as in equation (18). Then

$$\Delta S = \int \frac{\epsilon^2 \, dt}{\tau_K \, C_{vib} \, \bar{T}^2} \quad . \tag{26}$$

Since $\epsilon(t)$ depends on the compression profile and characteristics of the gas, the integral must be taken over that part of the flow for which ΔS is desired. By combining equations (14), (22), and (24) so as to eliminate the temperature, an equation for ϵ is obtained.

$$\frac{d\epsilon}{dt} + \frac{C_p}{C_p'} \frac{\epsilon}{\tau_K} = \frac{C_{vib}}{C_p'} \frac{M}{2} \frac{du^2}{dt} \quad . \tag{27}$$

The integral is

$$\epsilon(t_1) = \exp\left(-\int^{t_1} \frac{C_p \, dt}{\tau_K \, C_p'}\right) \int^{t_1} \exp\left(\int^{t_1} \frac{C_p \, dt}{\tau_K \, C_p'}\right) \frac{C_{vib}}{C_p'} \frac{d\left(\frac{M}{2} u^2\right)}{dt} \, dt \quad . \tag{28}$$

Knowledge of the velocity history of the flow and the specific heats for the gas now enable one to relate pressure differences to relaxation times.

This approach may now be utilized as an alternate method for deriving (19). Equation (27) may be rewritten as

$$\left(\frac{d\epsilon}{dt}\right) dt + \left(\frac{C_p \epsilon}{C_p'}\right) \frac{dt}{\tau_K} = \left(\frac{C_{vib}}{C_p'}\right)\left(\frac{d \frac{M}{2} u^2}{dt}\right) dt. \qquad (29)$$

As the time required for stopping becomes shorter the second term will become small compared to the other terms, and in the limit, when $\int \epsilon \frac{dt}{\tau_K}$ becomes negligible in comparison to the other two terms, the change in ϵ is

$$\Delta\epsilon_{(limit)} = \left(\frac{C_{vib}}{C_p'}\right) \Delta \left(\frac{M}{2} u^2\right) . \quad .$$

In the case being considered ϵ was originally zero and the velocity was u_1. A sudden stopping then produces a value of

$$\epsilon_o = \left(\frac{C_{vib}}{C_p'}\right) \frac{M}{2} u_1^2 .$$

With $u = 0$, (29) gives for the approach to equilibrium

$$\frac{d\epsilon}{dt} = - C_p \epsilon / C_p' \tau_K .$$

The entropy change for instantaneous compression is, accordingly,

$$\Delta S_{03})_{i.c.} = \int_{\epsilon_o}^{o} \frac{\epsilon^2 \, dt}{\tau_K \, C_{vib} \, \bar{T}^2} = \int_{\epsilon_o}^{o} \frac{C_p' \tau_K \, \epsilon \, d\epsilon}{C_p \, \tau_K \, C_{vib} \, \bar{T}^2}$$

$$= \frac{C_p'}{2 \, C_p \, C_{vib} \, \bar{T}^2} \left(\frac{C_{vib} \, M u_1^2}{2 \, C_p'}\right)^2 , \qquad (30)$$

which is, of course, identical with equation (19) since for instantaneous compression τ_K cancels out.

Since the expansion and compression take place adiabatically $\Delta H_{03} = 0$, which for a nonreacting ideal gas means that $T_3 = T_0$. The overall entropy change is therefore given by

$$\Delta S = R \ln p_0/p_3 \quad . \tag{31}$$

When the difference $(p_0-p_3) = \Delta p$ is small compared to p_0,

$$\frac{\Delta S}{R} \doteq \Delta p/p_0 \quad , \tag{32}$$

and from (19) or (30)

$$\frac{\Delta p_{i.c.}}{p_0} = \frac{C_p'}{2C_p\, C_{vib}\, R\bar{T}^2} \left(\frac{C_{vib}\, Mu_1^2}{2\, C_p'}\right)^2 \quad . \tag{33}$$

It is convenient at this point to substitute a set of dimensionless variables. Again using Kantrowitz' notation define the following:

$$\tau_K' = \frac{C_p'}{C_p}\,\frac{u_1\,\tau_K}{d} \qquad t' = \frac{u_1 t}{d}$$

$$\epsilon' = \frac{\epsilon}{(C_{vib}/C_p')(\frac{M}{2}\,u_1^2)} \qquad u' = u/u_1 \quad . \tag{34}$$

Using (30), (32), and (34) in equations (26) and (23) one obtains

$$\epsilon'(t') = \exp(-\frac{1}{\tau_K'}\int^{t'} dt')\left[\int^{t'} \exp(\frac{1}{\tau_K'}\int^{t'} dt')\frac{du'^2}{dt'}\,dt'\right] , \tag{35}$$

and

$$\frac{\Delta p}{\Delta p_{i.c.}} = \frac{2}{\tau_K'}\int_0^{\infty} \epsilon'^2\, dt' \quad . \tag{36}$$

The square bracketed portion of (35) arises from the fact that the energy input on compression occurs over a finite time interval rather than instantaneously. Equation (35) thus represents a folding of the energy input curve into the relaxation expression. From (36) one sees that $\Delta p/\Delta p_{i.c.}$ depends only on γ'_K for a given flow pattern. This is the great simplification obtained by running an experiment in which only small temperature changes occur.

In order to actually calculate relaxation times from observed pressure defects it is necessary to know the value of the integral appearing in (36), hence of $\epsilon'(t')$. The latter requires a detailed knowledge of the compression streamlines in the region around the face of the impact tube [i.e. of $\frac{du^2}{dt}(t)$] which, in turn, depend on the geometry of the impact tube. The flow around a source-shaped impact tube can be described analytically, and Kantrowitz has evaluated the above integral for this special case. For the square-tipped impact tubes used in our experiments no analytic solution is available, but Griffith has carried out the necessary computations numerically using Southwell's Relaxation Method[68] to obtain the flow pattern. This method rests upon the accuracy with which a difference equation can be made to approximate a differential equation. Assuming incompressible flow impinging axially upon a square-tipped impact tube having a hollow center of inside diameter equal to 0.620 times the outside diameter, he obtains the values

shown in figure 5 for the dependence of velocity on distance and the values shown in figure 6 for the dependence of ϵ' on the time. Upon integrating over the path for various τ' he obtains the following values:

τ_K'	1/10	1/3	1	3	10
$\Delta p/\Delta p_{i.c.}$	0.0828	0.226	0.480	0.723	0.908

For very short relaxation times the approximation formula $\Delta p/\Delta p_{i.c.} = 0.867\ \tau'$ may be used. This is valid for $\tau' < 0.08$. This completes the theory necessary for reducing observed pressure defects to relaxation times.

FIGURE 5

VELOCITY ALONG AXIS FOR FLOW AROUND A PITOT TUBE

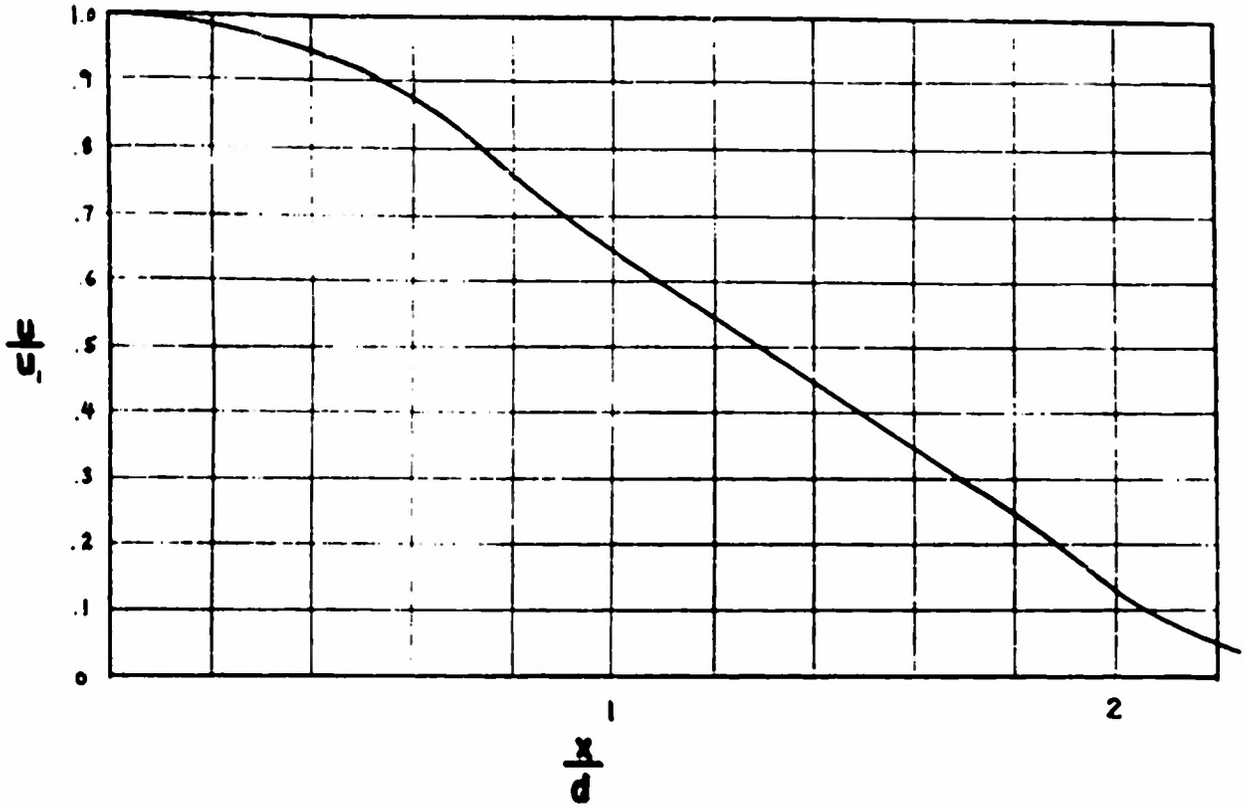

VELOCITY vs. TIME

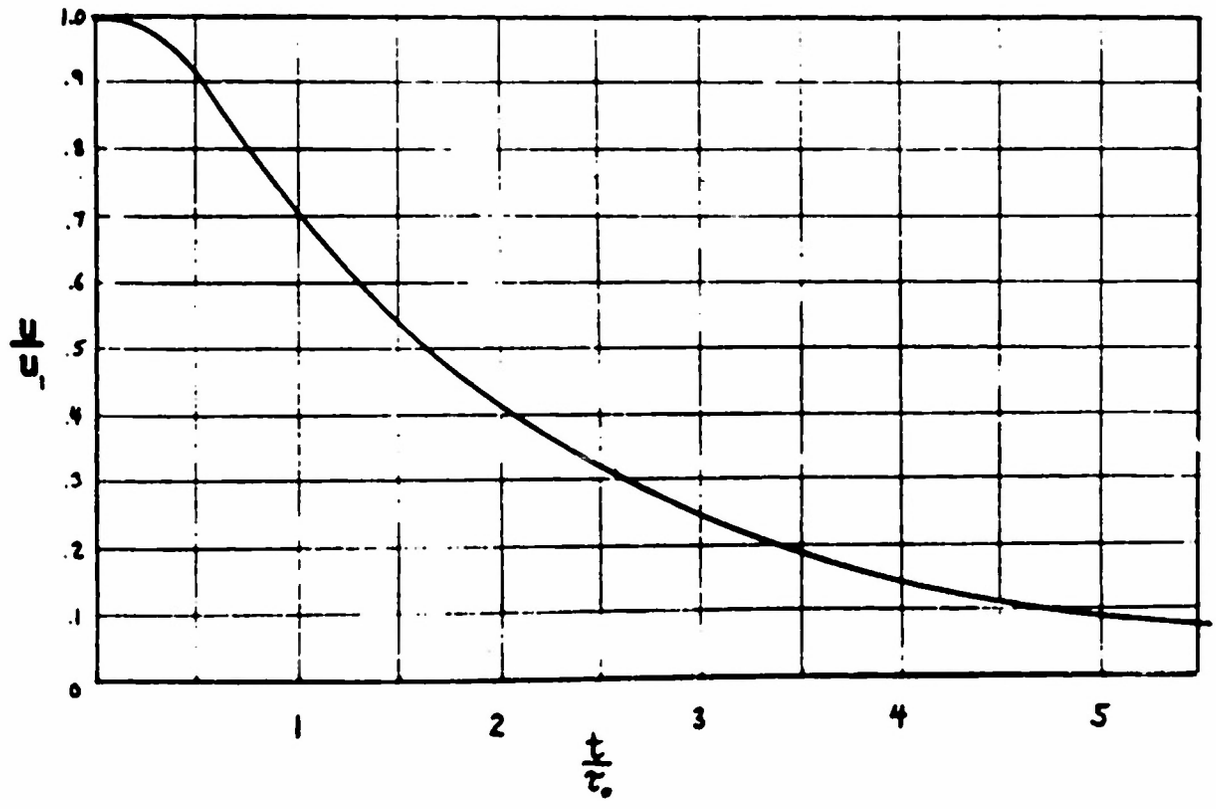

Figure 6

Energy Difference vs Time

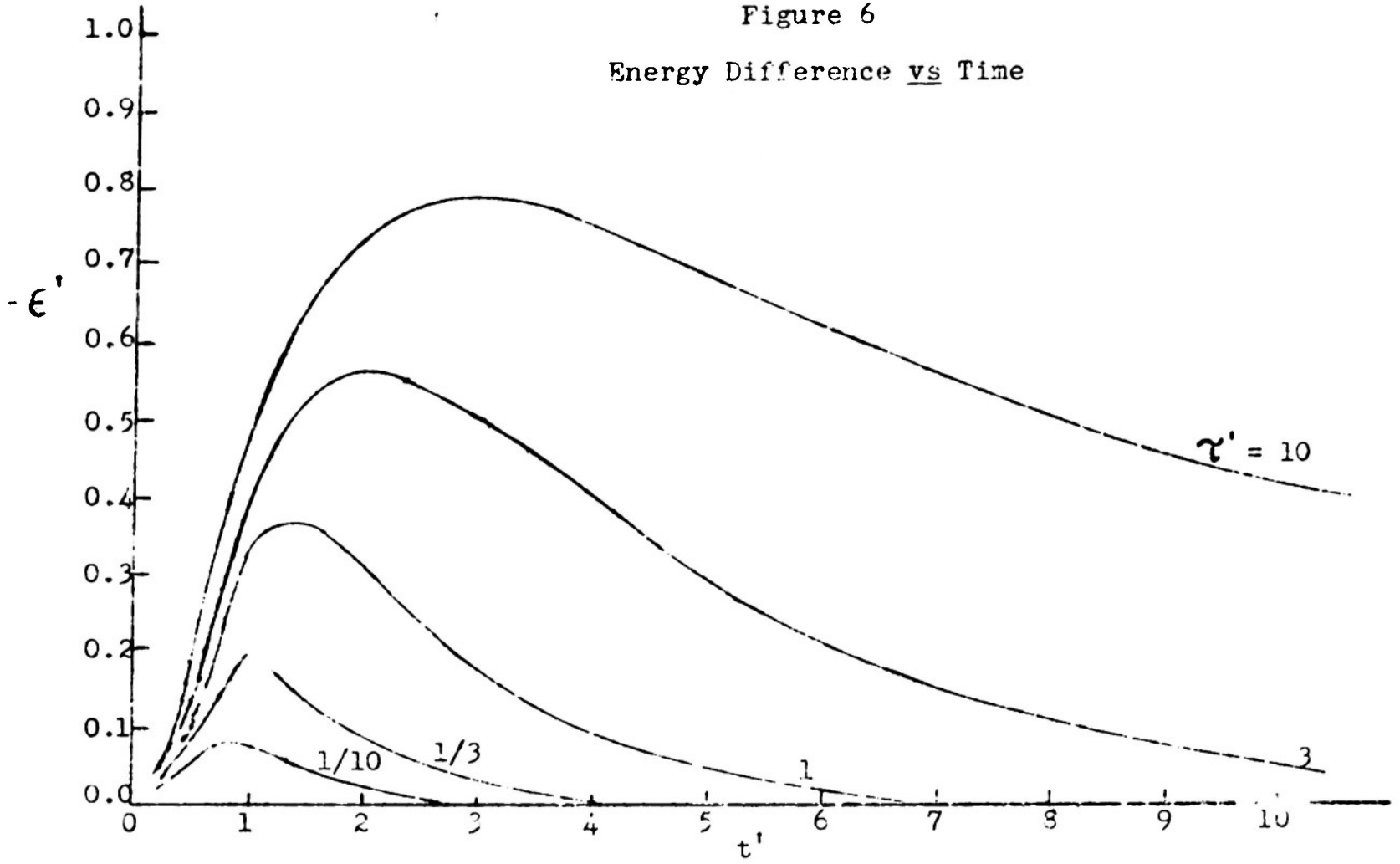

C. Theory for a Reacting Mixture of Ideal Gases

In this subsection the theoretical equations governing the impact tube experiment as applied to a reacting mixture of ideal gases are developed. This constitutes an extension of the application of this type of experiment, and was first discussed by Bauer[63]. For the purposes of the present analysis consideration will be limited to a gas which dissociates according to the equation $A_2 = 2A$, but the formulas obtained may be readily extended to other cases of pressure dependent chemical reactions. It will be assumed that the species A_2 and A individually obey the ideal gas law.

In order to specify completely the state of a typical dissociating gas like nitrogen tetroxide, the pressure and a single temperature suffice provided the system is in equilibrium. As has been noted in part A of this section, the nature of the impact tube experiment is such that at the face of the impact tube the translational energy of the gas is increased so rapidly that a condition of disequilibrium results. One then needs two additional variables to specify completely the state of the gas: α, the degree of dissociation and θ, the temperature in the Boltzmann formula corresponding to the pupulation distribution among vibrational states. This latter definition parallels that used for a non-dissociating gas and, as before, T is taken as the temperature in the Boltzmann

formula corresponding to the population distribution among translational and rotational states. (Note: At first though one might be inclined to postulate different θ's for the lagging modes of NO_2 and N_2O_4. Rigorously one should assume a different θ for each individual lagging degree of freedom. Since this exact assumption would lead to almost intractable mathematical expressions (see Bauer, ref. 63) we make the simplest assumption of a single θ for all of the lagging vibrational modes. A separate variable is used to describe the reaction which may be expected to adjust at an appreciably different rate from vibration.)

a. Thermodynamic Considerations.

The entropy change involved in each step of the impact tube method for the idealized case of instantaneous compression will now be discussed. This will clearly give the maximum possible entropy gain. The enthalpy changes will also be followed. Since ΔH and ΔS of reaction are given for changes at 25°C. and pressures for each component of one atmosphere (ΔH°_{298} and ΔS°_{298}), one must include suitable correction terms when the changes occur under conditions other than these. All quantities will be written per original mole of A_2 unless otherwise specified.

The expansion through the nozzle is sufficiently slow compared to the rate of equilibration that the process proceeds reversibly. The expansion is also adiabatic.

$$\Delta S_{01} = 0; \quad \Delta H_{01} = -\frac{M}{2} u_1^2 \quad . \tag{37}$$

Here M is the molecular weight of A_2, and u_1 is the unit mass velocity of the stream in state 1.

For a truly instantaneous compression the entropy change (ΔS_{12}) is equal to zero since the non-lagging modes follow reversibly while the lagging modes are in nowise affected. The energy of mass motion is returned as molecular enthalpy.

$$\Delta S_{12})_{i.c.} = 0; \quad \Delta H_{12})_{i.c.} = \frac{M}{2} u_1^2 . \tag{38}$$

During the equilibration period after such a compression the experiment is so arranged (see figure 2) that the pressure remains at p_2 while the non-lagging specific heat goes from T_2 to T_3, the lagging specific heat of the vibrational modes goes from T_1 to T_3, and the lagging degree of dissociation goes from α_1 to α_3. The entropy increases, but there is no change in the enthalpy.

$$\begin{aligned}
\Delta S_{23})_{i.c.} = & \left\{(1-\alpha_1)C'_{p(2)} + 2\alpha_1 C'_{p(1)}\right\} \ln T_o/T_2 \\
& + \left\{(1-\alpha_1) C_{\theta(2)} + 2\alpha_1 C_{\theta(1)}\right\} \ln T_o/T_1 \\
& + (1-\alpha_1)R \ln\left(\frac{1-\alpha_1}{1+\alpha_1} p_2\right) + 2\alpha_1 R\ln\left(\frac{2\alpha_1}{1+\alpha_1} p_2\right) \\
& + \Delta S^\circ(\alpha_3-\alpha_1) - (1-\alpha_3)R\ln\left(\frac{1-\alpha_3}{1+\alpha_3} p_2\right) \\
& - 2\alpha_3 R\ln\left(\frac{2\alpha_3}{1+\alpha_3} p_2\right) \\
& + \left\{(1-\alpha_3) C_{p(2)} + 2\alpha_3 C_{p(1)}\right\} \ln T_3/T_o
\end{aligned}$$

$$\Delta H_{23})_{i.c.} = 0. \tag{39}$$

Here $C_{p(i)}$ refers to the total specific heat, $C'_{p(i)}$ refers to the non-lagging specific heat (translation and rotation), and $C_{\theta(i)}$ refers to the lagging specific heat (vibration). The subscript i = 1 refers to species A_1 and i = 2 refers to species A_2. The specific heats are taken per formula weight of the substance indicated. This expression for $\Delta S_{23})_{i.c.}$ has been computed using a path such that the change in α occurs under conditions where ΔS°_{298} properly applies. Since this argument is used repeatedly the steps for this case are presented in detail below.

	State 2					State 3
α:	α_1	α_1	α_1	α_3	α_3	α_3
T:	T_2	T_o	T_o	T_o	T_o	T_3
θ:	T_1	T_o	T_o	T_o	T_o	T_3
p_{NO_2}:	$\frac{2\alpha_1}{1+\alpha_1}p_2$	$\frac{2\alpha_1}{1+\alpha_1}p_2$	1	1	$\frac{2\alpha_3}{1+\alpha_3}p_2$	$\frac{2\alpha_3}{1+\alpha_3}p_2$
$p_{N_2O_4}$:	$\frac{1-\alpha_1}{1+\alpha_1}p_2$	$\frac{1-\alpha_1}{1+\alpha_1}p_2$	1	1	$\frac{1-\alpha_3}{1+\alpha_3}p_2$	$\frac{1-\alpha_3}{1+\alpha_3}p_2$

It should be noted at this point that the specific heat terms of equation (39) demarked by curly brackets are strictly speaking temperature dependent and represent average values over a temperature interval with 1/T as the weighting function. Curly brackets will be used throughout this section to signify such special averages.

Now consider going directly from the initial state to the final state. The changes are:

$$\begin{array}{lll} p & p_o \longrightarrow p_2 & \\ T = \theta & T_o \longrightarrow T_3 & \\ \alpha & \alpha_o \longrightarrow \alpha_3 \ , & \text{and hence:} \end{array}$$

$$\Delta S_{o3})_{i.c.} = (1-\alpha_o)R\ln\left(\frac{1-\alpha_o}{1+\alpha_o}\, p_o\right) + 2\alpha_o R\ln\left(\frac{2\alpha_o}{1+\alpha_o}\, p_o\right)$$

$$-\Delta S^\circ(\alpha_o-\alpha_3) - (1-\alpha_3)\, R\ln\left(\frac{1-\alpha_3}{1+\alpha_3}\, p_2\right)$$

$$-2\alpha_3 R\ln\left(\frac{2\alpha_3}{1+\alpha_3}\, p_2\right) + \left\{(1-\alpha_3)C_{p(2)}\right.$$

$$\left. + 2\alpha_3\, C_{p(1)}\right\} \ln T_3/T_o \qquad (40)$$

and $\Delta H_{o3} = \left\{(1-\alpha)C_{p(2)} + 2\alpha C_{p(1)}\right\}(T_3-T_o) + \Delta H^\circ(\alpha_3-\alpha_o) = 0$.

Since any reversible path may be used to evaluate ΔS,

$$\Delta S_{o3})_{i.c.} = \Delta S_{o1})_{i.c.} + \Delta S_{12})_{i.c.} + \Delta S_{23})_{i.c.} \ ,$$

and upon substituting from equations (37), (38), (39), and (40) one gets after combining terms:

$$(1+\alpha_1)R\ln(p_o/p_2)_{i.c.} = \left\{(1-\alpha_1)C'_{p(2)} + 2\alpha_1 C'_{p(1)}\right\} \ln T_o/T_2$$

$$+ \left\{(1-\alpha_1)C_{\theta(2)} + 2\alpha_1 C_{\theta(1)}\right\} \ln T_o/T_1$$

$$+ \Delta S^\circ(\alpha_o-\alpha_1) - (1-\alpha_1)R\ln\left(\frac{1-\alpha_o}{1+\alpha_o} \cdot \frac{1+\alpha_1}{1-\alpha_1}\right)$$

$$- 2\alpha_1 R\ln\left(\frac{2\alpha_o}{1+\alpha_o} \cdot \frac{1+\alpha_1}{2\alpha_1}\right) - (\alpha_o-\alpha_1)R\ln K_p(T_o). \qquad (41)$$

Note that T_3 has canceled upon combining terms. $K_p(T)$ is the pressure independent equilibrium constant evaluated at T.

$$K_p(T) = \frac{4\alpha_e^2}{1-\alpha_e^2}\, p \quad . \qquad (42)$$

Here α_e is the equilibrium degree of dissociation at p, T.

Since all of these steps occur adiabatically, one may write $\Delta H_{02})_{i.c.} = 0$; hence

$$\left[\left\{(1-\alpha_1)C_{\theta(2)} + 2\alpha_1 C_{\theta(1)}\right\} T_1 - \left\{(1-\alpha_o)C_{\theta(2)} + 2\alpha_o C_{\theta(1)}\right\} T_o\right]$$

$$+ \left[\left\{(1-\alpha_1)C'_{p(2)} + 2\alpha_1 C'_{p(1)}\right\} T_2 - \left\{(1-\alpha_o)C'_{p(2)} + 2\alpha_o C'_{p(2)}\right\} T_o\right]$$

$$= 0 \quad . \qquad (43)$$

Writing the explicit equation for $\Delta S_{01} = 0$ yields the adiabatic relation:

* $$(1+\alpha_1)R\ln(p_o/p_1) = \left\{(1-\alpha_1)C_{p(2)} + 2\alpha_1 C_{p(1)}\right\} \ln T_o/T_1$$

$$+ \Delta S^\circ(\alpha_o-\alpha_1) - (1-\alpha_1)\, R \ln \left(\frac{1-\alpha_o}{1+\alpha_o} \cdot \frac{1+\alpha_1}{1-\alpha_1}\right)$$

$$- 2\alpha_1\, R \ln \left(\frac{2\alpha_o}{1+\alpha_o} \cdot \frac{1+\alpha_1}{2\alpha_1}\right) - (\alpha_o-\alpha_1)\, R \ln K_p(T_o) . \qquad (44)$$

Combination of equations (41), (42), (43), and (44) allows one to compute the maximum (instantaneous compression) pressure defect, $(p_o-p_2)_{i.c.}$, for a given p_o, T_o, p_1. Equation (43) is needed to give T_2.

One sees then, that the thermodynamic approach can only give limiting values: when the compression is very slow compared to the equilibration rate $\Delta S_{03} = 0$ and $p_2 = p_o$, when the compression is very rapid compared to the

---

* In eq. (44) and thereafter ΔS°_{298} will be abbreviated to ΔS° and ΔH°_{298} will be abbreviated to ΔH°.

equilibration rate $\Delta S_{03} \neq 0$ and $(p_o - p_2) > 0$ and is given by (41). In order to find the entropy increment for intermediate cases one must consider the details of the kinetic process and find the entropy increment as a function of the time rate of enthalpy input and of the rates of equilibration of the lagging modes.

b. Time Dependent Entropy Changes

For the general case of a mixture of two reacting gases related by $A_2 = 2A$ with both lagging and non-lagging degrees of freedom, the time rate of entropy change may be written as

$$\frac{dS}{dt} = \left(\frac{\partial S}{\partial p}\right)_{T,\theta,\alpha} \frac{dp}{dt} + \left(\frac{\partial S}{\partial T}\right)_{p,\theta,\alpha} \frac{dT}{dt} + \left(\frac{\partial S}{\partial \theta}\right)_{p,T,\alpha} \frac{d\theta}{dt} + \left(\frac{\partial S}{\partial \alpha}\right)_{p,T,\theta} \frac{d\alpha}{dt} . \qquad (45)$$

The coefficients to be used here are:

$$\left(\frac{\partial S}{\partial p}\right)_{T,\theta,\alpha} = - \left(\frac{\partial V}{\partial T}\right)_{p,\alpha,\theta} = - \frac{(1+\alpha)R}{p} \qquad \text{(individually ideal gases)}$$

$$\left(\frac{\partial S}{\partial T}\right)_{p,\theta,\alpha} = \frac{1}{T} \left\{(1-\alpha)C'_{p(2)}(T) + 2\alpha C'_{p(1)}(T)\right\}$$

$$\left(\frac{\partial S}{\partial \theta}\right)_{p,T,\alpha} = \frac{1}{\theta} \left\{(1-\alpha)C_{\theta(2)}(\theta) + 2\alpha C_{\theta(1)}(\theta)\right\} \qquad (46)$$

$$\left(\frac{\partial S}{\partial \alpha}\right)_{p,T,\theta} = - R \ln \left(\frac{4\alpha^2}{1-\alpha^2} p\right) + \left\{C'_{p(2)} - 2C_{p(1)}\right\} \ln T_o/T + \left\{C_{\theta(2)} - 2C_{\theta(1)}\right\} \ln T_o/\theta + \Delta S^\circ .$$

All of these coefficients are per initial mole of N_2O_4. The last coefficient was obtained by the method indicated in the discussion of equation (39), and the specific heats are the same type of weighted average values noted previously. The hydrodynamical momentum conservation equation yields

$$\frac{dp}{dt} = -\frac{\rho}{2}\frac{du^2}{dt} \quad , \qquad \text{which may be re-}$$

written for this case as

$$\frac{dp}{dt} = \frac{p}{(1+\alpha)RT}\left(-\frac{M}{2}\frac{du^2}{dt}\right) \quad . \tag{47}$$

T is used here rather than θ because only the translational energy is involved in the pressure. Substitution of (46) and (47) into (45) yields

$$\begin{aligned}\frac{dS}{dt} = {} & \frac{1}{T}\frac{M}{2}\frac{du^2}{dt} + \frac{1}{T}\left\{(1-\alpha)C'_{p(2)}(T) + 2\alpha C'_{P(1)}(T)\right\}\frac{dT}{dt} \\ & + \frac{1}{\theta}\left\{(1-\alpha)C_{\theta(2)}(\theta) + 2\alpha C_{\theta(1)}(\theta)\right\}\frac{d\theta}{dt} \\ & + \left[-R\ln\left(\frac{4\alpha^2}{1-\alpha^2}p\right) + \left\{C'_{p(2)} - 2C'_{p(1)}\right\}\ln T_o/T\right. \\ & \left. + \left\{C_{\theta(2)} - 2C_{\theta(1)}\right\}\ln T_o/\theta + \Delta S^o\right]\frac{d\alpha}{dt} \quad . \end{aligned} \tag{43}$$

Treating the time rate of enthalpy change in a similar manner:

$$\begin{aligned}\frac{dH}{dt} = {} & \left(\frac{\partial H}{\partial p}\right)_{T,\theta,\alpha}\frac{dp}{dt} + \left(\frac{\partial H}{\partial T}\right)_{p,\theta,\alpha}\frac{dT}{dt} + \left(\frac{\partial H}{\partial \theta}\right)_{p,T,\alpha}\frac{d\theta}{dt} \\ & + \left(\frac{\partial H}{\partial \alpha}\right)_{p,T,\theta}\frac{d\alpha}{dt} = -\frac{M}{2}\frac{du^2}{dt} \quad . \end{aligned} \tag{49}$$

For a mixture of <u>ideal</u> gases and with α constant, $\left(\frac{\partial H}{\partial p}\right)_{T,\theta,\alpha} = 0$, and substituting the appropriate values for the other coefficients gives

$$\frac{dH}{dt} = \left\{(1-\alpha)C'_{p(2)}(T) + 2\alpha C'_{p(1)}(T)\right\}\frac{dT}{dt} + \left\{(1-\alpha)C_{\theta(2)}(\theta) + 2\alpha C_{\theta(1)}(\theta)\right\}\frac{d\theta}{dt} + \left[+\Delta H^\circ + \left\{C'_{p(2)} - 2C'_{p(1)}\right\}(T_o - T) + \left\{C_{\theta(2)} - 2C_{\theta(1)}\right\}(T_o - \theta)\right]\frac{d\alpha}{dt}$$

$$= -\frac{M}{2}\frac{du^2}{dt} . \qquad (50)$$

Using (50) to eliminate the derivatives of u^2 and T from (43), yields the important relation

$$\frac{dS}{dt} = \left\{(1-\alpha)C_{\theta(2)}(\theta) + 2\alpha C_{\theta(1)}(\theta)\right\}\left(\frac{1}{\theta} - \frac{1}{T}\right)\frac{d\theta}{dt} - \frac{1}{T}\left[+\Delta H^\circ + \left\{C'_{p(2)} - 2C'_{p(1)}\right\}(T_o - T) + \left\{C_{\theta(2)} - 2C_{\theta(1)}\right\}(T_o - \theta)\right]\frac{d\alpha}{dt} + \left[-R \ln\left(\frac{4\alpha^2}{1-\alpha^2}\, p\right) + \left\{C'_{p(2)} - 2C'_{p(1)}\right\}\ln T_o/T + \left\{C_{\theta(2)} - 2C_{\theta(1)}\right\}\ln T_o/\theta + \Delta S^\circ\right]\frac{d\alpha}{dt} . \qquad (51)$$

This equation corresponds to equation (15) for a nonreacting gas. Comparison of the two indicates the added complexity which arises from the need to specify an additional variable, in this case, case α, as a measure of the chemical disequilibrium. The parallel with this earlier work may be continued if one sets $du^2/dt = 0$ in (50) and inte-

grates the resulting differential equation, using as a boundary condition $T = \theta = T_3$, $\alpha = \alpha_3$. This can be readily performed in this case only if the specific heats are assumed constant, and the coefficient of $\frac{d\alpha}{dt}$ is assumed to have a constant value of ΔH° to a first approximation; then one gets

$$\left\{(1-\alpha)C'_{p(2)}(T) + 2\alpha C'_{p(1)}(T)\right\} T + \left\{(1-\alpha)C_{\theta(2)}(\theta) + 2\alpha C_{\theta(1)}(\theta)\right\} \theta + \Delta H^\circ \alpha = \left\{(1-\alpha_3)C'_{p(2)}(T_3) + 2\alpha_3 C'_{p(1)}(T_3)\right\} T_3 + \left\{(1-\alpha_3)C_{\theta(2)}(T_3) + 2\alpha_3 C_{\theta(1)}(T_3)\right\} T_3 + \Delta H^\circ \alpha_3 .$$

Now by analogy, one uses this equation to substitute for T in (51) giving

$$\frac{dS}{dt} = \left\{(1-\alpha)C_{\theta(2)}(\theta) + 2\alpha C_{\theta(1)}(\theta)\right\} \left\{\frac{1}{\theta} - \frac{1}{T(\theta,\alpha)}\right\} \frac{d\theta}{dt} - \frac{1}{T(\theta,\alpha)} \left[+ \Delta H^\circ + \left\{C'_{p(2)} - 2C'_{p(1)}\right\} (T_o - T(\theta,\alpha)) + \left\{C_{\theta(2)} - 2C_{\theta(1)}\right\} (T_o - \theta)\right] \frac{d\alpha}{dt} + \left[-R \ln \left(\frac{4\alpha^2}{1-\alpha^2} p\right) + \left\{C'_{p(2)} - 2C'_{p(1)}\right\} \ln (T_o/T(\theta,\alpha)) + \left\{C_{\theta(2)} - 2C_{\theta(1)}\right\} \ln T_o/\theta + \Delta S^\circ\right] \frac{d\alpha}{dt} ,$$

where $T(\theta,\alpha)$ is given by

$$T(\theta,\alpha) = - \frac{\left\{(1-\alpha)C_{\theta(2)}(\theta) + 2\alpha C_{\theta(1)}(\theta)\right\}}{\left\{(1-\alpha)C'_{p(2)}(T) + 2\alpha C'_{p(1)}(T)\right\}} \theta$$

$$- \frac{\Delta H^\circ}{\{(1-\alpha)C'_{p(2)}(T) + 2\alpha C'_{p(1)}(T)\}}\,\alpha$$

$$+ \frac{\{(1-\alpha_3)C'_{p(2)}(T_3) + 2\alpha_3 C'_{p(1)}(T_3)\}}{\{(1-\alpha)C'_{p(2)}(T) + 2\alpha C'_{p(1)}(T)\}}\,T_3$$

$$+ \frac{\{(1-\alpha_3)C_{\theta(2)}(T_3) + 2\alpha_3 C_{\theta(1)}(T_3)\}}{\{(1-\alpha)C'_{p(2)}(T) + 2\alpha C'_{p(1)}(T)\}}\,T_3$$

$$+ \frac{\Delta H^\circ}{\{(1-\alpha)C'_{p(2)}(T) + 2\alpha C'_{p(1)}(T)\}}\,\alpha_3 \,.$$

Unfortunately this substitution leaves θ, α and their differentials inconveniently scrambled so that the next step in the earlier procedure of integrating between limits is not feasible until θ and α have been expressed as functions of the time. To obtain $\theta(t)$ and $\alpha(t)$ one must consider the detailed kinetics of the process. Then substitution of (51) into

$$\Delta S_{03} = \Delta S_{13} = \int_{t_0}^{\infty} \left(\frac{dS}{dt}\right) dt \,, \qquad (52)$$

and integration over the compression path gives the entropy gain in terms of the kinetic parameters. Or, reversing this procedure, experimentally determined values of the entropy gain could be used to deduce values of the kinetic parameters.

c. Consideration of the Kinetic Details

In order to carry out the integration indicated in (52) one needs the time dependence of p, T, θ, and α. To determine these time dependent functions one needs four independent differential equations of which two are provided by the hydrodynamic condition (47) and the enthalpy condition (50). An equation identical to the vibrational relaxation equation (20) of the previous section might be assumed to hold here also. A fourth equation may be derived from a consideration of the kinetics of the reaction. If one writes simply

$$A_2 \underset{k_d}{\overset{k_a}{\rightleftharpoons}} 2A \quad , \qquad \text{then}$$

$$\left(\frac{d\alpha}{dt}\right)_{\text{reaction}} = \frac{M}{\rho}\left(\frac{dn}{dt}\right)_{\text{reaction}}$$

$$\frac{1}{1+\alpha}\left(\frac{d\alpha}{dt}\right)_r = \frac{RT}{p}\left(\frac{dn}{dt}\right)_r = \frac{RT}{p}\left[k_d n_{A_2} - k_a n_A^2\right]$$

$$= \frac{RT}{p}\left[\frac{k_a}{K_{eq}}(1-\alpha)\frac{\rho}{M} - k_a\left(2\alpha\frac{\rho}{M}\right)^2\right]$$

$$= k_a\left[\frac{1}{K_{eq}}\left(\frac{1-\alpha}{1+\alpha}\right) - \frac{p}{RT}\left(\frac{2\alpha}{1+\alpha}\right)^2\right] .$$

The boundary conditions for solution are clearly:

at t_o: $\alpha = \alpha_1$ $T = T_1$ $\theta = T_1$ $p = p_1$

$t \to \infty$: $\alpha = \alpha_3$ $T = T_3$ $\theta = T_3$ $p = p_2$.

Conceptually this represents a complete solution to the problem since the four independent differential equations plus boundary conditions specify a solution. Bauer[63] has

outlined an iterative procedure by which in principle one may compute p, T, θ and α as functions of the time in terms of the parameters ρ_o, T_o, p_1, the two rate constants, and the heat of activation for dissociation. Evaluation of (52) for ranges of values in these parameters, and comparison of the calculated results with experimentally determined values would enable one to determine the parameters.

While in principle such an iterative procedure may be utilized, in actual practice this method would be difficult to carry out and there would also be the question of finding the most rapidly converging procedure.

d. Introduction of Relaxation Times

An alternate method of approach follows from the extension of the concept of a "relaxation time" to chemical equilibration. One then considers only the over-all rate and glosses over details of the mechanism. It is possible to apply this simplifying concept because one is dealing with a system which is displaced only slightly from equilibrium.

A number of investigators have discussed the general problem of the return of a system to equilibrium. Manes,

Hofer, and Weiler[65a] have shown that in general for reversible reactions close to equilibrium the net over-all reaction rate is proportional to ΔX, where X is any one of the thermodynamic functions. That the approach to equilibrium is first order, irrespective of the type of rate laws which govern the opposing reactions, has previously been pointed out by Damköhler.[59] Gilkerson, Jones, and Gallop[69] have shown that the conclusions of Manes et al. may also be arrived at as a consequence of the theory of absolute reaction rates.

Bauer pointed out that the criterion of "small displacements from equilibrium" appears to be a necessary but not a sufficient condition for the conclusions reached by Manes. Clearly for a perturbation no matter how small, which involves a metastable intermediate, the rate of return to equilibrium would not be proportional to the displacement from equilibrium, as measured by the difference in free energy. Certainly a single relaxation time would not suffice to characterize the path followed on equilibration for such a system. Bauer suggested that a sufficient condition would be either that (a) one consider only old systems - i.e., systems in which the perturbation occurred sufficiently long ago so that the equilibration rate has

settled down to its final decay rate, or (b) the perturbation must be induced in that part of the system which is associated with a process having the longest time constant.

In the discussion which follows we shall therefore only postulate the applicability of a first-order decay law to the equilibration process for adjacent steps in a simplified mechanism. Since the enthalpy input is continuous rather than instantaneous the mathematical analysis is somewhat cumbersome and is dealt with in detail in Appendix I. For a perturbation, $h(t)$, the departure from equilibrium, $\eta(t)$, is given by

$$\eta(t) = e^{-t/\tau} r \int_0^t \frac{\partial h(t^*)}{\partial t^*} e^{t^*/\tau} dt^* , \qquad (53)$$

where $h(t) = 0$ for $t < 0$, and r is the ratio of "departure" to "perturbation" which has been assumed to be additive and linear.

In the impact tube experiment the perturbation consists of conversion of energy of mass flow into enthalpy of the gas, and following equation (50)

$$\frac{\partial h(t)}{\partial t} = - \frac{M}{2} \frac{du^2}{dt} . \qquad (54)$$

Substitution of (54) into (53) yields

$$\eta(t) = \frac{M}{2} e^{-t/\tau} r \int_t^0 \frac{du^2}{dt^*} e^{t^*/\tau} dt^* . \qquad (55)$$

This is the generalized derivation of Kantrowitz's equation (11) or Griffith's equation (28).

At this point a comparison between the impact tube experiments and shock tube experiments (see Section I, Parts B.b. and C.c.) is easily drawn. The shock tube experiments are clearly one limit of the above description; that is, in that case h(t) is a step function, and corresponds to the instantaneous compression limit, h°, with

$$h^{\circ} = \frac{M}{2} u_1^2 \quad . \tag{56}$$

The effect of approaching such a limit is illustrated by the histograms of figure 7. For a given τ this limit may be approached by going to larger u, or smaller d and thus decreasing the time over which the enthalpy injection occurs. Or, for a fixed value of d/u_1, one may consider systems having increasing τ in which case in the limit the enthalpy injection occurs over times infinitesimal compared to τ. If we define τ_o, the characteristic compression time for the experiment, as

$$\tau_o \equiv d/u_1 \quad , \tag{57}$$

then the impact tube experiment approaches the shock tube experiment as $\tau_o/\tau \longrightarrow 0$.

It is also clear that (55) is simplified considerably in this limit, but at the same time this analysis points to the obvious restriction of shock tube experiments to <u>instantaneous</u> perturbations, which must be at least as <u>strong</u> as the weakest shock which can be accurately measured. In turn, this means that the departures from equilibrium

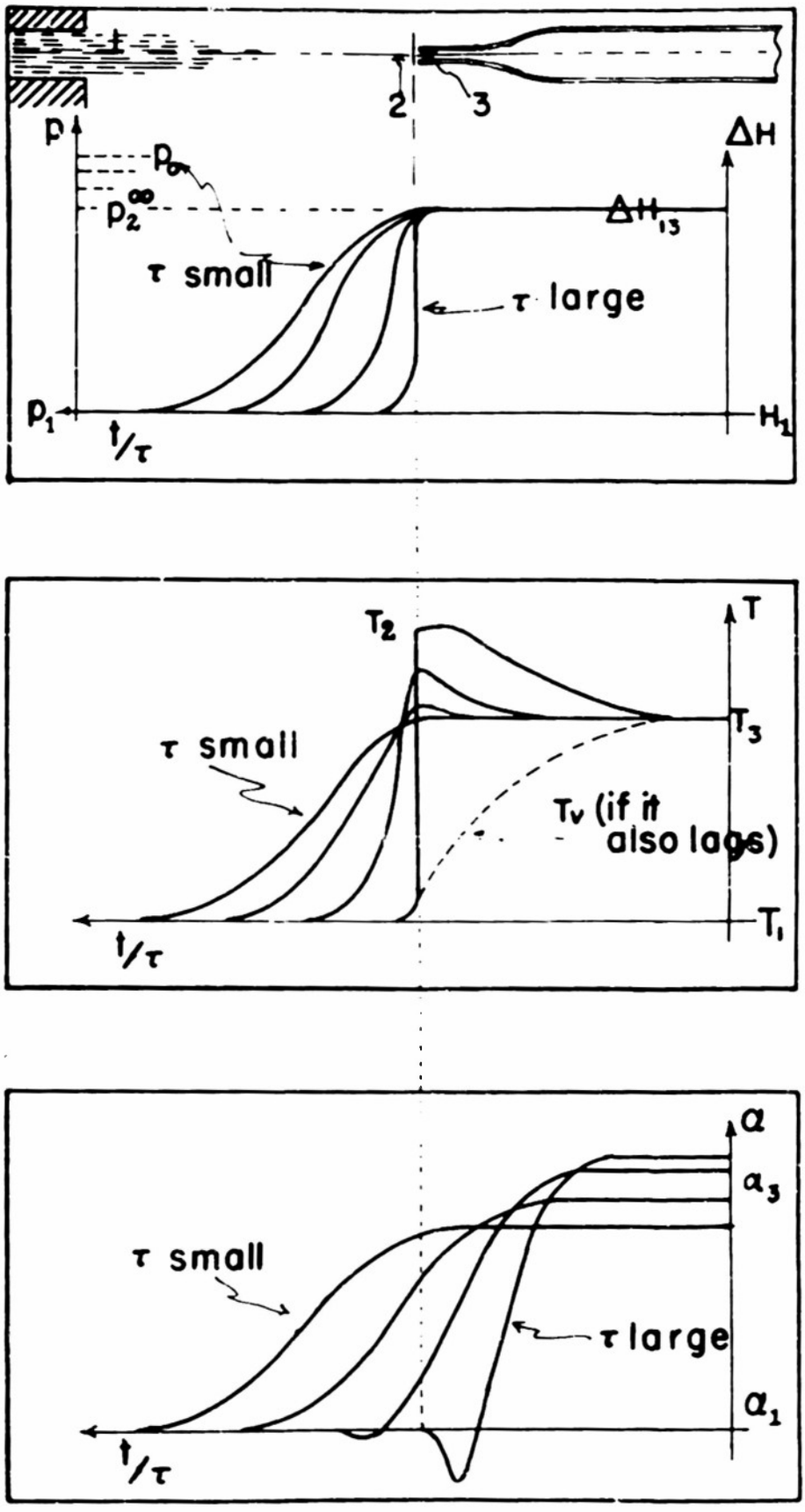

FIGURE 7

Histograms for (d/u_1) specified; α lagging

for the shock tube experiment will be large compared to those encountered in the ordinary range of the impact tube experiment where equilibration proceeds apace with perturbation. For the impact tube experiment the adjustment of u also permits considerable variation in the magnitude of the total entropy injection.

One must now formulate expressions for the departures from equilibrium in terms of the time and kinetic parameters describing the rate of vibrational energy and reaction equilibration.

Define the following measures of departure from equilibrium:

$\eta_T \equiv$ excess energy in non-lagging modes over final equilibrium value

$\eta_\epsilon \equiv$ excess energy in lagging (vibrational) modes over final equilibrium value

$\eta_\alpha \equiv$ excess energy in reaction mode over final equilibrium value.

It is clear that since at final equilibrium $T = T_3$, $\theta = T_3$, and $\alpha = \alpha_3$ one may write:

$$\begin{aligned} \eta_1 &= \bar{C}_p' \,(T-T_3) \\ \eta_\theta &= \bar{C}_\theta \,(\theta-T_3) \\ \eta_\alpha &= \Delta H^\circ \,(\alpha-\alpha_3) \,. \end{aligned} \tag{58}$$

The specific heat terms used here are defined as

$$\begin{aligned} \bar{C}_p' &\equiv \left\{(1-\alpha)C_{p(2)}' + 2\alpha C_{p(1)}'\right\} \\ \bar{C}_\theta &\equiv \left\{(1-\alpha)C_{\theta(2)} + 2\alpha C_{\theta(1)}\right\} \,. \end{aligned} \tag{59}$$

These are in general functions of both α and T, while ΔH° is a function only of T.

Let us now consider the equilibration process as taking place in two steps. That is, the energy of mass kinetic motion which is injected into the gas at the face of the impact tube will be pictured as going first into translation, from which it flows into the vibrational modes and then into the chemical degree of freedom. Diagrammatically

$$\left(\begin{matrix}\text{Translational} + \\ \text{Rotational Energy}\end{matrix}\right) \underset{k_1'}{\overset{k_1}{\rightleftharpoons}} \left(\begin{matrix}\text{Vibrational} \\ \text{Energy}\end{matrix}\right) \underset{k_2'}{\overset{k_2}{\rightleftharpoons}} \left(\begin{matrix}\text{Chemical} \\ \text{Energy}\end{matrix}\right) .$$

This picture is further clarified by reference to figure 8. Here T_1 is an intermediate temperature corresponding to the maximum temperature which would be reached by the vibrational modes if the chemical reaction lagged indefinitely. From the above it follows that

$$\begin{aligned}
\frac{d\eta_T}{dt} &= -k_1 \eta_T + k_1' \eta_\theta \\
\frac{d\eta_\alpha}{dt} &= -k_2' \eta_\alpha + k_2 \eta_\theta \qquad (60) \\
\frac{d\eta_\theta}{dt} &= -k_2 \eta_\theta + k_2' \eta_\alpha - k_1' \eta_\theta + k_1 \eta_T .
\end{aligned}$$

These three simultaneous differential equations may be arranged in the following pattern:

$$\begin{aligned}
\left(\frac{d}{dt} + k_1\right)\eta_T + (-k_1')\eta_\theta + 0 &= 0 \\
(-k_1)\eta_T + \left(\frac{d}{dt} + k_2 + k_1'\right)\eta_\theta + (-k_2)\eta_\alpha &= 0 \qquad (61) \\
0 + (-k_2)\eta_\theta + \left(\frac{d}{dt} + k_2'\right)\eta_\alpha &= 0 .
\end{aligned}$$

Figure 8

Relaxation Curves following an Instantaneous Compression

Case of $\tau_1 < \tau_2$

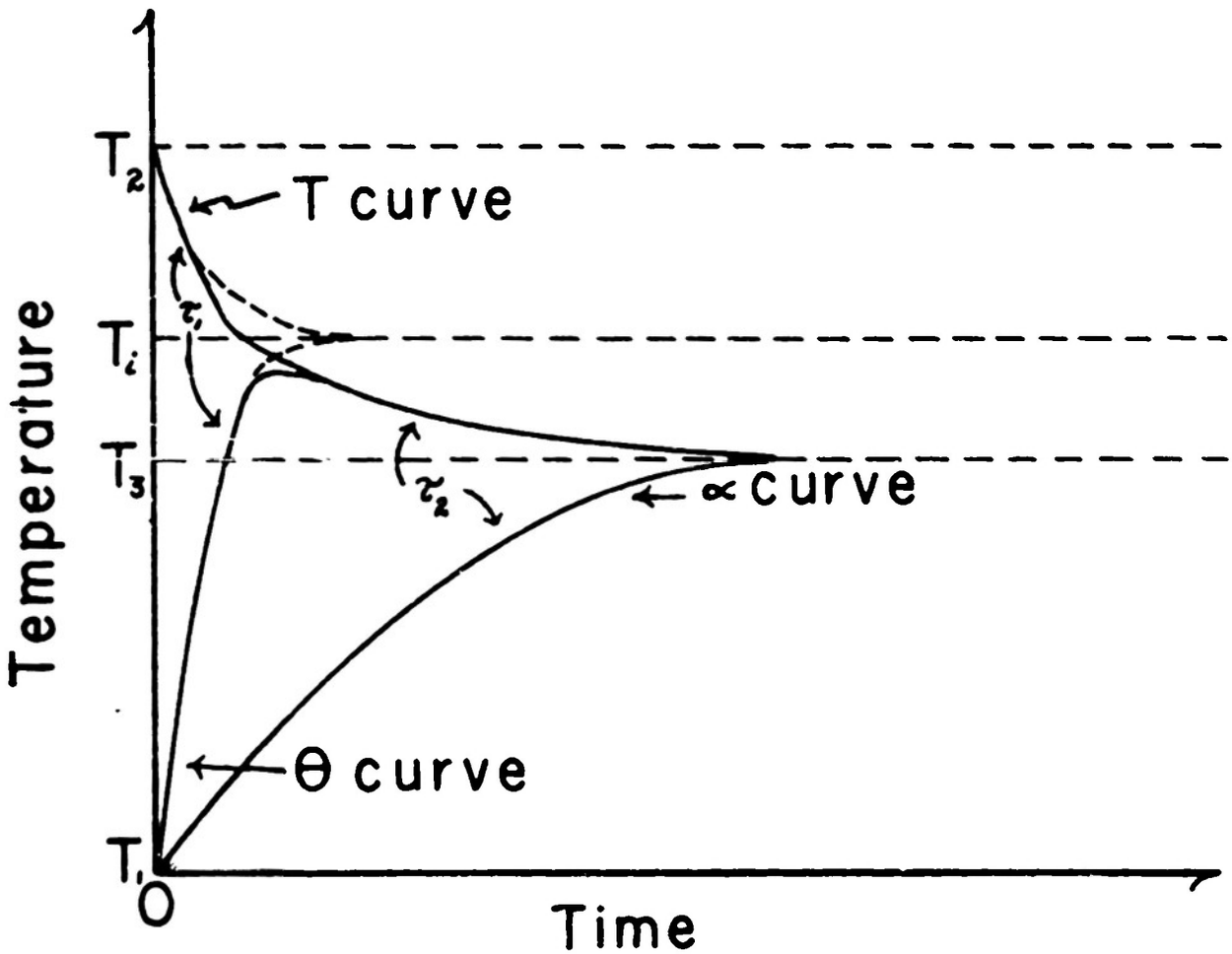

Now if one introduces trial solutions of the form

$$\eta_i(t) = \sum_{j=1}^{3} A_{ij}\, e^{-p_j t}, \quad i = T,\theta,\alpha \quad , \tag{62}$$

and substitues these into (61), then the condition that such solutions exist is

$$\begin{vmatrix} k_1-p & -k_1' & 0 \\ -k_1 & k_2+k_1'-p & -k_2 \\ 0 & -k_2 & k_2'-p \end{vmatrix} = 0 \quad , \tag{63}$$

the roots of which are the p_j's in (62). This means that for a system of the type being discussed there are three effective relaxation times: $1/p_1$, $1/p_2$, $1/p_3$.

At this point suppose we simplify the kinetic assumption (60) by writing

$$\frac{d\eta_i}{dt} = -\eta_i/\tau_i \quad . \tag{64}$$

This clearly implies that for each i only one of the A_{ij}'s of equation (62) has an appreciable magnitude depending upon the form of the initial perturbation. Generally, this is not valid; in our case, due to the different natures of the two equilibration steps, it is not a poor approximation. $\eta_i(t)$ is given as a result of the folding operation by equation (55), and for an instantaneous compression, h° is given by (56); or, its equivalent

$$h^\circ = \bar{c}_p'(T_2-T_1) \quad . \tag{65}$$

The instantaneous disequilibrations produced by such an instantaneous compression are

$$\eta_T^\circ = \bar{C}_p'(T_2-T_3) \qquad \eta_\theta^\circ = \bar{C}_\theta(T_1-T_3) \qquad \eta_\alpha^\circ = \Delta H^\circ(\alpha_1-\alpha_3). \quad (66)$$

Hence on dividing, one gets for the ratio r,

$$r_T = \frac{T_2-T_3}{T_2-T_1} \qquad r_\theta = \frac{T_1-T_3}{T_2-T_1}\frac{\bar{C}_\theta}{\bar{C}_p'} \qquad r_\alpha = \frac{\alpha_1-\alpha_3}{T_2-T_1}\frac{\Delta H^\circ}{\bar{C}_p'} . \quad (67)$$

If one now defines the following dimensionless variables:

$$t' \equiv t/\frac{d}{u_1} \quad , \quad \tau_i' \equiv \tau_i/\frac{d}{u_1} \quad , \quad u' \equiv u/u_1, \quad \eta_i'(t) \equiv \eta_i(t)/\eta_i^\circ , \quad (68)$$

then (55) may be rewritten as

$$\eta_i'(t) = \frac{M}{2}\frac{r_i}{\eta_i^\circ} u_1^2 \, e^{-t'/\tau_i'} \int_t^\circ \frac{du'^2}{dt'} e^{-t'/\tau_i'} \, dt' . \quad (69)$$

Note that the integral depends only on τ_i', and on the <u>shape</u> (not the size) of the impact tube.

These formulas may now be applied to the calculation of ΔS_{13}. Equation (51) may be approximated to first order as

$$\frac{dS}{dt} = \frac{\bar{C}_\theta}{\bar{T}^2}(\theta-T)\frac{d\theta}{dt} + \frac{\Delta H^\circ}{\bar{T}^2}(T-T_o)\frac{d\alpha}{dt} \quad (70)$$

since $\left|\frac{T_o-T}{T_o}\right| \ll 1$, $\left|\frac{T_o-\theta}{T_o}\right| \ll 1$, and $\left|\frac{\alpha_o-\alpha}{\alpha_o}\right| \ll 1$. That is, (70) follows from (51) by neglecting squares and higher powers of the above terms in the expansion. $\bar{T}$ represents an average temperature and may be taken as T_o to this same accuracy.

Combining (58) with (64) yields

$$(T-T_o) = \eta_T/\bar{C}_p' \qquad (T-\theta) = \frac{\eta_T}{\bar{C}_p'} - \frac{\eta_\theta}{\bar{C}_\theta}$$

$$\frac{d\theta}{dt} = \frac{1}{\bar{C}_\theta}\frac{d\eta_\theta}{dt} = -\frac{1}{\bar{C}_\theta}\frac{\eta_\theta}{\tau_\theta} \tag{71}$$

$$\frac{d\alpha}{dt} = \frac{1}{\Delta H^\circ}\frac{d\eta_\alpha}{dt} = -\frac{1}{\Delta H^\circ}\frac{\eta_\alpha}{\tau_\alpha} \quad .$$

Substitution of these equations into (70) and then into (52), yields

$$\Delta S_{o3} = \oint_{t_o}^{\infty} -\frac{1}{\bar{T}^2}\left\{\frac{\eta_T\,\eta_\theta}{\bar{C}_p'\,\tau_\theta} - \frac{\eta_\theta^2}{\bar{C}_\theta\,\tau_\theta} + \frac{\eta_T}{\bar{C}_p'}\frac{\eta_\alpha}{\tau_\alpha}\right\} dt \quad . \tag{72}$$

With the aid of this (68) reduces to dimensionless variables:

$$\Delta S_{o3} = -\frac{d}{u_1}\frac{1}{\bar{T}^2}\frac{(T_2-T_3)\bar{C}_\theta(T_1-T_3)}{\tau_e}\int_{t_o}^{\infty} \eta_T'\,\eta_\theta'\,dt'$$

$$+\frac{d}{u_1}\frac{1}{\bar{T}^2}\frac{\bar{C}_\theta(T_1-T_3)^2}{\tau_\theta}\int_{t_o}^{\infty} \eta_\theta'^2\,dt'$$

$$-\frac{d}{u_1}\frac{1}{\bar{T}^2}\frac{(T_2-T_3)\Delta H^\circ(\alpha_1-\alpha_2)}{\tau_\alpha}\int_{t_o}^{\infty} \eta_T'\,\eta_\alpha'\,dt' \quad . \tag{73}$$

This solves the problem of computing ΔS_{o3} as a function of the kinetic parameters, since (69) may be used to evaluate $\eta_i'(t)$ for a square-ended impact tube (figure 6), and these $\eta_i'(t)$ may then be inserted into (73) to compute ΔS_{o3}.

The complexity of the calculations is reduced considerably if one assumes that $\tau'_T = \tau'_\theta = \tau'_\alpha = \tau'$. This implies that $\tau_T = \tau_\theta = \tau_\alpha = \tau$, or that, by virtue of (64), the ratio of the rates of approach to zero of two $\eta_i(t)$'s is proportional to the ratio of their displacements; i.e.,

$$\frac{d\eta_i(t)/dt}{d\eta_j(t)/dt} = \eta_i(t)/\eta_j(t) \quad . \tag{74}$$

This is to all appearances a reasonable assumption to use as a first approximation. (Note that this assumption also removes the restriction imposed by (64), which implied a restriction on the relative magnitudes of the A_{ij} of (62), since the terms add for this less general case.) Reference to (69) and the values of the constants therein as given by (66) and (67) shows that this assumption also requires that

$$\eta'_T(t) = \eta'_\theta(t) = \eta'_\alpha(t) = \eta'(t) \quad . \tag{75}$$

This clearly follows from (74) on substitution of the dimensionless forms. Hence, the consequence of assuming equal τ's is that (73) may be rewritten as:

$$\Delta S_{03} = \frac{1}{\tau'} \frac{1}{\bar{T}^2} \left[\bar{C}_\theta (T_3 - T_1)(T_2 - T_1) - \Delta H^\circ (T_2 - T_3)(\alpha_1 - \alpha_3) \right] \times \int_{t_o}^{\infty} \eta'(t')^2 \, dt' \quad . \tag{76}$$

An interesting result may be obtained by going back and computing $\Delta S_{03})_{i.c.}$ under the same degree of approximation. For the instantaneous compression case the initial magni-

tudes of disequilibrium are given by (66), and for $\tau_T = \tau_\theta = \tau_\alpha = \tau$ one gets for their time dependence

$$\eta_T^\circ(t) = \bar{C}_p'(T_2-T_3)\, e^{-t/\tau}$$

$$\eta_\theta^\circ(t) = \bar{C}_\theta(T_1-T_3)\, e^{-t/\tau} \qquad (77)$$

$$\eta_\alpha^\circ(t) = \Delta H^\circ(\alpha_1-\alpha_3)\, e^{-t/\tau}.$$

Substitution of these equations into (72) yields

$$\Delta S_{03})_{i.c.} = \int_0^\infty -\frac{1}{\bar{T}^2}\left\{\frac{\bar{C}_p'(T_2-T_3)\bar{C}_\theta(T_1-T_3)}{\bar{C}_p'} - \frac{\bar{C}_\theta^{\,2}(T_1-T_3)^2}{\bar{C}_\theta} + \frac{\bar{C}_p'(T_2-T_3)\Delta H^\circ(\alpha_1-\alpha_3)}{\bar{C}_p'}\right\}\frac{1}{\tau} e^{-2t/\tau}\, dt,$$

or

$$\Delta S_{03})_{i.c.} = \frac{1}{\bar{T}^2}\left[\bar{C}_\theta(T_3-T_1)(T_2-T_1) - \Delta H^\circ(T_2-T_3)(\alpha_1-\alpha_3)\right]\frac{1}{2}. \qquad (78)$$

Comparison of (78) with (76) now permits one to write

$$\Delta S' = \frac{2}{\tau'}\int_{t_o}^{\infty} \eta'(t')^2\, dt' \quad , \qquad (79)$$

where

$$\Delta S' \equiv \Delta S_{03}/\Delta S_{03})_{i.c.} \quad . \qquad (80)$$

Equation (79) is identical in turn with Griffith's equation (29) or Kantrowitz' equation (16). One sees that $\Delta S'$ depends only on τ' for a given flow pattern. This is

the simplification which follows from the fact that in the impact tube experiment only small departures from equilibrium are introduced.

The method to be used for analyzing the data is now quite clear. Experimentally one determines $(p_o - p_2)$ for a given set of flow conditions. This corresponds to an entropy increase which is to be compared with the instantaneous compression entropy increase computed for the same set of flow conditions. The resulting value of $\Delta S'$ is converted to a value of τ' using equation (79), and from this value and the known ratio d/u, the relaxation time, τ, may be computed.

III. Equipment and Procedure

A. Equipment

The experimental procedures required for the impact tube exceriment are of three types. They involve the preparation in adequate amounts of the pure gases, the setting up of a gas circulation system which maintains the desired non-turbulent flow under conditions such that the temperature, pressure, and velocity of the streaming gas are at known and controllable values, and the construction of an impact tube with attendant pressure sensing device.

Both the carbon dioxide and the nitrogen tetroxide used in these experiments were purchased in tanks as the liquified gases from The Matheson Company.

Adequate drying of the carbon dioxide presented a serious problem. Eventually a high pressure tank was constructed in which the gas to be dried was allowed to come to equilibrium with phosphoric anhydride at a pressure of about 60 atmospheres. The carbon dioxide used in the reported results was Matheson "Bone Dry" grade (purity specified at 99.956%; remainder water). Twelve pounds of this gas were held over three pounds of reagent grade phosphoric anhydride for one month at 60 atmospheres before being used. Due to the pronounced dependence of the relaxation time of carbon dioxide on moisture content, the consistency of our data is good indication of the purity

of the gas used. Of course, there was no way to prevent the gas from picking up minute amounts of impurities during flow, from the tubing, valves, etc.

While the carbon dioxide flowed readily from the tank at room temperature, such was not the case for the nitrogen tetroxide which boils at 21.3°C. and has a heat of vaporization of 99.0 cal./g. at 21.0°C. In order to assure a sufficiently rapid flow of this gas it was necessary to heat the tank. The heater was constructed from three 600w. glow coil elements using for a core a brass tube 5 1/4" inside diameter and 13" long, with asbestos and sand as the insulating materials. The heater could be operated at 600, 900, 1200, and 1800 w. input, and the air temperature between the cylinder and heated jacket was roughly 250°C. during the course of most runs. It was observed that the gas flow increased rapidly when the nitrogen tetroxide reached the vicinity of its critical temperature of 158.2°C. The gas was taken from No. 3 cylinders (each having a capacity of 10 lbs.) and was specified as having a minimum purity of 99% with only 0.01% of water and traces of lower nitrogen oxides. A record was kept as to which cylinder was used for each run, for although each cylinder gave self consistent results there appeared to be a consistent difference between runs made using different cylinders. Even with the above arrangement the highest pressures reported were reached only with

difficulty and the data obtained suffered somewhat from this limitation.

After leaving the tank both gases were passed through an "after-heater". In the case of the carbon dioxide this heater was used to compensate for the cooling due to the Joule-Thomson effect. For the nitrogen tetroxide it was needed to insure complete vaporization. From here the gas passed through tygon tubing to the system past a thermocouple and through a bubbler, the latter serving both to keep the input pressure from greatly exceeding atmospheric and as a simple indicator for adjusting the gas flow. (See figure 9, which also shows the equipment involved in the following discussion.)

To sweep the apparatus free of moisture, for purposes of alignment, and the taking of null readings a tank of nitrogen was also attached to this input. The nitrogen used was Seaford "dry nitrogen" from Airco, specified as 99.99% pure with H_2 as the sole impurity.

The gas then passed through approximately 10 feet of glass tubing before entering the first of two 12L. reservoirs, which were connected through a pressure regulator. When the "after-heater" was adjusted so that the input temperature of the gas was very nearly room temperature the time of holdup in the connecting tubing and reservoirs was sufficient to insure that the gas had come to thermal equilibrium. When working with nitrogen tetroxide care

Figure 9. The Flow System

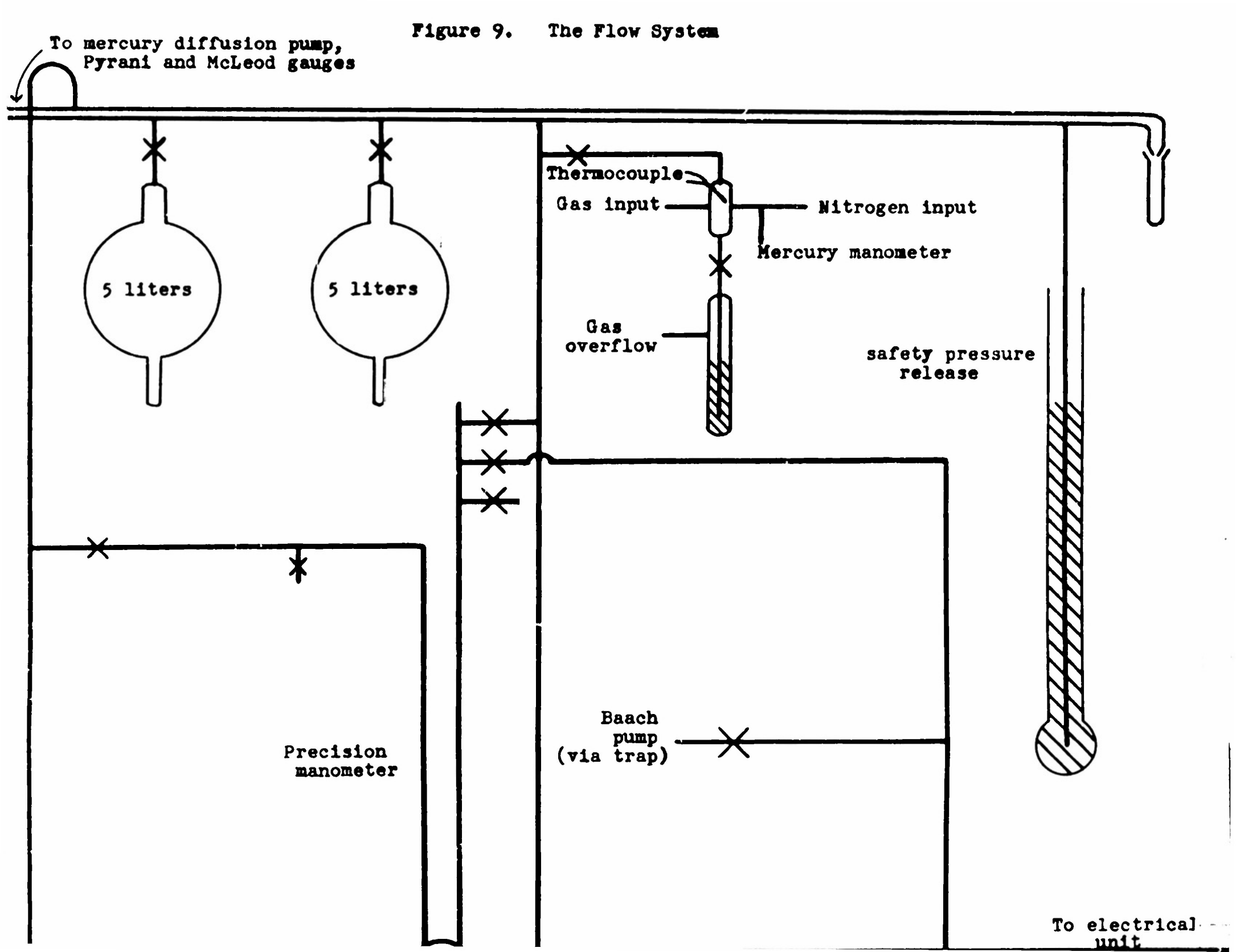

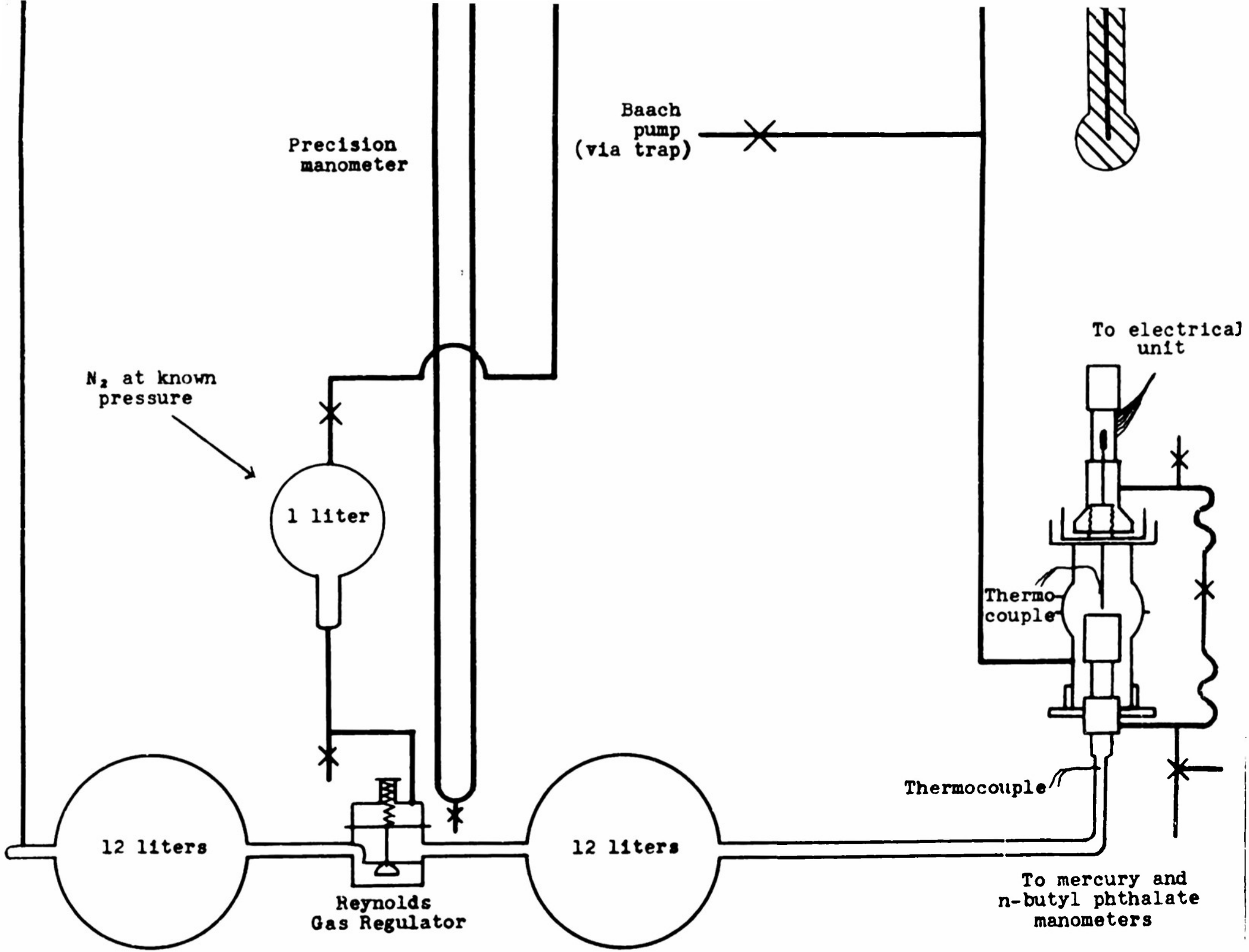
Baach
pump
(via trap)
Precision
manometer
To electrical
unit
N_2 at known
pressure
1 liter
Thermo-
couple
Thermocouple
12 liters
12 liters
Reynolds
Gas Regulator
To mercury and
n-butyl phthalate
manometers

was taken to have the room temperature stabilized at 25°C., or slightly higher, thus insuring no condensation.

The pressure regulator was of the diaphragm valve type, being a Reynolds gas regulator utilized commercially for maintaining constant flame height despite variation in pressure in the gas mains. An arbitrarily variable pressure of a standard reference bulb was substituted for the "atmospheric" side, and hence it was possible to set the regulator so that the pressure in the second 12L. bulb was held constant (to ±0.1 mm. Hg) at any value less than our supply pressure of one atmosphere. A serious difficulty arose because of the corrosion of the diaphragm and valve by the nitrogen tetroxide. Eventually it was found that a diaphragm cut from an 0.010" thick sheet of Visqueen* polymer had the necessary flexibility and was only slowly attacked by oxidizing agents. A portion of the valve was constructed of stainless steel which appreciably reduced leakage due to corrosion.

From the second reservoir bulb the gas passed through a stopcock and then into the impact apparatus proper. This equipment is shown in cross-section in figure 10, with the gas entering at R. In this apparatus the gas flows up the glass tube and over a thermocouple which measures the temperature, T_o, before expansion. In all runs this tempera-

---

* The Visking Corp., Chicago 38, Ill.

Figure 10
The Impact Apparatus

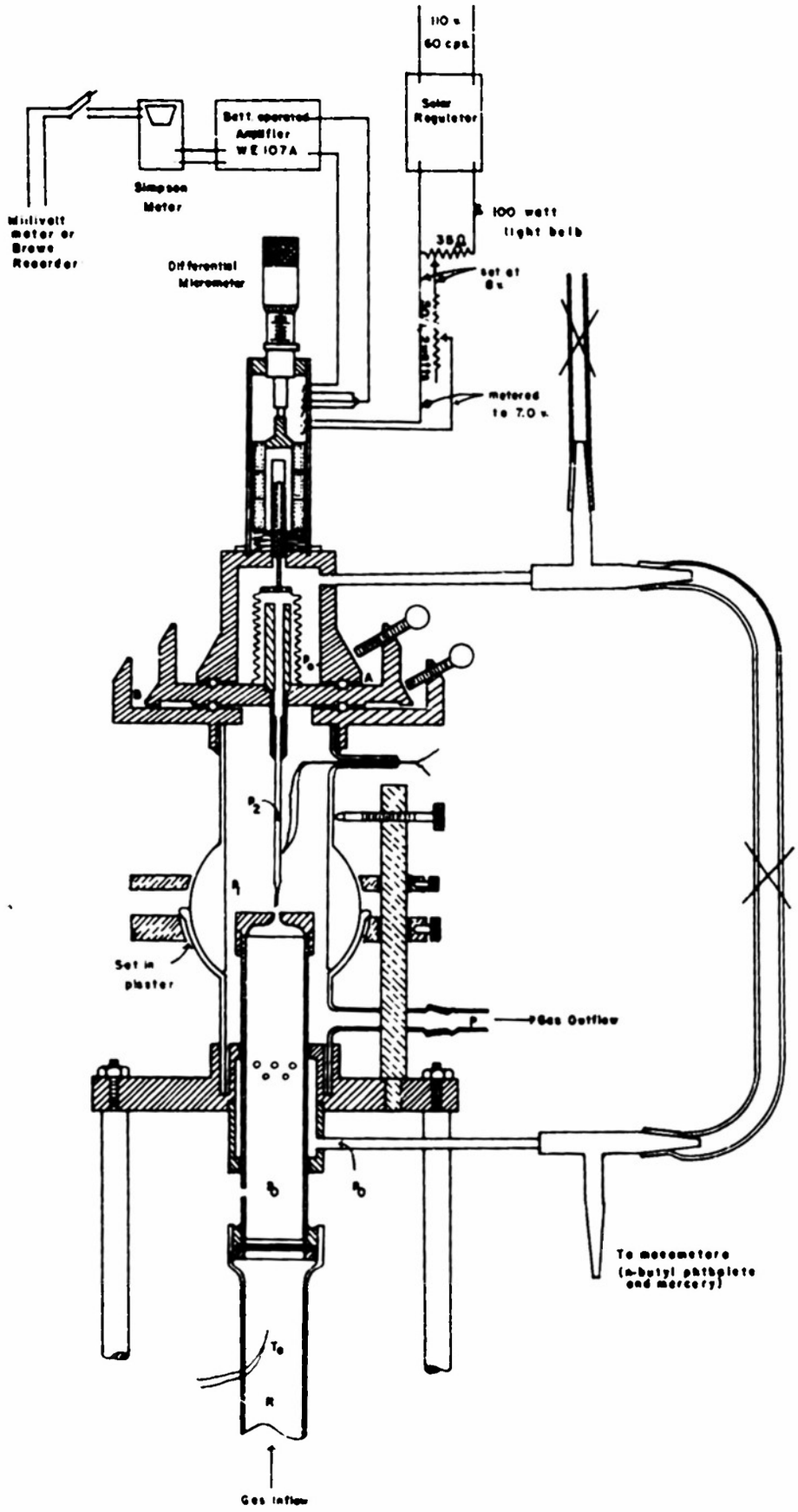

ture was very nearly 25°C. and differed by at most a couple of degrees from room temperature. Comparison of this thermocouple with that in the bubbler gave a measure of the extent of temperature change undergone by the gas in the equipment.

The gas next passed through a 200 mesh monel metal screen sandwiched between two pieces of coarser monel screening. (Initially copper screening was used, but corrosion by the nitrogen tetroxide was quite rapid.) This acted as a field of point sources and led to a smooth laminar flow up the polished stainless steel tube to the nozzle. Part way up this tube small holes connected it to a jacket so that the input pressure could be applied to a manometer which measured the initial pressure, p_o; this pressure could also be applied to the outside of a metal bellows as indicated in the drawing. When steady state conditions were established no gas flowed through these holes and therefore their presence clearly could not effect the flow.

In designing the nozzle through which the gas flows into the expansion chamber it is important to make the time rate of energy change as small as possible so that complete equilibrium is maintained at all times. From the equations of section IIB it is clear that $d\zeta/dt$ is minimized when dT/dt is smallest; that is, when the acceleration occurs with a small rate of temperature drop. For the

work with carbon dioxide a 1/2" long nozzle shaped like those of previous investigators was used. For the work with nitrogen tetroxide a new nozzle was constructed. This was designed following the equations[70]

$$ur^2 = \text{cons't.}$$

$$r^6x = \text{cons't.} \quad ,$$

where r is the radius of the hole and u the flow velocity of the gas at a distance x from the base of the nozzle. The design was based on a length of 1.6" and an orifice diameter of 0.0700" before introducing the boundary layer correction. The outlet velocity was taken to be 17.2 m./sec. and the von Doenhoff boundary-layer displacement thickness was computed using a value of 120×10^{-6} poises for the viscosity and an average density of 1.279×10^{-3} gm./cm.^{3}. These values correspond to optimum conditions for p_o = 0.500 atm., $p_o/p_1 = 1.44$, $T_o = 25°C$. The final nozzle dimensions were:

x	r	x	r
0.01	.0816	0.60	.0415
0.03	.0679	0.30	.0397
0.07	.0590	1.00	.0385
0.10	.0556	1.20	.0376
0.20	.0495	1.40	.0370
0.40	.0442	1.60	.0366

Corrosion of the brass nozzle used with carbon dioxide was found to be quite rapid when nitrogen tetroxide was used, and the nozzle could not be gold plated without running the risk of introducing rough spots in the carefully shaped throat. An attempt to machine the longer nozzle of dimen-

sions noted above out of stainless steel proved frustratingly unsuccessful due to breakage of the reaming tool. It was observed, however, that duraluminum (24ST) withstood the action of the gas for a considerable period. Hence the nozzle was made out of a stainless steel jacket surrounding a duraluminum plug, in which the throat had been machined. With this nozzle no corrosion problems were encountered.

The expansion chamber was pumped on at the point marked "gas outflow" in figure 10 by a two stage hi-vac pump of very large capactiy.* It is necessary that the pump used should be able to maintain a pressure drop of a factor of two across the nozzle when p_o = 1.0 atm. For the nozzle already described this requires a pumping rate of approximately 20 L. (S.T.P.) per minute. A mercury manometer was also attached to the expansion chamber at this point to permit measurement of p_1. It was found that for a fixed p_o any expansion ratio could easily be selected by adjusting a stopcock interposed between the chamber and the pump.

A thermocouple was also mounted in the expansion chamber alongside the region of smooth flow. In later designs this was removed as it served no useful purpose, and always gave essentially the same value as did the input thermocouple.

---

* Manufactured by: International Machine Works, North Bergen, N. J.

The requirements for the impact tube are quite simple, however, considerable practice is required to meet them. They are:

i) The tube must be round and have the center hole concentric with the outer edge.

ii) The ratio of the inside diameter to outside diameter should be close to 0.620 since this is the value for which theoretical calculations are available.[44]

iii) The tip surface must be at right angles to the axis of the tube.

iv) The tube should smoothly widen to its maximum diameter, but this must occur over a short distance so that the gas flow through the tip to reach equilibrium will not be greatly impeded.

The tubes may be constructed from ordinary 4 mm. pyrex tubing by drawing out in two steps. In the first step the tube is drawn down to about 1/4 of its initial diameter and the walls thinned. In the second step the tube is then drawn down to the required outside diameter of from 0.02 to 0.08 cm. Two steps are required to get the proper wall thickness (otherwise only very low i.d./o.d. can ordinarily be obtained). It is quite important that the tube be heated evenly if a circular cross-section is to result. If the glass is twisted while being drawn the symmetry is considerably improved and the resultant tip is more often coaxial with the base of the tube. The tubes may then be broken

off by scratching slightly with a small crystal of carborundum and applying pressure. With considerable luck as well as practice this breaking can be done so as to yield a perpendicular non-chipped surface. More often it is necessary to grind the tip flat and perpendicular to the tube axis on a very fine stone. Washing the tubes with a strong solution of detergent followed by large quantities of distilled water usually proved to be sufficient cleaning. They were then checked and measured under a microscope with a graduated eyepiece reading to ±0.0002 cm. One could easily tell whether the surface was really smooth and the inside and outside surfaces coaxial. Measurements of both diameters were taken at two positions separated by 90 degrees to check for eccentricity. The impact tube was then mounted with black wax in the brass tube projecting from the movable stage A so that it was connected to the inside of the bellows previously mentioned. A small "square" was used to set the impact tube perpendicular to the ground surface at B. The extension of the tube below the ground surface was adjusted so that the tip was between one and two times the nozzle diameter from the nozzle face, as this distance was found by Griffith to give the most consistent results.

The only portion of the equipment remaining to be described is the differential pressure sensing device---that portion of the equipment which measures the difference

between the initial pressure, p_o, and the final pressure, p_2, which exists at the face of the impact tube where the gas has been brought to rest. These two pressures are applied respectively to the outside and inside of a stainless steel bellows. The bellows used had a wall thickness of 0.0085", was 1 1/2" long by 3/4" in diameter, and had 23 convolutions. Its flexibility was such that a pressure differential of one atmosphere produced a change in length of about 0.05". Most of the inside of this bellows was filled with a brass plug so that very little gas need flow through the impact tube to adjust to a given pressure defect. Thus its time constant was minimized. The top of the bellows was closed with a stainless steel plug which carried a stainless steel rod 1 1/2" long with the core of a differential transformer mounted at its tip. This entire unit was enclosed in a brass shell which was connected to the jacket, and thus maintained at the pressure p_o. On the outside of this shell and around the soft iron core the differential transformer* was mounted. As may be seen in figure 10, the central winding of the transformer was powered by a Sola Voltage Regulator (1.04 amp., 115 v. output) which was fed by a Stabline Voltage Regulator. A combination of resistances was chosen so as to load the Sola at near its rated capacity, and to provide 7.0 v. as a safe

---

* Schaevitz Engineering, Camden 11, N. J.
Series S, Type 18L
Sensitivity 0.0008v/.001"/volt in. at 60 CPS

continuous operating input for the differential transformer. Sixty cycle current was utilized in preference to a higher frequency (which gave a higher output) because no oscillator which had sufficiently good amplitude stability was available. The outputs of the two secondary coils of the differential transformer were connected in opposition to a Western Electric 107A battery operated amplifier (gain circa 800) which was shock mounted to reduce troublesome microphonics. The amplifier output, taken from the primary of the output transformer (no load on secondary), was fed into a Simpson meter (model 260). This meter responds when set in the "a.c. volts" position by rectifying the applied voltage and applying the resultant direct current to a suitably calibrated microammeter. By tapping across this microammeter one obtains the input current suitably rectified for use on a recorder, and at the same time the meter serves both as a rough indicator for adjusting the differential transformer to minimum position and as a sensitivity control. As actually used, the level of the rectified voltage was controlled at the Simpson meter and its zero was set by means of a bucking circuit; the net voltage was finally recorded by a Brown high speed instrument (Model No. 153X12V-W6-30, full deflection 10 mv.).

In addition to being very poisonous, nitrogen tetroxide is a highly corrosive gas. Insofar as was possible all equipment subject to its attack was constructed of glass or

stainless steel. Another metal which resists its action quite well is duraluminum (24ST), which has an advantage over stainless steel in being much easier to machine. In several instances gold plated brass was used in our equipment, and this proved resistant to everything except direct exposure to a constant stream of the gas. Stopcocks were lubricated with a halocarbon grease, which resists attack for some time, but this grease has a high viscosity at room temperature. In the case of those ground surfaces where the gas had very little opportunity for direct attack Apeizon grease (L) was found to be satisfactory over long periods. The metal and glass parts were sealed together using black Apeizon wax. In designing the equipment one must be careful that such joints are well protected from direct blasts of nitrogen tetroxide which oxidizes exposed regions to produce a porous crumbly mass. With suitable care in design such joints last quite well, however. Tygon tubing was the only plastic tubing used in these experiments, and while it became more rigid with continued exposure to the gas no layer of corrosion products was noted.

B. Procedure

a. Alignment

There are two alignment steps to be taken before the equipment becomes ready for calibration. The first is adjustment of the differential transformer and its core, and the second is positioning of the impact tube with respect to the flow stream.

As can be seen from figure 10, the position of the brass tube surrounding the transformer core can be varied by using the top ring of three thumbscrews which move the top portion (at A) with respect to the impact tube carrying section. If the core is initially perpendicular to the base plate, and the bellows free from strains so that it moves only axially on compression, this lateral motion permits centering the core so that nowheres does it touch the surrounding brass tube. The core may be adjudged to be moving freely when the calibration curve (see below) is reproducible and shows no hysteresis. Mounted atop the differential transformer carriage is a differential micrometer (not shown in detail) constructed by attaching a left hand threaded section of 42 threads per inch in opposition to a commercial right hand micrometer having 40 threads per inch. With this arrangement the probe is advanced 0.0012 inches for one full turn, and one can easily select one three-hundredth of this. The probe presses down on the differential transformer in opposition

to a spring mounted below; it is used to adjust the core to approximately 2 mv. off null position where the response curve is very nearly linear and the sensitivity highest.

The initial adjustment on the impact tube which determines its distance from the nozzle has already been described. The lower ring of thumbscrews at the top of the impact apparatus (figure 10) permits one to move the tube in the horizontal plane, at B, without disturbing the pressure sensing unit. Lateral transverses showed that a considerable fraction of the nozzle area was free from turbulence since the defect measured with nitrogen was quite small and constant. Beyond this area the pressure in the impact tube changed quite pronouncedly. The angle of attack was adjustable via the lowest ring of thumbscrews shown in that diagram; these work on the ball-joint which has as its center the tip of the impact tube. We found, as had Griffith, that the observed defects were constant as long as the angle of attack was within 5° of zero. Also, it was found possible to construct impact tubes so that their tips were so nearly perpendicular to the axis of the tube that no angular adjustment was needed. Hence, after this was ascertained, the ball-joint section was replaced by a straight glass column with ends ground perpendicular to its axis, and with only a single side tube for outflow. This simpler design was also substantially more resistant to breakage than its more complicated forerunner and removed a potential point of leakage.

b. Calibration and Sensitivity

A pressure differential could be applied across the pressure sensing device by opening the stopcock at the top of the apparatus (figure 10) to the air, closing the stopcock between the bellows' chamber and expansion chamber, and evacuating the rest of the inner chamber slightly. For calibration purposes an n-butyl phthalate open end manometer attached as shown in figure 9 was used to read the pressure difference. The ratio of the density of n-butyl phthalate to that of mercury was found to be as 1:12.80; hence, a pressure difference could easily be read to $\pm 0.02 \times 10^{-3}$ atm. ($\pm$ 2x0.01 cm. of n-butyl phthalate).

A typical calibration curve is shown in figure 11. The points have been numbered in the sequence in which they were taken (nos. 1, 6, and 12 were at zero pressure differential). The stability, reproducility, and absence of hysteresis are indicative of proper core centering and high stability in the electrical circuit. With the Brown recorder set for full scale deflection at 10 mv. it was possible to read to $\pm$ 0.02 mv., and hence a pressure difference could be determined to within the equivalent of $\pm$ 0.04 mv. Reference to the calibration plot indicates that the response was about 3.3 mv./cm. of n-butyl phthalate, hence pressure differentials could be read to a precision of $\sim 1.2 \times 10^{-5}$ atm. In some later runs the sensitivity was increased by about 35% by finer adjustment.

Figure 11

Typical Calibration Plot

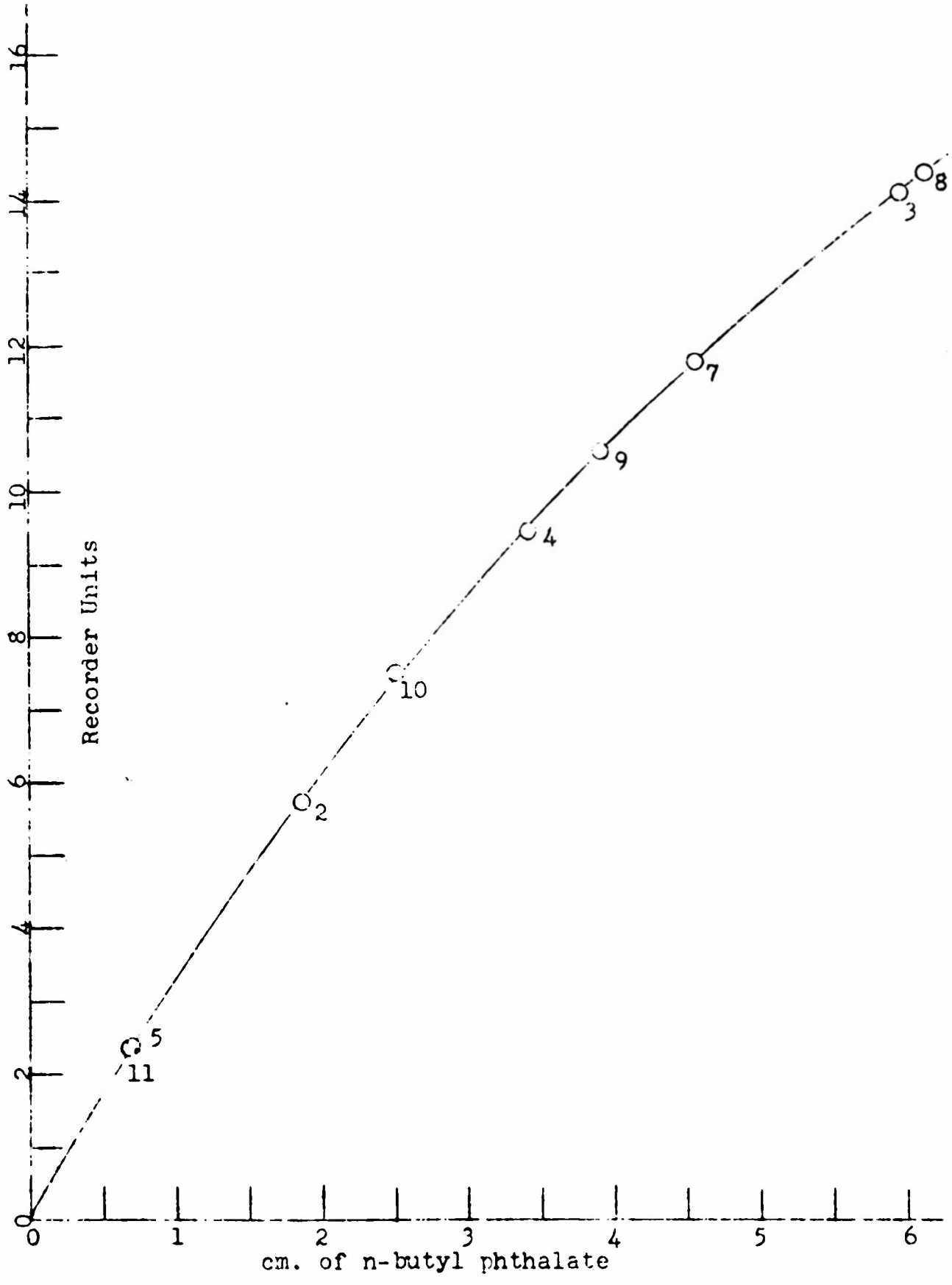

The greatest difficulty in this setup was a gradual wandering of the zero point, which therefore had to be redetermined after every few readings, so that the true zero could be interpolated. Higher quality electrical components would doubtless reduce this difficulty to the point where it would cease to be significant. The response time of the whole pressure sensing device was limited by that of the recorder (2 seconds for full scale deflection).

In view of the observed stability and reproducibility, the sensitivity of this unit could quite easily be increased by using an amplifier with greater gain. Other possibilities are: increasing the cross-section of the bellows, using a longer bellows with more convolutions, using a bellows of more flexible material, using a recorder of greater sensitivity, or using a differential transformer of higher voltage output (step up ratio).

c. Nitrogen Background

In order to check flow conditions one must make a run with a gas whose rotational and vibrational relaxation times are very much smaller than the compression time of the equipment. Nitrogen is such a gas since the vibrational contribution to its specific heat is negligible at room temperature and its rotational specific heat has a relaxation time shorter than 10^{-9} sec. at room temperature and atmospheric pressure.[1b] The results of a typical run with

nitrogen are shown in figure 12. The sharp break at an expansion ratio of about 2.2 is due to the setting in of turbulence and will be discussed more fully in section IV. The smooth curve and low value of the defect compared to that for carbon dioxide indicates a regular background effect which can be corrected for. The fact that the nitrogen defect curve is small and linear below p_o/p_1 = 2.0 and passes through the origin is in line with the fact that ordinary hydrodynamic effects such as misalignment of the impact tube, temperature or pressure inhomogeneities, turbulence, etc. would be expected to produce a total-head defect which varies directly as $(p_o/p_1 - 1)$. This is, of course, not the case for a defect depending on a heat capacity lag.

d. Procedure for Carbon Dioxide Runs

The following stepwise procedure was followed in making all observations on carbon dioxide recorded in section IV.

i) For greater stability the electrical equipment supplying the input to the differential transformer was not turned off between runs. The system was checked for leaks before each set of runs using an auxiliary mercury diffusion pump circuit with McLeod and Pyrani gauges.

ii) The battery powered amplifier, rectifier, bucking circuit, and recorder were turned on about one

Figure 12

Pressure Defect Curves for CO_2 and N_2

at p_o = 0.534 atm., T_o = 300.2°K.

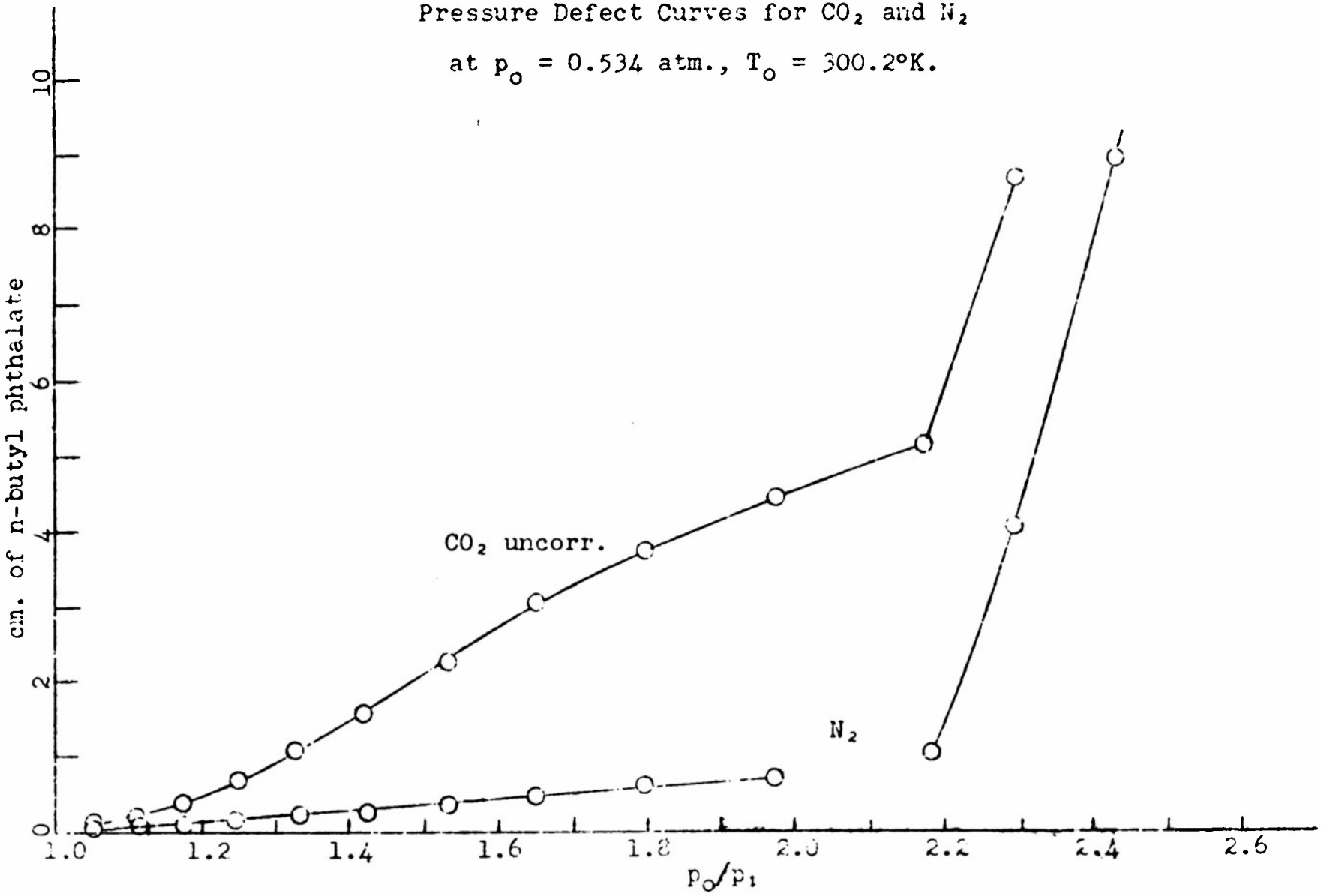

hour before the start of the actual run. The end of their required warm-up period was ascertained by a trace of constant deflection on the recorder. During this period the thermocouple cold junction was filled and the thermocouples checked, the pump serviced and started, the continuously monitored input carefully adjusted to 7.00 v., the position of the transformer with respect to the core adjusted, the barometric reading recorded, p_o control set to approximately the value desired, and the room brought to an even temperature.

iii) A complete calibration curve of recorder displacements versus n-butyl phthalate manometer readings was taken for later use. This curve also indicated by its lack of hysteresis that the core was well centered and served as an extra check on the leak-tightness of the central portion of the equipment.

iv) A background run was made with dry nitrogen over the pressure ratio range, $1.2 \leqslant (p_o/p_1) \leqslant 2.0$, giving the magnitude of the hydrodynamic correction. This also served to check for proper alignment of the impact tube, permitted final adjustment of p_o, and swept the apparatus free of foreign gases.

v) The system was flushed with carbon dioxide at an intermediate pressure ratio until a constant pressure

defect was observed. The after heater was adjusted for proper temperature of the input gas.

vi) Measurements were recorded for the pressure defect of carbon dioxide over the pressure ratio range, $1.2 \leqslant (p_o/p_1) \leqslant 2.0$, starting with the smallest ratios. Thermocouple readings were taken at the bubbler and input stations while the gas was flowing.

At all times the input voltage was monitored to check on its consistency. The recorder readings at zero pressure defect were noted before and after steps iii, iv, and vi. If there were appreciable fluctuations in this null position, or if for any reason a suspicion arose that the apparatus was functioning not quite satisfactorily, operations were suspended, and the run started anew. All of these steps were repeated at each p_o, the runs being spaced by sufficient time so that the batteries would not be adversely affected.

e. Procedure for Nitrogen Tetroxide Runs

The procedure followed here closely paralleled that described above for carbon dioxide. Additional time was required for step v since the tank of compressed gas had first to be brought to a high enough temperature to maintain the desired p_o over the range of expansion ratios. The highest p_o which could be maintained over the whole range of expansion ratios was 0.7 atm., and this only with

a comparatively full tank. After the run it was necessary to remove the heated tank from its heater and cool it with cloths soaked in ice water until evolution slowed before closing the cylinder. The corrosive gas was then swept from the equipment with dry nitrogen.

Due to the heating requirements plus corrosion problems, runs with nitrogen tetroxide proceeded considerably less smoothly than those with carbon dioxide, and therefore, as will be seen, the results showed less consistency. Otherwise the runs followed very closely the same pattern, and the added experience obtained from earlier work helped to mitigate the increased difficulties.

IV. Carbon Dioxide

In this section heat capacity lag measurements taken on carbon dioxide are recorded; their reduction to relaxation times, and a critical interpretation of the results are then presented.

A. The Data

The purity of the gas used and the procedure followed has already been described in section III. A typical calibration plot is shown in figure 11, while figure 12 shows a typical plot of nitrogen and carbon dioxide defects *vs* expansion ratio. The sharp breaks at $(p_o/p_1) \cong 2.2$ correspond to the setting up of shock waves at the nozzle and in front of the impact tube, when the Mach number reaches unity. The decline in slope of the pressure defect curve of carbon dioxide above $(p_o/p_1) = 1.5$ appears to be common to all of the runs, independent of p_o. This has not been satisfactorily accounted for; it may be due to slight imperfections in the throat surface. Points above expansion ratios of 1.5 were not used in the computation of relaxation times.

From a graph of the type shown in figure 12 values of the carbon dioxide defect minus that for nitrogen at selected expansion ratios were obtained. Attempts to secure useful data at $p_o = 0.2$ atm. and below were frustrated by the fact that the nitrogen background correction then be-

comes an appreciable fraction ($\sim 50\%$) of the values observed for carbon dioxide, so that the precision of the data is quite poor. The results of measurements at p_o = 0.967, 0.752, 0.534, and 0.341 atms. are shown in figure 13, where the relative pressure defects are plotted vs the expansion ratios. The impact tube used in all of these runs had an outside diameter of 0.0770 cm., with (I.D./O.D.) = 0.56 and maximum eccentricity < 3%.

It is important to note that within the margins of the experimental accuracy these curves are superposable. As will be discussed later, this is due to the bimolecular nature of the collision process. It may be noted here, however, that such consistent data were not obtained with less pure or slightly moist carbon dioxide. Indeed, one may consider this sort of a check as a sensitive criterion for the purity of the gas. Previous investigators using the impact tube method were restricted to the fixed value p_1 = 1 atm., but could vary p_o, and hence obtained only one such curve. They had no such internal check on either the purity of the gas or the bimolecular nature of the reaction.

Figure 13

Relative Pressure Defect vs Expansion Ratio for CO_2 at $T_0 = 299.7°K$.

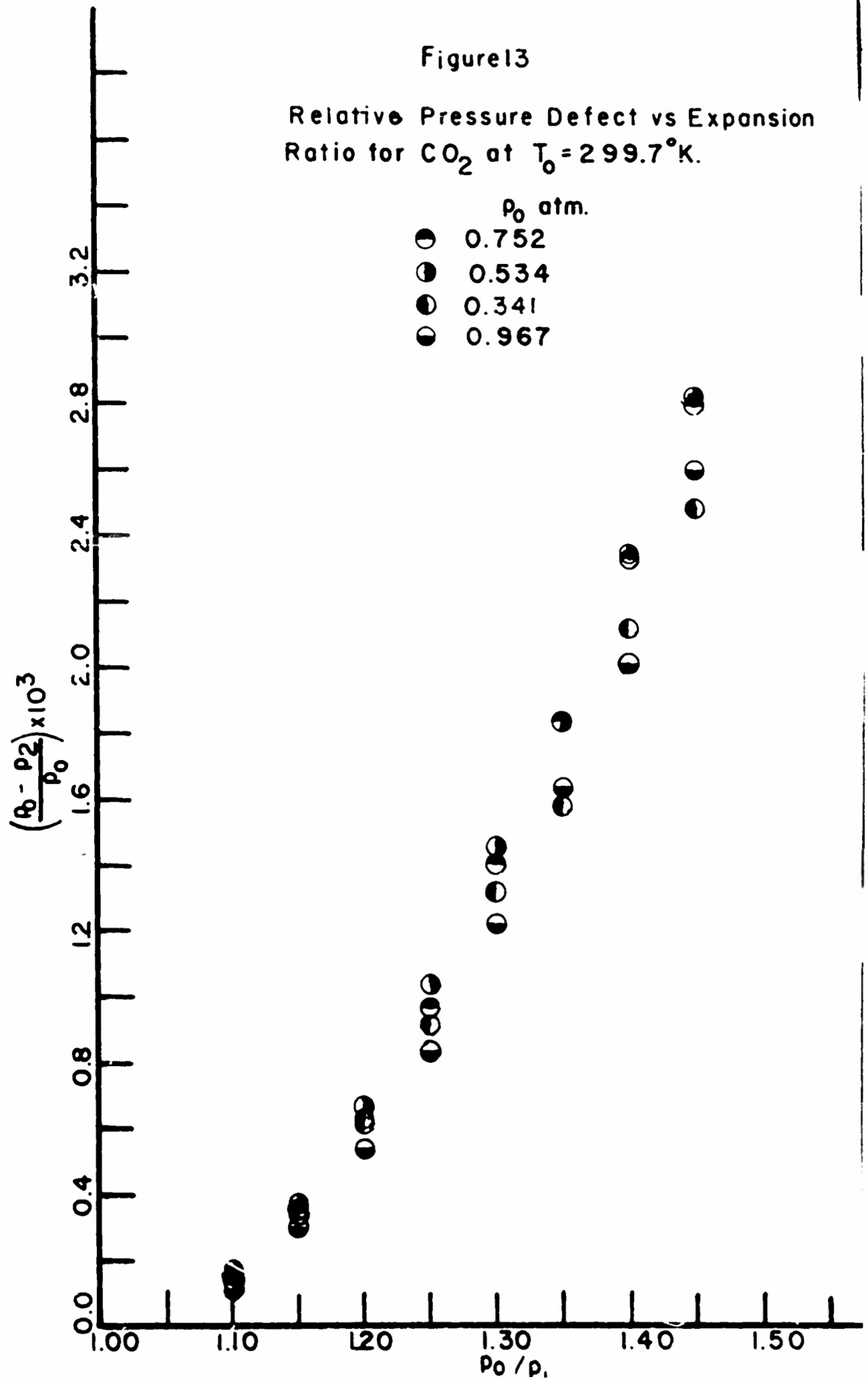

B. Treatment of Data

The impact tube experiment yielded values of the pressure defect for various combinations of p_o, T_o, and p_1. These data have been used to determine the relaxation time following the theory developed in section II. The experimentally determined entropy gain was compared with the entropy gain computed for instantaneous compression and, from this ratio, the ratio of the unknown relaxation time of the gas to the known characteristic compression time of the equipment was determined. A stepwise description of the method of computation follows; table I contains tabulated values of the more significant quantities computed.

1. The relative pressure defects vs expansion ratios were tabulated for each p_o, T_o (columns 1a, 1b, 1c).
2. Using the adiabatic expansion equation (8), T_1 was calculated for each p_o, T_o, and p_1 (column 2a). As a first approximation C_p^{71} was taken at T_o, and henceforth at $\bar{T} = \frac{1}{2}(T_o + T_1)$. Two successive iterations were sufficient to give T_1 to the same accuracy as T_o (columns 2b, 2c).
3. The free flow energy, $\frac{M}{2}u_1^2$, in calories per mole was calculated using

$$\frac{M}{2}u_1^2 = C_p(\bar{T}) \left\{T_o - T_1\right\} \quad , \tag{91}$$

and the free flow unit mass velocity, u_1, in cm./sec. computed therefrom (column 3).

4. From equation (33) the pressure defect for instantaneous compression was computed (column 4). For carbon dioxide $C_p' = \frac{7}{2} R$, and C_{vib} was taken as the difference between C_p and C_p'.

5. The ratio of the experimental to the instantaneous entropy gain was calculated to a first approximation from

$$\Delta S'_{total} = \frac{\Delta S_{exp.}}{\Delta S_{i.c.}} = \frac{R \ln \frac{p_o}{p_3})_{exp.}}{R \ln \frac{p_o}{p_3})_{i.c.}} \cong \frac{\Delta p_{exp}/p_o}{\Delta p_{i.c.}/p_o} \text{ , (column 5).} \tag{82}$$

6. A large scale graph of the values of τ_K' vs $\Delta S'$ computed by Griffith for a square ended impact tube (see table of values in section IIB) was then utilized to obtain a first approximation to τ_K'.

7. A correction was then applied for entropy gain in the nozzle. Although a square ended impact tube was used, the correction term derived by Kantrowitz and based on a source shaped impact tube was applied. Since the correction is for the nozzle contribution, the shape of the impact tube is not material. Only an approximate value of $\Delta S_n'$ is needed as the term is a small correction. The formula utilized was

$$\Delta S_n' = \frac{4}{3} \frac{1}{K_n} - \frac{16}{9K_n^2} \left[1-\exp(-\tfrac{2}{3} K_n)\right] + \frac{4}{9K_n^2} \left[1-\exp(-3K_n)\right] \text{ ,} \tag{83}$$

with

$$K_n = \frac{D}{l} \times \frac{\tau'_K}{C_p} C'_p \quad . \tag{84}$$

Here l is the nozzle length ($\frac{1}{2}$" for the experiments on carbon dioxide), and D = 3xradius of the impact tube. Now

$$\Delta S'_{total} = \Delta S' + \Delta S'_n \quad , \tag{85}$$

where $\Delta S'_{total}$ is the relative entropy gain for the overall process, i.e. the result of step 5, $\Delta S'_n$ is the relative entropy gain in the nozzle, and $\Delta S'$ is the relative entropy gain on compression. Subtracting $\Delta S'_n$ [eqns. (83,84)] from $\Delta S'_{total}$ [eqn. (82)] gave a second approximation for $\Delta S'$. From this a new τ'_K was obtained. This value was averaged with the previous approximation to τ'_K, and a new $\Delta S'_n$ computed therefrom (column 7a). This was then subtracted from $\Delta S'_{total}$ of step 5 and a still better approximation to $\Delta S'$ obtained. This procedure was repeated until $\Delta S'$ was determined to within the accuracy of the experimental results (column 7b). This required three iterations, and in all cases only the first term in (83) was appreciable. Only final values of the relative entropy gains are recorded in table I.

8. The value of τ'_K corresponding to the final corrected value of $\Delta S'$ (column 7c) was used to compute τ_K according to the equation

$$\tau_K = \tau'_K \frac{C'_p}{C_p} \frac{d}{u_1} \text{ (column 8)} \quad , \tag{86}$$

Table I

(1a) p_o/p_1	(1b) $\frac{\Delta p_{exp}}{p_o} \times 10^3$	(1c) p_1 (atm)	(2a) T_1 (°K.)	(2b) $\bar{T}$ (°K.)	(2c) $C_p(\bar{T})$ (cal./deg.mole)
p_o = 0.967 atm., T_o = 298°K.					
1.100	0.11	0.879	291.7	294.8	8.84
1.150	0.30	.841	288.7	293.4	8.82
1.200	0.54	.806	286.0	292.0	8.80
1.250	0.83	.774	283.3	290.6	8.79
1.300	1.22	.744	280.8	289.4	8.78
1.350	1.64	.716	278.4	288.2	8.76
1.400	2.10	.691	276.1	287.0	8.75
1.450	2.60	.667	273.8	285.9	8.74
p_o = 0.752 atm., T_o = 299.8°K.					
1.100	0.14	0.684	293.5	296.6	8.86
1.150	0.36	.653	290.5	295.2	8.84
1.200	0.63	.626	287.8	293.8	8.82
1.250	0.97	.601	285.1	292.4	8.81
1.300	1.40	.578	282.6	291.2	8.80
1.350	1.84	.557	280.2	290.0	8.78
1.400	2.33	.537	277.8	288.8	8.77
1.450	2.80	.519	275.6	287.7	8.76
p_o = 0.534 atm., T_o = 300.2°K.					
1.100	0.17	0.485	293.9	297.0	8.86
1.150	0.37	.464	290.9	295.6	8.84
1.200	0.67	.445	288.1	294.2	8.83
1.250	1.04	.427	285.5	292.8	8.81
1.300	1.46	.410	283.0	291.6	8.80
1.350	1.84	.395	280.5	290.4	8.79
1.400	2.34	.381	278.2	289.2	8.77
1.450	2.82	.368	276.0	288.1	8.76
p_o = 0.341 atm., T_o = 299.2°K.					
1.100	0.16	0.310	292.9	296.0	8.85
1.150	0.34	.297	289.9	294.6	8.83
1.200	0.62	.284	287.2	293.2	8.82
1.250	0.92	.273	284.5	291.8	8.80
1.300	1.32	.262	282.0	290.6	8.79
1.350	1.58	.252	279.6	289.4	8.78
1.400	2.12	.244	277.3	288.2	8.76
1.450	2.48	.235	275.0	287.1	8.75

Table I (Cont'd.)

(1a)	(3)	(4)	(5)	(7a)	(7b)
p_o/p_1	$u_1 \times 10^{-3}$ (cm./sec.)	$\frac{\Delta p_{i.c.}}{p_o} \times 10^3$	ΔS_{total} (calories/deg. mole)	ΔS_n	$\Delta S'$
	p_o = 0.967 atm.,	T_o = 298°K.			
1.100	10.3	0.27	0.41	0.04	0.37
1.150	12.5	0.60	0.50	0.07	0.43
1.200	14.2	1.00	0.54	0.08	0.46
1.250	15.7	1.50	0.55	0.09	0.46
1.300	17.0	2.06	0.59	0.11	0.48
1.350	18.1	2.66	0.62	0.12	0.50
1.400	19.2	3.33	0.63	0.13	0.50
1.450	20.1	4.04	0.64	0.14	0.50
	p_o = 0.752 atm.,	T_o = 299.8°K.			
1.100	10.3	0.27	0.52	0.06	0.46
1.150	12.5	0.60	0.60	0.08	0.52
1.200	14.2	1.00	0.63	0.08	0.55
1.250	15.7	1.50	0.65	0.09	0.56
1.300	17.0	2.06	0.68	0.09	0.59
1.350	18.1	2.66	0.69	0.10	0.59
1.400	19.2	3.33	0.70	0.10	0.60
1.450	20.1	4.04	0.69	0.10	0.59
	p_o = 0.534 atm.,	T_o = 300.2°K.			
1.100	10.3	0.27	0.63	0.08	0.55
1.150	12.5	0.60	0.62	0.09	0.53
1.200	14.2	1.00	0.67	0.09	0.58
1.250	15.7	1.50	0.69	0.10	0.59
1.300	17.0	2.06	0.71	0.10	0.61
1.350	18.1	2.66	0.69	0.10	0.59
1.400	19.2	3.33	0.70	0.10	0.60
1.450	20.1	4.04	0.70	0.10	0.60
	p_o = 0.341 atm.,	T_o = 299.2°K.			
1.100	10.3	0.27	0.59	0.07	0.52
1.150	12.5	0.60	0.57	0.07	0.50
1.200	14.2	1.00	0.62	0.08	0.54
1.250	15.7	1.50	0.61	0.08	0.53
1.300	17.0	2.06	0.64	0.08	0.56
1.350	18.1	2.66	0.59	0.08	0.51
1.400	19.2	3.33	0.64	0.09	0.55
1.450	20.1	4.04	0.61	0.08	0.53

Table I (Cont'd.)

(1a) p_o/p_1	(7c) τ_K'	(3) $\tau_K \times 10^6$ (sec.)	(9) $\bar{p}$ (atm.)	$\bar{p} \times \tau_K \times 10^6$ (atm.sec.)
p_o = 0.967 atm., T_o = 298°K.				
1.100	0.64	3.8	0.923	3.5
1.150	0.82	4.0	.904	3.6
1.200	0.92	3.9	.886	3.5
1.250	0.92	3.6	.870	3.1
1.300	1.00	3.6	.856	3.1
1.350	1.08	3.6	.842	3.0
1.400	1.08	3.4	.829	2.8
1.450	1.08	3.3	.817	2.7
p_o = 0.752 atm., T_o = 299.8°K.				
1.100	0.92	5.4	0.718	3.9
1.150	1.17	5.7	.702	4.0
1.200	1.32	5.6	.689	3.9
1.250	1.38	5.4	.676	3.7
1.300	1.57	5.6	.665	3.7
1.350	1.57	5.3	.654	3.5
1.400	1.65	5.2	.644	3.4
1.450	1.57	4.7	.636	3.0
p_o = 0.534 atm., T_o = 300.2°K.				
1.100	1.32	7.8	0.510	4.0
1.150	1.21	5.9	.499	2.9
1.200	1.50	6.4	.490	3.1
1.250	1.57	6.1	.480	2.9
1.300	1.72	6.1	.472	2.9
1.350	1.57	5.3	.464	2.5
1.400	1.65	5.2	.458	2.4
1.450	1.65	5.0	.451	2.3
p_o = 0.341 atm., T_o = 299.2°K.				
1.100	1.17	6.9	0.326	2.3
1.150	1.08	5.2	.319	1.7
1.200	1.27	5.4	.312	1.7
1.250	1.21	4.7	.307	1.4
1.300	1.38	4.9	.302	1.5
1.350	1.12	3.8	.296	1.1
1.400	1.32	4.2	.292	1.2
1.450	1.21	3.6	.288	1.0

where d is the diameter of the impact tube.

9. The mean pressure during relaxation, $\bar{p}$, was taken as $\frac{1}{2}(p_o+p_1)$, since $\frac{(p_o-p_3)}{(p_o-p_1)} << 1$ (column 9).

When the values for each p_o are averaged, one gets:

p_o (atm.)	$\bar{p}_{ave.}$ (atm.)	$\tau_{K(ave.)}$ (μ sec.)	Ave. dev. in τ_K
0.967	0.866	3.6	6%
0.752	0.673	5.4	4%
0.534	0.478	6.0	10%
0.341	0.305	4.8	17%

The precision decreases with p_o essentially due to the fixed precision in the differential pressure measurement by the recording manometer, and to the proportionately larger nitrogen background correction. The above results at higher p_o's show average deviations which are smaller than that for the series of points quoted by Kantrowitz, for $p_o > 1$ atm.

C. Critical Interpretation

To check on the origin of the fluctuations in the values of the relaxation times we have thus obtained, a variety of plots were made in an attempt to pin down obvious trends in the data. In figure 14 values of τ_K are plotted vs p_o/p_1. The three lowest pressures check each other fairly well, wherein there is a strong suggestion of a decreasing trend with increasing expansion ratio. Relaxation times computed from the run at $p_o = 0.967$ appear to be independent of p_o/p_1; these check the data of Kantrowitz more closely (the latter were not corrected for entropy loss in the nozzle).

In figure 15 the relaxation times are plotted vs $\bar{p}$. One may conclude firstly, for any one run, there is an obvious trend with $\bar{p}$, but the slope of this trend decreases markedly with increasing pressure. This suggests that there are deviations from laminar flow in the nozzle, which become aggravated at the lower pressures and higher flow velocities. It is quite likely that the nozzle used for these runs was too short, and its throat was not sufficiently smooth; a longer nozzle, such as that used for the work on nitrogen tetroxide, would certainly reduce the correction term. Secondly, the relaxation times decrease with increasing average pressure (as $1/\bar{p}$), except for values derived from the lowest pressure run. Assuming that the transfer of energy is bimolecular, one would anticipate

Figure 14

Variation of Relaxation Time with Expansion Ratio for CO_2 at $T_{ave.} \pm 300°K.$

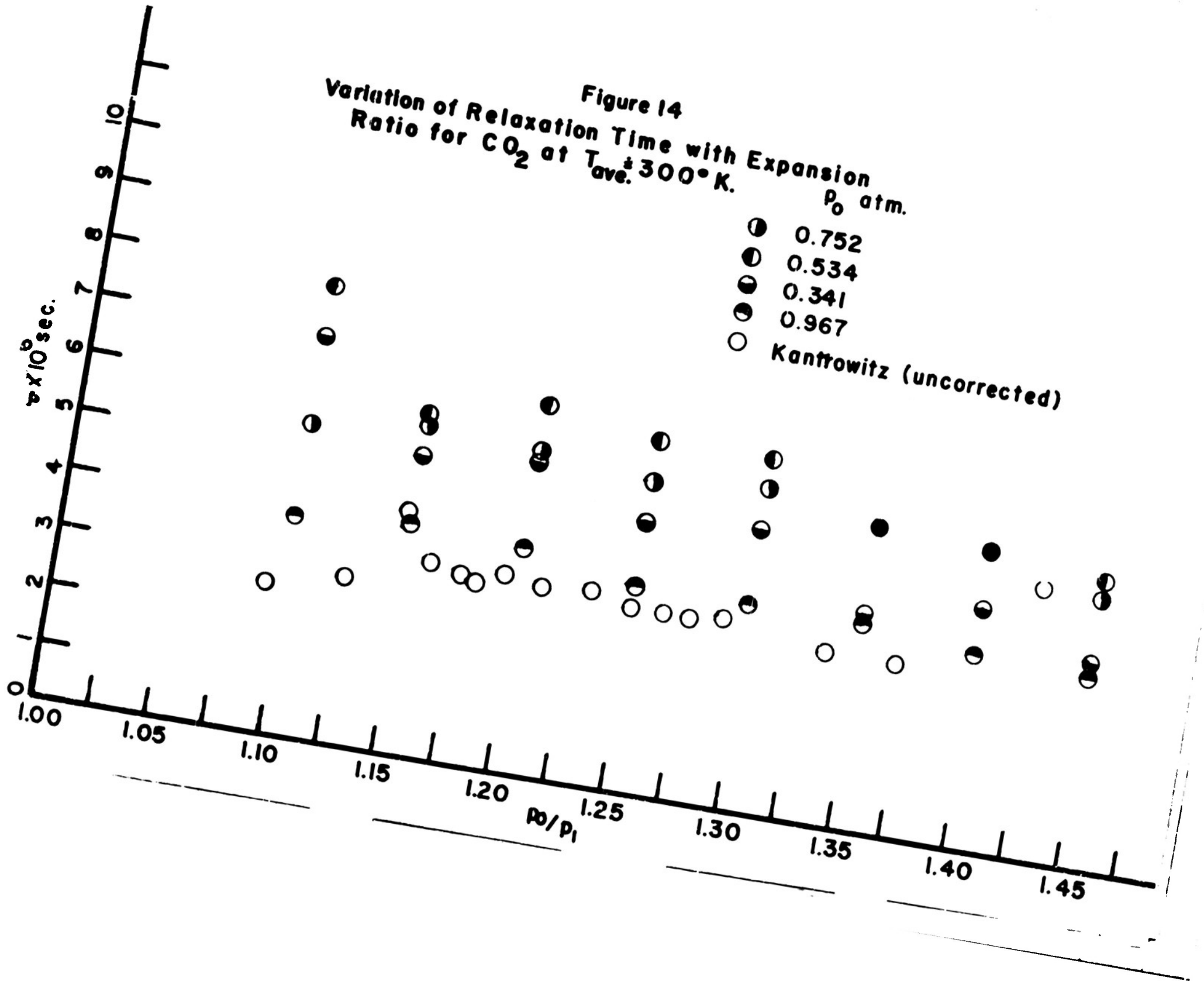

Figure 15

τ vs $\bar{p}$ for CO_2
(various p_0's)

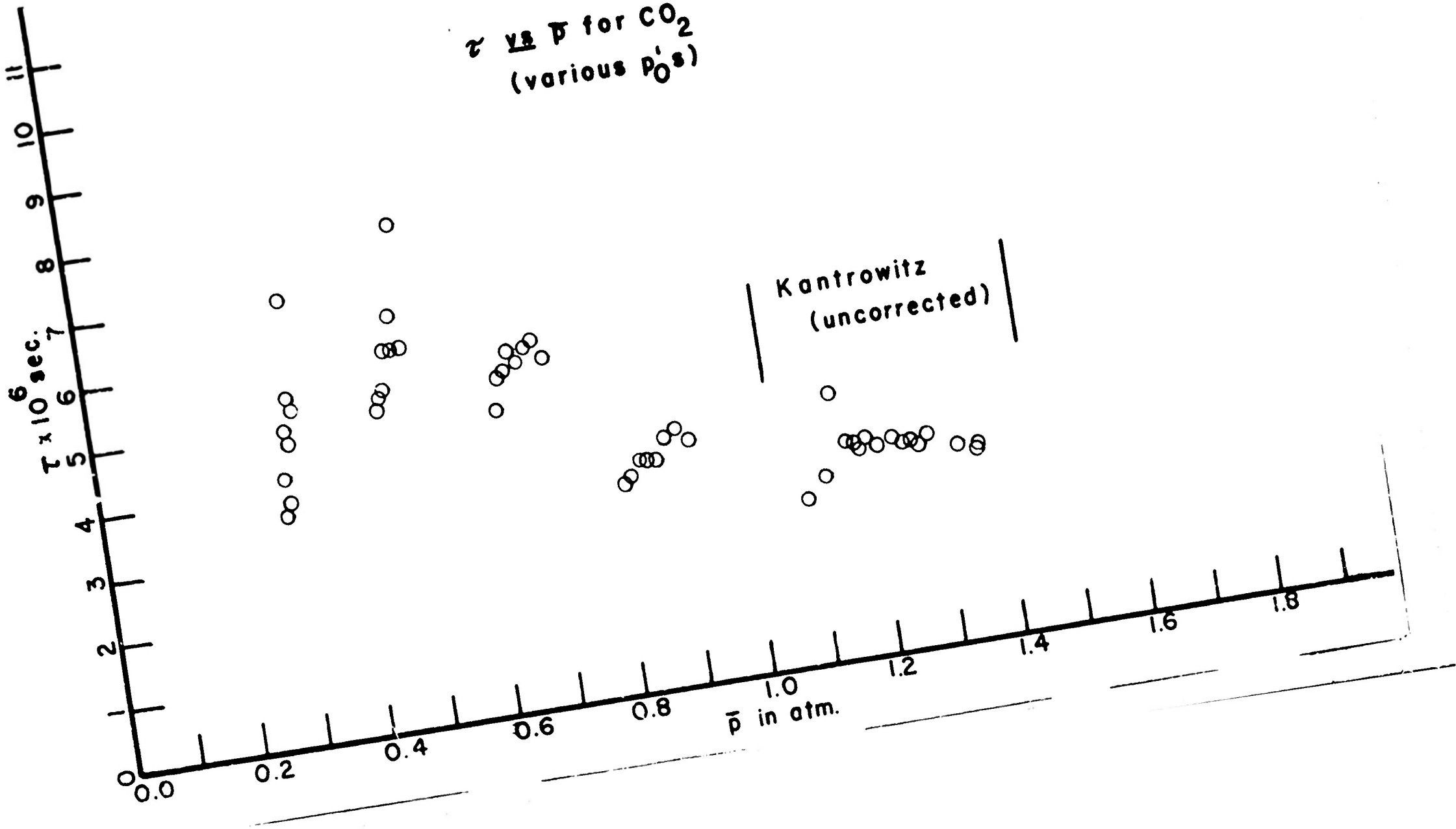

that the product, $\bar{p}x\,\tau_K$, which is proportional to the "collision number", would remain constant as long as the temperature and composition are not varied. This is demonstrated in figure 16. Such a check on the bimolecular nature of the energy exchange process has previously been made by means of sonic measurements.[72] In this figure one also notes a general decrease in $\bar{p}x\,\tau_K$ with decreasing $\bar{p}$. This trend suggests that slight but constant amounts of impurity were picked up by the gas from the flow system.

The average of the results for the runs at the three highest p_o's, for carbon dioxide at $\bar{T}$ = 291.5±0.9°K. is:

$$(\tau_K \times \bar{p})_{ave} = 3.2\times10^{-6} \text{ sec. atm.}$$

(average deviation $\tilde{=}$ 10%)

Upon correcting for the rate expression used by Kantrowitz as noted in section II B,

$$(\tau \times \bar{p})_{ave} = 2.5 \times 10^{-6} \text{ sec. atm.} \quad ,$$

or collision number[73] $= 2.2 \times 10^4$.

The computation of a "collision number" from $(\tau \times \bar{p})_{ave}$, using the mean of the initial and final pressure values, is clearly a first approximation. Refinement of the kinetic theory of this dependence is needed to deduce an appropriate weighting function.

The relation of the above result to other available data can be seen most clearly from figure 1.

It should be pointed out that it is not simple to compare the scatter in the "collision number" for sonic

Figure 16

$\bar{p} \times \tau$ vs $\bar{p}$ for CO_2
(various p's)

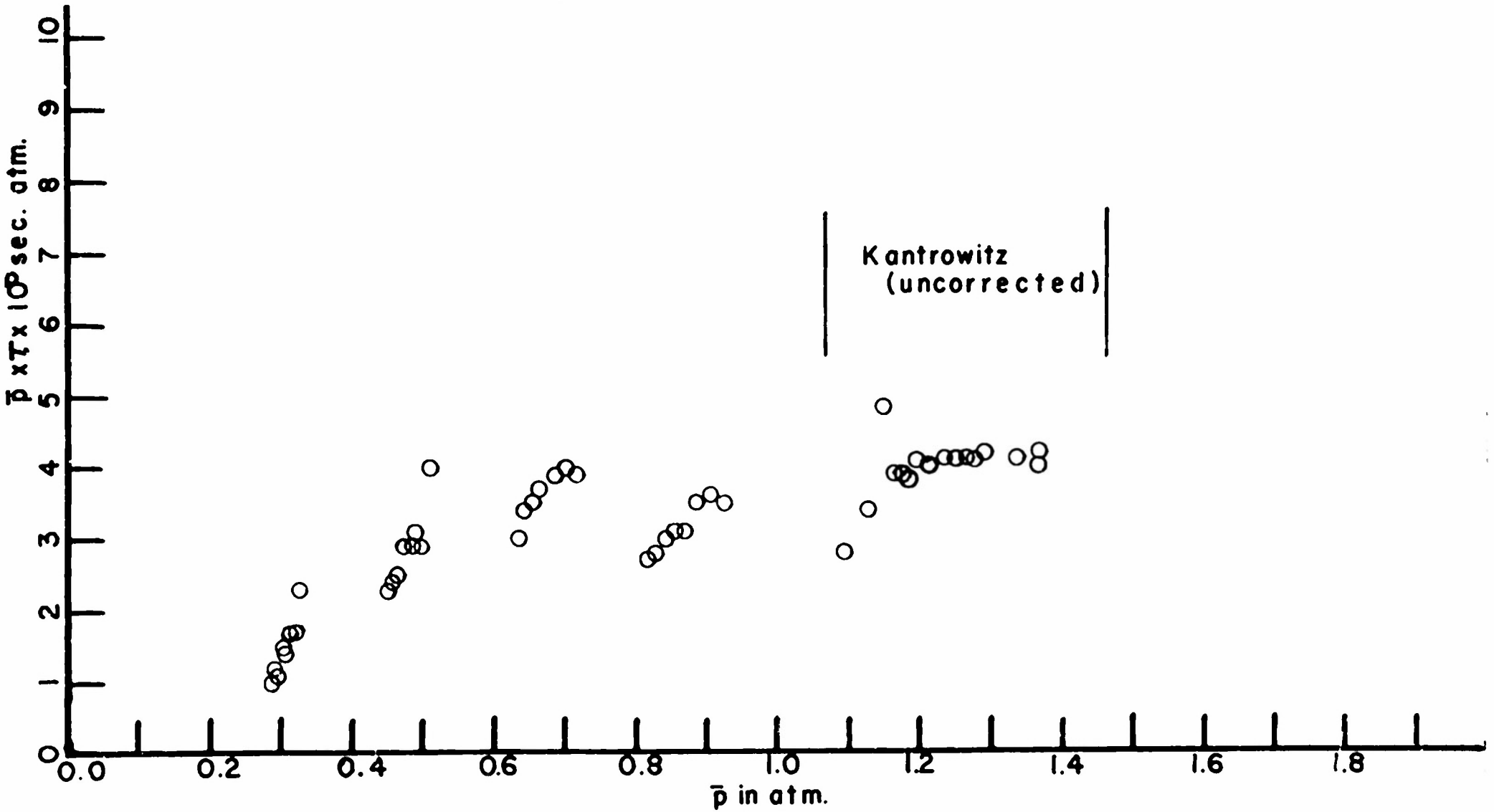

experiments with that for our method. In sonic experiments one does not usually locate the point of maximum inflection of a complete velocity versus frequency curve for a series of pressures. Rather one substantiates the fact that the reaction is of second order by showing that all data reduce to the same "s" shaped curve when the velocity squared is plotted versus the log of the ratio of the frequency to the pressure. Strictly speaking, one should differentiate the "order" of the reaction, which indeed has been demonstrated to be of the second degree, from the "molecularity" which is inferred from the inverse pressure dependence of τ.

This work on carbon dioxide was not meant to be definitive, but rather to serve as a test of our equipment and to develop a definite procedure for its use. In the next section results from the application of the impact tube experiment to a mixture of reacting gases are presented.

V. Nitrogen Tetroxide

In this section heat capacity lag measurements on nitrogen tetroxide are recorded and analyzed. Limitations of the impact tube method are then discussed.

A. The Data

The purity of the gas used and the procedure followed have already been described in section III. The calibration plots obtained for these runs were similar to that shown in figure 11, except that further adjustment to the null position of the differential transformer with respect to its core increased the sensitivity approximately 35%. A typical plot of nitrogen and nitrogen tetroxide defects vs expansion ratio is shown in figure 17. It should be noted that for a given expansion ratio the pressure defect (uncorrected for background) found for nitrogen tetroxide is approximate 1/3 that for carbon dioxide. Corrected for background the ratio becomes nearly 1:4. This decrease in magnitude of effect is only partially compensated for by the increase in sensitivity noted above. The net effect is an increase in the per cent average deviation of the nitrogen tetroxide results when compared to those for carbon dioxide.

In contrast with the carbon dioxide data no decline in the slope of the pressure defect curve above intermediate expansion ratios was noticed, nor were sharp breaks found

Figure 17

Pressure Defect Curves for N_2O_4 and N_2 at p_o = 0.485 atm., T_o = 298°K.

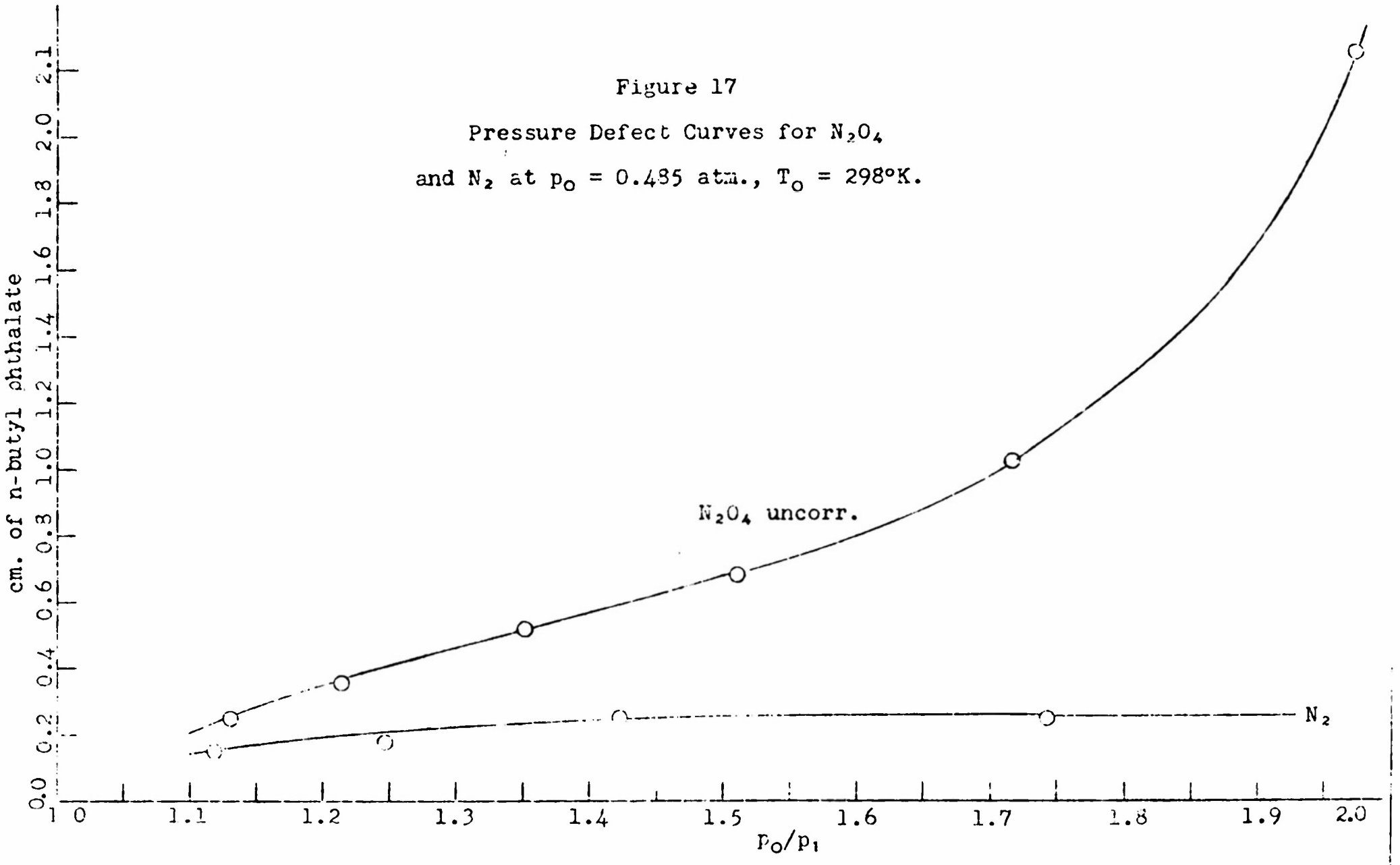

in the curve when the orifice exit velocity of the gas approached a Mach number of unity. The elimination of the former phenomenon is very probably due to the use of the longer and more carefully machined nozzle which is described in section III. The absence of a sharp break in the nitrogen tetroxide defect curves for expansion ratios around two is possibly a result of very small temperature inhomogeneities due to operation close to the condensation temperature of the gas. The measured defect did increase quite strongly in this region indicating a marked increase in turbulence.

Since the exact point at which this turbulence begins to contribute significantly to the magnitude of the observed defect is difficult to ascertain, no data above $(p_o/p_1) = 1.7$ were used to determine the relaxation time. In general, for $(p_o/p_1) < 1.3$ the nitrogen background becomes such a large fraction of the defect observed for nitrogen tetroxide that variations in this background are large compared to the difference between the nitrogen tetroxide defect and nitrogen defect. Hence, values below $(p_o/p_1) = 1.3$ were also omitted from consideration.

From a graph of the type shown in figure 17 values of the nitrogen tetroxide defect minus that for nitrogen at selected expansion ratios were obtained. Attempts to secure useful data at significantly less than 0.3 atm. were frustrated by the smallness of the difference between the

defects observed for nitrogen tetroxide and those observed for nitrogen compared to fluctuations in the nitrogen background and zero point reading. The results of measurements at $p_o \doteq 0.7$, 0.5, and 0.3 atm. taken from smooth curves through the corrected pressure defects are displayed in table II, which includes data for two different tanks and two different impact tubes. When a run was repeated under the same conditions with the same tank of gas a given set of results was customarily reproducible to within ±10%.

The impact tubes used had the following characteristics:

Tube A:

O.D. = 0.0292 cm., I.D./O.D. = 0.55,

eccentricity < 1% .

Tube B:

O.D. = 0.0440 cm., I.D./O.D. = 0.51,

eccentricity < 1%.

For the purposes of easy reference each of these eight runs has been assigned a roman numeral identification number.

Runs I, II, and III are believed to be representative, and it is on these that attention will be primarily focused in the following analyses. Runs IV, V, and VI are included to illustrate variations due to sample impurity (tanks M, N), while runs VII and VIII are included to illustrate the effect of changing the diameter of the impact tube.

Table II

Pressure Defect Data on Nitrogen Tetroxide

Run	Experiment No.	Tank	Impact tube	p_o (atm)	Net* defect in cm. n-butyl phthalate at $\frac{p_o}{p_1}$ = 1.30	1.40	1.50	1.60	1.70
I	8-29-52	M	A	0.492	0.54	0.67	0.80	0.96	1.13
II	9-1-52	M	A	0.699	0.80	0.86	0.96	1.11	1.33
III	9-1-52(II)	M	A	0.311	0.31	0.44	0.58	0.73	0.90
IV	9-4-52	N	A	0.704	1.14	1.23	1.33	1.44	1.56
V	9-4-52(II)	N	A	0.502	0.63	0.75	0.89	1.06	1.27
VI	9-4-52(III)	N	A	0.307	0.29	0.37	0.47	0.58	0.71
VII	9-16-52	N	B	0.485	0.24	0.32	0.43	0.56	0.73
VIII	9-18-52	N	B	0.289	0.23	0.30	0.38	0.49	0.62

* After correction for nitrogen background

(cm. n-butyl phthalate)/972.8 = atm.

B. Treatment of Data

The impact tube experiment yields values of the pressure defect for various combinations of p_o, T_o, and p_1. These data have been used to determine the relaxation time following the theory developed in section II. The experimentally determined entropy gain is compared with the entropy gain computed for instantaneous compression and, from this ratio, the ratio of the unknown relaxation time of the gas to the known characteristic compression time of the equipment is determined. Two cases will be considered: (i) both the vibrational degrees of freedom and the chemical reaction lag, and (ii) only the chemical reaction lags. A stepwise description of the method of computation follows; tables of the more significant quantities computed have also been included.

1. The thermodynamic quantities needed for this computation are the heat capacities and the equilibrium constant as functions of the temperature.

   i) For NO_2 the fundamental frequencies used to calculate the heat capacity are[74] ν = 648, 1320, and 1621 cm.$^{-1}$. The values obtained are:

$C_p(NO_2)$ in cal. mole^{-1} degree^{-1}	T°K.
9.07	293.2
9.03	293.2
8.99	288.2

ii) For N_2O_4 the fundamental frequencies used to calculate the heat capacity are[75]: $\nu_1 = 1265$, $\nu_2 = 1360$, $\nu_3 = 752$, $\nu_4 = 813$, $\nu_5 = \nu_6 = 1744$, $\nu_7 = ?$, $\nu_8 = 283$, $\nu_9 = \nu_{11} = 380$, $\nu_{10} = \nu_{12} = 500$ cm.$^{-1}$. ν_7 represents the torsional mode and is assumed to be sufficiently low so that the equipartition value, R, of the heat capacity is reached at room temperature. The values obtained are:

$C_p(N_2O_4)$ in cal. mole^{-1}degree^{-1}	T°K.
18.88	298.2
18.73	293.2
18.58	288.2

The heat capacities at other temperatures have been obtained by linear interpolation.

iii) The values of the measured ideal equilibrium constants (extrapolated to zero pressure) have been taken from the paper by Verhock and Daniels.[76]

$K_{eq.}$(atm)	T°C.
0.1426	25
0.3183	35
0.6706	45

The logarithm of $K_{eq.}$ was plotted vs the reciprocal of the absolute temperature, and according to the equation

$$\ln K_p = -\frac{\Delta H^\circ}{RT} + \frac{\Delta S^\circ}{R}$$

a straight line was drawn through the points; $\Delta H°$ and $\Delta S°$ were calculated from its slope and intercept respectively. The values obtained are:

$$\Delta H^{\circ}_{298} = 14649 \text{ cal. mole}^{-1}$$

$$\Delta S^{\circ}_{298} = 45.26 \text{ cal. degree}^{-1}\text{mole}^{-1} .$$

These check well with the values given by the authors; they were recomputed to insure that a consistent set of constants were being used.

2. The computation of the flow conditions starts with a specified set of values for p_o, T_o, and p_1, to determine T_1 and u_1. The procedure actually followed was for a selected (p_o, T_o) to compute p_1 and u_1 for several selected T_1. A plot of T_1 and u_1 vs (p_o/p_1) was then prepared, and values for any given expansion ratio read therefrom. Values of p_1 were computed from eqn. (44). written in the form:

$$(1+\alpha_1)\, R \ln \frac{p_o}{p_1} + (1-\alpha_1)\, R \ln \left(\frac{1-\alpha_o}{1+\alpha_o} \cdot \frac{1+\alpha_1}{1-\alpha_1}\right)$$

$$+ 2\alpha_1\, R \ln \left(\frac{2\alpha_o}{1+\alpha_o} \cdot \frac{1+\alpha_1}{2\alpha_1}\right) + (\alpha_o-\alpha_1)\, R \ln K_p(T_o)$$

$$+ \Delta S°(\alpha_1-\alpha_o) + \left\{(1-\alpha_1)C_{p(2)} + 2\alpha_1 C_{p(1)}\right\} \ln \frac{T_1}{T_o}$$

$$= \text{residue} . \qquad (37)$$

The value of p_1 consistent with reducing the residue to zero was obtained by computing the residue for several p's very close to p_1 and interpolating. The quantity $(\frac{M}{2} u_1^2)$ was computed from (37), rewritten as

$$\Delta H_{o1} = -\frac{M}{2} u_1^2$$

$$= \Delta H^o(\alpha_1-\alpha_o) + \left\{(1-\alpha_1)C_{p(2)} + 2\alpha_1 C_{p(1)}\right\}(T_1-T_o) .$$

These values are recorded in table III.

3. One now must compute $\Delta S'$. For small changes in the entropy,

$$\Delta S = \left(\frac{\partial S}{\partial p}\right)_{T,\theta,\alpha} \Delta p + \left(\frac{\partial S}{\partial T}\right)_{p,\theta,\alpha}\left(\frac{\partial T}{\partial p}\right)_{\theta,\alpha} \Delta p$$

$$+ \left(\frac{\partial S}{\partial \theta}\right)_{p,T,\alpha}\left(\frac{\partial \theta}{\partial p}\right)_{T,\alpha} \Delta p + \left(\frac{\partial S}{\partial \alpha}\right)_{p,T,\theta}\left(\frac{\partial \alpha}{\partial p}\right)_{T,\theta} \Delta p ,$$

and since all of the partial coefficients change but slightly for small changes around (p_o, T_o, α_o), to a good approximation

$$\Delta S \propto \Delta p . \tag{88}$$

Then one may write, using (80),

$$\Delta S' = \frac{(p_o-p_2)}{(p_o-p_2)_{i.c.}} . \tag{89}$$

Values for (p_o-p_2) are observed. The instantaneous compression values are computed from equation (41) and tabulated in table IV. The "corr." term in this table is precisely

$$\text{corr.} \equiv + (1-\alpha_1)\, R \ln\left(\frac{1-\alpha_o}{1+\alpha_o} \cdot \frac{1+\alpha_1}{1-\alpha_1}\right)$$

$$+ 2\alpha_1\, R \ln\left(\frac{2\alpha_o}{1+\alpha_o} \cdot \frac{1+\alpha_1}{2\alpha_1}\right) . \tag{90}$$

However, to a second order in $\left|\frac{\alpha_o-\alpha_1}{\alpha_o}\right| << 1$, this term may be approximated by

Table III

Summary of Computed Values:

$0 \rightarrow 1$ Transition, $T_o = 25°C.$

p_o (atm.)	T_1°C.	p_1 (atm.)	$\frac{p_o}{p_1}$	a_1	$\frac{M}{2} u_1^2$ ($\frac{cal.}{mole}$)	u_1 ($\frac{cm.}{sec.}$)$\times 10^{-4}$
0.3000	25	0.3000	1.0000	0.3259	0.0	0.00
	22	.2449	1.2250	.3189	158.6	1.20
	19	.1993	1.5053	.3119	317.1	1.70
	16	.1614	1.8587	.3048	475.7	2.08
0.5000	25	0.5000	1.0000	0.2530	0.0	0.00
	22	.4097	1.2204	.2518	147.1	1.16
	19	.3348	1.4934	.2455	293.6	1.63
	16	.2725	1.8349	.2391	442.5	2.01
0.7000	25	0.7000	1.0000	0.2201	0.0	0.00
	22	.5756	1.2161	.2144	140.5	1.13
	19	.4720	1.4830	.2086	280.4	1.60
	16	.3856	1.8154	.2027	421.9	1.96

$$\text{corr.} = -R(\alpha_o-\alpha_1)^2 \left\{ \frac{1}{2} \cdot \frac{1}{(1-\alpha_o)} + \frac{1}{\alpha_o} \right\} . \qquad (91)$$

T_2 was computed from equation (38), rewritten as follows:

$$\Delta H_{1,2} = \frac{M}{2} u_1^2 = \left\{ (1-\alpha_1) C'_{p(2)} + 2\alpha_1 C'_{(p_1)} \right\} (T_2-T_1). \qquad (92)$$

In table IV $(p_o-p_2)_{i.c.}$ has been tabulated for two cases.

i) The vibrational degrees of freedom and the chemical reaction both lag; then $C'_p(NO_2) = 4$ R, $C'_p(N_2O_4) = 5$ R, and $C_{\theta(i)}$ is obtained by subtracting $C'_{p(i)}$ from $C_{p(i)}$. Note that the torsional mode (ν_7) has been included in $C'_p(N_2O_4)$ as part of the non-lagging heat capacity. This follows from the comment in lii) above.

ii) Only the chemical reaction lags, in which case $C'_{p(i)} = C_{p(i)}$ and $C_{\theta(i)} = 0$. This simplifies the computation somewhat in that one of the terms in (41) drops out; however, one must also note that $C'_{p(i)}$ is now temperature dependent.

$\Delta S'$ was computed for the two cases according to (89) by taking the ratio of the experimental and "instantaneous compression" pressure defects. Final values have been recorded in table V. Figure 18 shows $(p_o-p_2)_{i.c.}$ vs $\frac{p_o}{p_1}$ for $T_o = 25°C.$ and various p_o's for the case where both the vibrational modes and chemical reaction lag, and for the case where only the chemical

Table IV

Instantaneous Compression Values

					Both vibrational modes and chemical reaction lagging					
p_o	T_1	$(\alpha_o-\alpha_1)\cdot \Delta S^\circ$	$(\alpha_o-\alpha_1)R\cdot \ln K_p(T_o)$	corr.	$\bar{C}_\theta \ln \frac{T_o}{T_1}$	T_2	$\bar{C}'_p \ln \frac{T_2}{T_o}$	$(1+\alpha_1)R\cdot \ln(\frac{p_o}{p_2})_{i.c.}$	$(\frac{p_o}{p_2})_{i.c.}$	$(p_o-p_2)_{i.c.}$
(atm.)	(°C.)	(*)	(*)	(*)	(*)	(°C.)	(*)	(*)		(atm.)
0.3000	25	0.0000	-.0000	-.0000	0.0000	25.00	0.0000	0.0000	1.0000	0.0000
	22	.3177	.0272	.0004	.0685	35.41	.4059	.0079	1.0030	.0009
	19	.6355	.0543	.0011	.1377	45.90	.7987	.0299	1.0116	.0035
	16	.9545	.0816	.0034	.2078	56.49	1.1796	.0677	1.0265	.0080
0.5000	25	0.0000	-.0000	-.0000	0.0000	25.00	0.0000	0.0000	1.0000	0.0000
	22	.2815	.0241	.0003	.0730	34.87	.3722	.0067	1.0027	.0014
	19	.5621	.0481	.0014	.1468	44.78	.7315	.0269	1.0110	.0055
	16	.8504	.0727	.0032	.2213	54.95	1.0874	.0602	1.0249	.0124
0.7000	25	0.0000	-.0000	-.0000	0.0000	25.00	0.0000	0.0000	1.0000	0.0000
	22	.2612	.0223	.0003	.0755	34.53	.3526	.0067	1.0028	.0020
	19	.5209	.0445	.0014	.1517	44.08	.6933	.0252	1.0106	.0074
	16	.7862	.0672	.0031	.2287	53.87	1.0293	.0559	1.0237	.0166

(*) $(\frac{\text{cal.}}{\text{deg.}} \cdot \frac{1}{\text{mole}})$

Table IV (Con't.)

		Only the chemical reaction lagging				
p_o	T_1	T_2	$\bar{C}_p \ln \frac{T_2}{T_o}$	$(1+\alpha_1)R \cdot \ln(\frac{p_o}{p_2})_{i.c.}$	$(\frac{p_o}{p_2})_{i.c.}$	$(p_o-p_2)_{i.c.}$
(atm.)	(°C.)	(°C.)	(*)	(*)		(atm.)
0.3000	25	25.00	0.0000	0.0000	1.0000	0.0000
	22	30.49	.3411	.0042	1.0016	.0005
	19	35.95	.6776	.0133	1.0051	.0015
	16	41.36	1.0071	.0324	1.0126	.0038
0.5000	25	25.00	0.0000	0.0000	1.0000	0.0000
	22	29.86	.3032	.0027	1.0011	.0006
	19	34.66	.5998	.0118	1.0048	.0024
	16	39.56	.9013	.0250	1.0103	.0052
0.7000	25	25.00	0.0000	0.0000	1.0000	0.0000
	22	29.49	.2806	.0032	1.0013	.0009
	19	33.94	.5568	.0100	1.0042	.0029
	16	38.45	.8343	.0222	1.0093	.0065

(*) $(\frac{\text{cal.}}{\text{deg.}} \cdot \frac{1}{\text{mole}})$

Table V

Evaluation of τ for both vibrational modes and chemical reaction lagging

Impact Tube A				Tank M			Tank N		
$\frac{p_o}{p_1}$	u_1 ($\frac{cm.}{sec.} \times 10^{-4}$)	$(p_o-p_2)_{i.c.}$ (atm.$\times 10^{+3}$)	τ_o (sec.$\times 10^{+6}$)	$\Delta S'$	τ'	τ (sec.$\times 10^{+6}$)	$\Delta S'$	τ'	τ (sec.$\times 10^{+6}$)
p_o = 0.30 atm.				Run III			Run VI		
1.30	1.37	1.5	2.13	0.212	0.307	0.65	0.199	0.280	0.60
1.40	1.55	2.3	1.88	0.197	0.277	0.52	0.165	0.222	0.42
1.50	1.69	3.4	1.73	0.176	0.240	0.42	0.142	0.184	0.32
1.60	1.83	4.5	1.60	0.167	0.223	0.36	0.132	0.165	0.27
1.70	1.94	5.8	1.51	0.160	0.213	0.32	0.126	0.160	0.24
p_o = 0.50 atm.				Run I			Run V		
1.30	1.32	2.4	2.21	0.231	0.338	0.75	0.270	0.413	0.91
1.40	1.49	3.9	1.96	0.177	0.240	0.47	0.198	0.280	0.55
1.50	1.64	5.6	1.78	0.147	0.191	0.34	0.163	0.218	0.39
1.60	1.77	7.5	1.65	0.132	0.168	0.28	0.145	0.188	0.31
1.70	1.88	9.5	1.55	0.122	0.154	0.24	0.137	0.176	0.27
p_o = 0.70 atm.				Run II			Run IV		
1.30	1.30	3.4	2.25	0.242	0.360	0.81	0.344	0.575	1.29
1.40	1.48	5.5	1.97	0.161	0.216	0.43	0.230	0.337	0.66
1.50	1.62	7.9	1.80	0.125	0.158	0.28	0.173	0.237	0.43
1.60	1.75	10.5	1.67	0.109	0.135	0.23	0.141	0.182	0.30
1.70	1.85	13.3	1.58	0.103	0.127	0.20	0.120	0.151	0.24

Table V (Con't.)

Evaluation of τ for only chemical reaction lagging

Impact Tube A				Tank M			Tank N		
$\frac{p_o}{p_1}$	u_1 ($\frac{cm.}{sec.} \times 10^{-4}$)	$(p_o-p_2)_{i.c.}$ (atm.$\times 10^{+3}$)	τ_o (sec.$\times 10^{+6}$)	$\Delta S'$	τ'	τ (sec.$\times 10^{+6}$)	$\Delta S'$	τ'	τ (sec.$\times 10^{+6}$)
p_o = 0.30 atm.				Run III			Run VI		
1.30	1.37	0.7	2.13	0.46	0.92	1.96	0.43	0.82	1.75
1.40	1.55	1.0	1.88	0.45	0.88	1.66	0.38	0.66	1.24
1.50	1.69	1.5	1.73	0.40	0.72	1.25	0.32	0.52	0.90
1.60	1.83	2.0	1.60	0.38	0.66	1.06	0.29	0.45	0.72
1.70	1.94	2.6	1.51	0.36	0.61	0.92	0.28	0.43	0.65
p_o = 0.50 atm.				Run I			Run V		
1.30	1.32	1.0	2.21	0.56	1.38	3.05	0.65	2.07	4.58
1.40	1.49	1.7	1.96	0.40	0.72	1.41	0.45	0.83	1.72
1.50	1.64	2.4	1.78	0.34	0.56	1.00	0.38	0.65	1.18
1.60	1.77	3.2	1.65	0.31	0.50	0.82	0.34	0.56	0.92
1.70	1.88	4.1	1.55	0.28	0.43	0.67	0.32	0.52	0.81
p_o = 0.70 atm.				Run II			Run IV		
1.30	1.30	1.4	2.25	0.59	1.58	3.56	0.84	6.10	13.73
1.40	1.48	2.1	1.97	0.42	0.78	1.54	0.60	1.65	3.25
1.50	1.62	3.0	1.80	0.33	0.54	0.97	0.46	0.92	1.66
1.60	1.75	4.0	1.67	0.29	0.46	0.77	0.37	0.64	1.07
1.70	1.85	5.1	1.58	0.27	0.41	0.65	0.31	0.50	0.79

Table V (Con't.)

Evaluation of τ for both vibrational modes and chemical reaction lagging

Impact Tube B				Tank N		
$\frac{p_o}{p_1}$	u_1 ($\frac{cm.}{sec.} \times 10^{-4}$)	$(p_o-p_2)_{i.c.}$ (atm.$\times 10^{+3}$)	τ_o (sec.$\times 10^{+6}$)	$\Delta S'$	τ'	τ (sec.$\times 10^{+6}$)
p_o = 0.30 atm.				Run VIII		
1.30	1.37	1.5	3.21	0.158	0.210	0.67
1.40	1.55	2.3	2.84	0.134	0.172	0.49
1.50	1.69	3.4	2.60	0.115	0.144	0.37
1.60	1.83	4.5	2.40	0.112	0.139	0.33
1.70	1.94	5.8	2.27	0.110	0.137	0.31
p_o = 0.50 atm.				Run VII		
1.30	1.32	2.4	3.33	0.103	0.127	0.42
1.40	1.49	3.9	2.95	0.084	0.102	0.30
1.50	1.64	5.6	2.68	0.079	0.094	0.25
1.60	1.77	7.5	2.48	0.077	0.092	0.23
1.70	1.88	9.5	2.34	0.079	0.094	0.22

Evaluation of τ for only chemical reaction lagging

Impact Tube B				Tank N		
$\frac{p_o}{p_1}$	u_1 ($\frac{cm.}{sec.} \times 10^{-4}$)	$(p_o-p_2)_{i.c.}$ (atm.$\times 10^{+3}$)	τ_o (sec.$\times 10^{+6}$)	$\Delta S'$	τ'	τ (sec.$\times 10^{+6}$)
p_o = 0.30 atm.				Run VIII		
1.30	1.37	0.7	3.21	0.338	0.56	1.30
1.40	1.55	1.0	2.84	0.308	0.49	1.39
1.50	1.69	1.5	2.60	0.260	0.40	1.04
1.60	1.83	2.0	2.40	0.252	0.38	0.91
1.70	1.94	2.6	2.27	0.245	0.37	0.84
p_o = 0.50 atm.				Run VII		
1.30	1.32	1.0	3.33	0.247	0.37	1.23
1.40	1.49	1.7	2.95	0.194	0.272	0.80
1.50	1.64	2.4	2.68	0.134	0.254	0.68
1.60	1.77	3.2	2.48	0.180	0.247	0.61
1.70	1.88	4.1	2.34	0.183	0.253	0.59

Figure 18

$(p_o-p_2)_{i.c.}$ vs p_o/p_1 for T_o = 25°C.

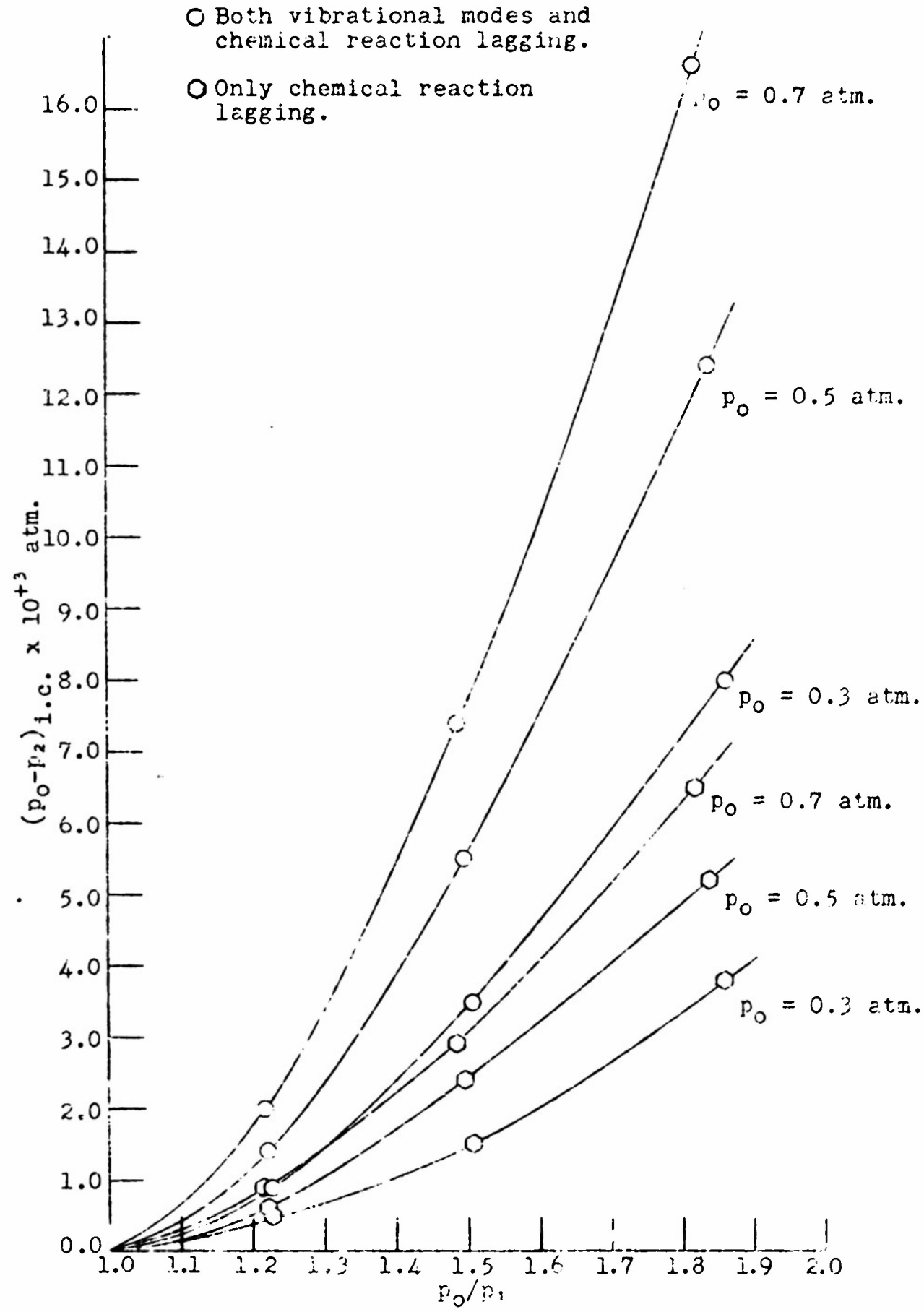

reaction lags. From these graphs values of $(p_o-p_2)_{i.c.}$ may be read at selected p_o/p_1 for comparison with the experimental quantities. A similar graph was used to deduce interpolated values of u_1. Figure 19 shows the dependence of u_1, T_1, p_1, a_1, and T_2 (vibrational modes and chemical reaction both lagging) on p_o/p_1 for p_o = 0.500 atm. and T_o = 25°C.

4. To compute τ' from $\Delta S'$ one uses equation (79). For the case of a square ended impact tube the integral has been evaluated by Griffith[44] and the values presented at the end of section II B. From a graph of these values plotted as log τ' vs $\Delta S'$, values of τ' for the determined values of $\Delta S'$ have been obtained. These are presented in table V. τ_o was found from (57) by taking the ratio of the measured diameter of the impact tube to the computed streaming velocity in state 1; then τ was computed according to (68). Values of τ_o and τ are presented in table V.

This completes the reduction of the measured pressure defects to relaxation times according to the theory outlined in section II C.

Figure 19

u_1, T_1, p_1, α_1, T_2 (both vib. and react. lagging) vs. p_o/p_1 for $p_o = 0.500$ atm. and $T_o = 25°C$.

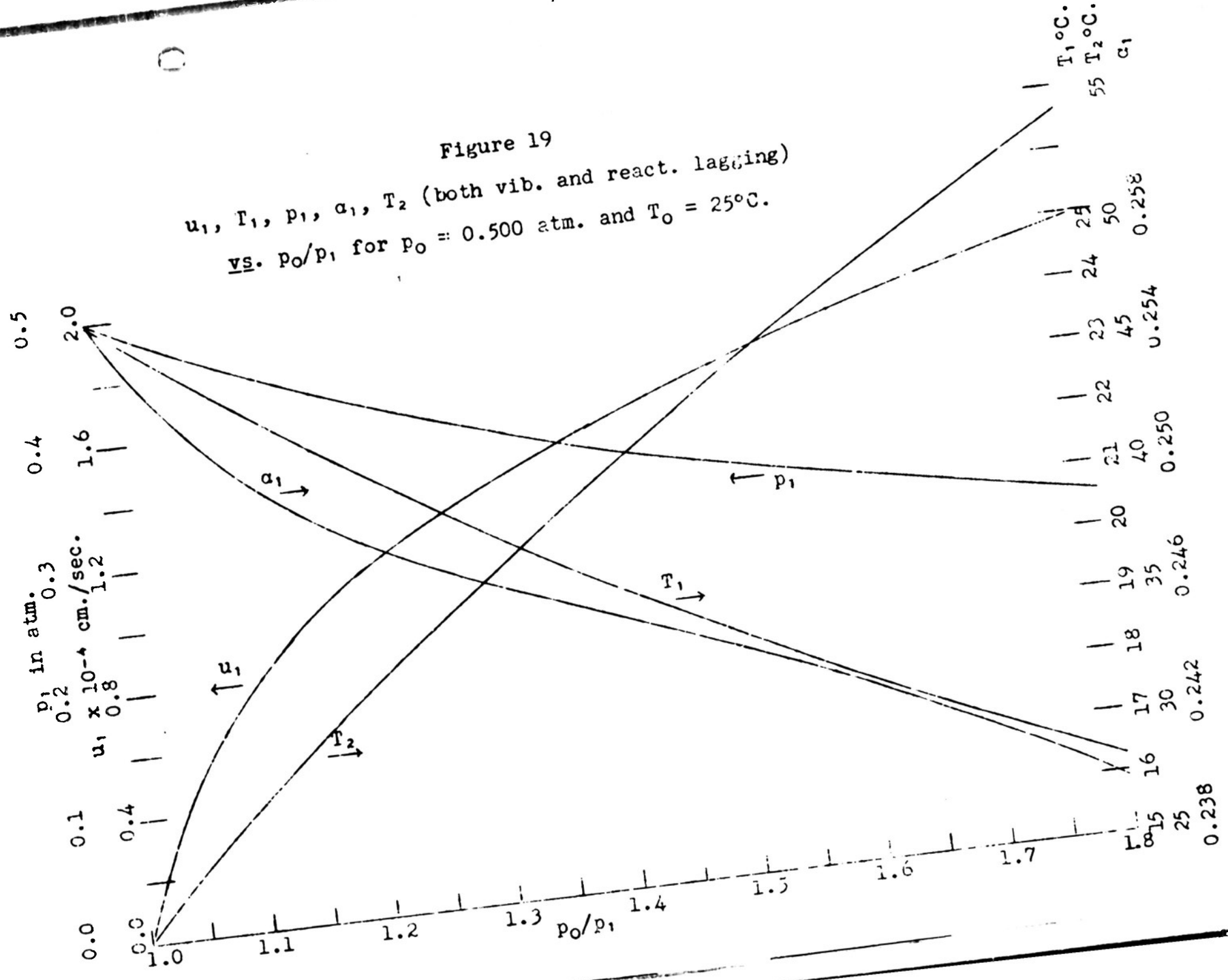

C. Discussion

a. Interpretation of the Data.

If the transfer of energy is bimolecular and only one relaxation time is operative, the product, $\bar{p} \times \tau$ [$\bar{p}$ is the average pressure, and is taken to be $\frac{1}{2}(p_o+p_1)$], which is proportional to the "collision number" should remain constant as long as the temperature and composition are not varied. In table VI values of $\bar{p}$ and ($\bar{p} \times \tau$) are displayed for runs I, II, and III, where τ has been computed for both vibrational modes and chemical reaction lagging and for only the chemical reaction lagging. Figure 20 is a plot of $\bar{p} \times \tau$ *vs* $\bar{p}$ for these two cases. If one of the procedures used to reduce the measured pressure defects to relaxation times is completely correct then for that case all of the points in figure 20 should fall on the same horizontal line. Clearly this is not the case. One notes, however, that when reduced on the basis of both vibrational modes and chemical reaction lagging the points cover a considerably narrower range than when reduced on the basis of only the chemical reaction lagging. This argues in favor of the inclusion of both types of lag in the reduction of these data. One further notes from table VI (or figure 20) that there is a strong trend in the values of τ computed for any one run. This dependence cannot be due to the pressure, since $\bar{p}$ varies by at most 15% within a run. Nor can it be due to temperature variations since $\bar{T} = \frac{1}{2}(T_1+T_2)$

Table VI

Evaluation of $\bar{p}$ and $\bar{p} \times \tau$ for Runs I, II, and III

Run	$\frac{p_o}{p_1}$	$\bar{p}$	$\bar{p} \times \tau$ for both θ and α lagging	$\bar{p} \times \tau$ for only α lagging
III, p_o = 0.30 atm.	1.30	0.266	0.17	0.52
	1.40	0.257	0.13	0.43
	1.50	0.250	0.10	0.31
	1.60	0.244	0.09	0.26
	1.70	0.238	0.08	0.22
I, p_o = 0.50 atm.	1.30	0.442	0.33	1.35
	1.40	0.429	0.22	0.60
	1.50	0.417	0.14	0.42
	1.60	0.406	0.11	0.33
	1.70	0.397	0.10	0.27
II, p_o = 0.70 atm.	1.30	0.619	0.50	2.20
	1.40	0.600	0.26	0.92
	1.50	0.583	0.16	0.57
	1.60	0.569	0.13	0.44
	1.70	0.556	0.11	0.36

Figure 20

$\tau \times \bar{p}$ vs $\bar{p}$ for Tank M (Runs I, II, III)

○ Calculated on basis of both vibrational modes and chemical reaction lagging.

● Calculated on basis of only chemical reaction lagging.

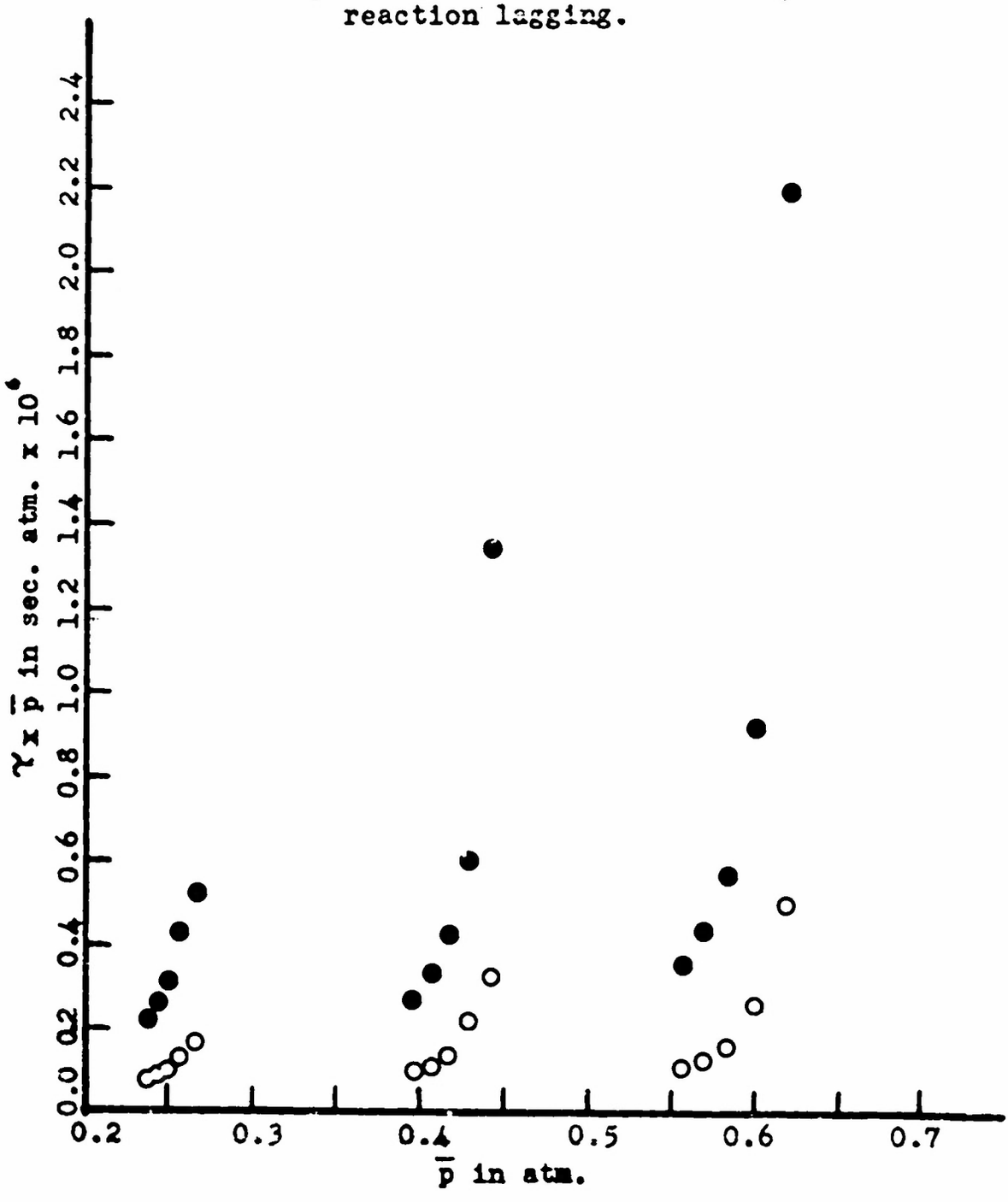

varies by at most 2% (note that lower T_1's are balanced by accompanying higher T_2's) within a run. This variation is reduced when one considers both vibrational modes and chemical reaction lagging, which suggests that further modifications of the simplified procedure used to reduce the measured pressure defects to relaxation times are in order. The next step would be to consider three different relaxation times, as initially set up in section III C. In this connection it is valuable to note that a similar trend was noted in our measurements on carbon dioxide. It is probable that the use of three different relaxation times associated with the different vibrational frequencies would also effect a more complete reduction of the data in that case. Further conclusions on this question may be derived from table V. It is clear that the only effect of changing the diameter of the impact tube is to change τ_o. Having allowed for this factor the relaxation times computed for all impact tubes should be identical Comparison of the results of runs at identical values of p_o and p_o/p_1, and with the same tank of gas, leads to the following ratios:

p_o	$\frac{p_o}{p_1}$	$\frac{\tau \text{ determined with impact tube A}}{\tau \text{ determined with impact tube B}}$
0.30 atm.	1.30	0.90
	1.40	0.86
	1.50	0.86
	1.60	0.82
	1.70	0.77
0.50 atm.	1.30	2.16
	1.40	1.88
	1.50	1.56
	1.60	1.35
	1.70	1.23

Clearly the ratio of τ's for the two impact tubes depends on $\bar{p}$. This again indicates that two or more relaxation times are necessary to properly reduce the data.

From figure 20 an estimate of the average relaxation time may be made by drawing the best horizontal line through those points calculated on the assumption that both the vibrational modes and chemical reaction lag. At 25°C. and 1 atm. total pressure, this gives

$$\boxed{\tau = 0.14 \ \mu \text{ sec.}}$$

b. Sources of Error

The above result is subject to four primary sources of error.

i) Since reduction of the data is not complete the above value represents an average. The average deviation from this value including all points is 0.07. The elimination of one point whose deviation is five times this

value gives an average deviation of 0.05. This is the single largest error involved in this experiment. However, reduction of this error depends only upon the use of a more complex theory for converting the measured pressure defects to relaxation times. The very regularity of the trend for each run in figure 20 augurs well for the success of a more complete theoretical treatment.

ii) The effect of impurities is indicated in table V by data for comparable runs on two different tanks. The average difference between τ values for the two tanks is approximately 30%; however, the ratio of the value of τ obtained with tank N compared to tank M varies from less to greater than unity, depending on p_o. In part this may be involved with the theoretical problem referred to above, or more likely to a greater dilution of a fixed amount of impurities desorbed from the flow system at higher p_o's. The purity specifications on the gas as supplied by the manufacturer (see section III) indicate that the gas contains only very small amounts of impurities which might be expected to be troublesome. It should also be noted that before use the system was always swept clean with "dry" nitrogen and before data were taken the nitrogen tetroxide was run through the system until at a fixed p_o and p_o/p_1 a constant pressure defect was observed. It seems improbable that impurities would be present in the flow system in such amount and desorb in such a manner as to produce such

a constant measured defect for any appreciable time. It was also found possible at the end of a run to return to any stipulated set of conditions and obtain very nearly (see point iv below) the same value for the pressure defect. All of these factors argue against the probability of gross impurities being introduced by the flow system, and indicate that the impurities in the gas as supplied by the manufacturer vary from tank to tank. The absolute magnitude of the error in τ caused by these impurities is impossible to ascertain, but it is probably less than a factor of two. The error from this source is not inherent in the experiment. Its removal depends only on obtaining adequately purified nitrogen tetroxide in sufficiently large amounts.

iii) An error is introduced into the computations due to the lack of precise values for the necessary thermodynamic parameters. The magnitude of the error introduced in this manner may be investigated by computing the value of $\left(\frac{p_o}{p_2}\right)_{i.c.}$ using equation (41) for various assumed values of the thermodynamic constants. One finds for the range of values used in this thesis that a 0.1% change in $C_{p(2)}$ changes the value of $\left(\frac{p_o}{p_2}\right)_{i.c.}$ by approximately 10%. A change of 0.1% in ΔS° also causes a change in $\left(\frac{p_o}{p_2}\right)_{i.c.}$ of this same order of magnitude. These parameters are known to approximately 0.1% and their method of computation (see section V B) assures the maximum of self-consistency. Hence,

one may conclude that lack of sufficiently accurate knowledge of the thermodynamic parameters introduces an error into the computed value of $(\frac{p_o}{p_2})_{i.c.}$ of roughly ± 10%. The error subsequently introduced in the magnitude of τ is of this order of magnitude. It should be noted that this is not an error in the data obtained from this experiment, but reflects the lack of adequate knowledge of the parameters necessary to interpret the experimental data. That the interpretation of the experiment depends so strongly on the values of these thermodynamic parameters is not surprising in view of the fact that $\frac{1}{p_o}(p_o-p_2)_{i.c.} \cong 2\times10^{-3}$. In the experiment (p_o-p_2) is determined directly by applying the two pressures to different sides of the pressure sensing bellows. The calculated values are obtained by subtracting two large numbers, and an error of 0.01% in the computed value of p_2 will change the computed value of (p_o-p_2) by roughly 10%.

iv) The errors inherent in the present equipment are those due to lack of precision in reading the pressure, turbulence background, and zero point wandering. All of these have been considered in detail in section III. As indicated there, pressure differentials can be read to a precision of 1.0×10^{-5} atm. Reference to figure 17 shows that the nitrogen defect over the region used amounted to approximately 2.0×10^{-4} atm. Assuming that this defect was the same for the nitrogen tetroxide part of the run

probably involves an error of roughly 10% of this quantity, or 2×10^{-5}. Errors introduced by wandering of the zero point were considerably reduced by frequent readings of this quantity. The maximum value of this uncertainty as actually observed over many experiments is ± 0.2 mv. at the recorder or ± 5×10^{-5} atm. Hence the maximum error in determining the corrected pressure defect of N_2O_4 is ± 8×10^{-5} atm. Since a typical corrected pressure defect (see table II) amounted to 0.5×10^{-3} atm. this is equivalent to an error of ± 15%. As discussed in section III, the largest part of the error which is due to zero point wandering could be greatly reduced by the use of more stable electrical components. A reduction of this source of fluctuations to 20% of its present value would increase the precision of the measurements by a factor of 2, i.e., to ± 8%.

One further point should be mentioned with respect to errors, and that is the possibility of entropy gain in the nozzle. The nozzle utilized for the experiments on nitrogen tetroxide has a length of 1.6 inches, and for a typical exit velocity of 1.6×10^4 cm./sec. the time taken by the gas to expand through the nozzle is greater than 250 μ sec. Comparing this with the value of τ quoted above the time taken to expand through the nozzle is approximately 1700 times the relaxation time. Clearly the entropy gain in the nozzle due to this relatively slow expansion

must be negligible compared to the entropy gain on compression at the face of the impact tube.

c. Comparison with other Methods

As noted in section I, a number of methods have been suggested for determining the rate of dissociation of nitrogen tetroxide, but only one, involving the use of a shock tube, had any pronounced success. The bimolecular and unimolecular rate constants determined by Carrington and Davidson using this method have been quoted at the end of section I. Manes[65] discussed the relationship between the relaxation time and the postulated reaction mechanism for a general case which includes a large number of simple rate laws. He obtained the result[65b] that for a reaction of the type

$$aA + bB + \cdots \rightleftharpoons qQ + rR + \cdots$$

near equilibrium, for most cases τ is given by

$$\frac{1}{\tau} = r_f \left[\frac{a^2}{C_A} + \cdots + \frac{q^2}{C_Q} + \cdots \right] \quad , \qquad \text{where}$$

C_A is the concentration of species A and r_f is the rate of the forward reaction as written above. Utilizing the relation $K_{eq} = \frac{k_f}{k_r}$ and applying the above formula to the unimolecular case

$$N_2O_4 \underset{k_r}{\overset{k_f}{\rightleftharpoons}} 2NO_2 \qquad \text{gives}$$

$$\frac{1}{\tau} = k_f + k_r \, 4C_{NO_2} \quad .$$

Substituting Carrington and Davidson's unimolecular rate constant for k_f gives $\tau = 0.022$ μsec. For the bimolecular case

$$M + N_2O_4 \underset{k_r}{\overset{k_f}{\rightleftharpoons}} 2NO_2 + M$$

$$\frac{1}{\tau} = k_r \, 4 \, C_M \, C_{NO_2} + k_f \, (C_M + 2 \, C_{N_2O_4}), \quad \text{and}$$

using Carrington and Davidson's bimolecular rate constant for k_f gives $\tau = 0.99$ μsec. One can easily show that the condition for deactivation by collision or chemical decomposition to be equally probable is that the total concentration of molecules satisfies the equation

$$\left(\frac{k_{bimol.}}{k_{unimol.}}\right) C_T = 1 \quad .$$

Substituting in the values of the rate constants used above gives $C_T = 0.5 \frac{m}{l}$. This checks as well as can be expected with Carrington and Davidson's conclusion based on a plot of experimental values of log $k_{unimol.}$ vs log C_T, that the reaction is nearly second order at $0.05 \frac{m}{l}$, i.e. when the total concentration is decreased to one-tenth of C_T.

One atmosphere corresponds to a total concentration of $\sim 0.04 \frac{m}{l}$, and hence all of the data reported in this thesis were taken in the range where the bimolecular rate law applies. It should be noted then that the average τ deduced from the impact tube experiment is approximately one-seventh that calculated from the bimolecular rate constant based on the shock tube experiments. The differ-

ence may be interpreted as being due to the greater efficiency of collisions with nitrogen dioxide and tetroxide in exciting the nitrogen tetroxide molecule over collisions with nitrogen which was used as the carrier gas in the shock tube experiments. The conclusion is that the two experiments agree in the area of comparison.

The most important consequence of these two experiments is that both definitely indicate the presence of a lag in equilibration. This should be contrasted with the acoustic method which has led to many conflicting reports even as to whether there was or was not a velocity change (see section I).

It is interesting to compare the shock tube and the impact tube methods for measuring the rates of rapid chemical reactions in the gas phase since such a comparison most clearly indicates the advantages and disadvantages of each.

The success of the impact tube method is due to its being a differential experiment. The shock tube method relies on the rapidity with which a shock produces a large change in energy. This points up the primary difference between these two methods. The resulting difference in theoretical treatment has been partially indicated in section II C. A further difference results from the fact that since the displacements from equilibrium are small in the impact tube experiment approximations can be made which

are not applicable to the large displacements of the shock tube experiment. On the other hand, the amount one can learn about the mechanism from such small displacements from equilibrium us ultimately less than that which can be deduced from a larger range of perturbations.

In general, the theoretical treatments of both experiments are hampered by a lack of adequate hydrodynamic theories. In the impact tube experiment this manifests itself in the inaccuracies involved in converting the measured pressure defects into relaxation times. These inaccuracies have already been discussed. In the shock tube experiment this difficulty manifests itself in the lack of ability to compute precisely the conditions behind the shock wave. Carrington and Davidson have estimated that an error of 0.6% in the shock velocity means an error of 1.5° in the calculated temperature and an error of 15% in the rate constant. Even if the shock velocity were known more accurately other workers have pointed out that simple theories do not predict the density fluctuations with much accuracy.[77]

In the shock tube experiment the limit of resolution is set primarily by the time constant of the detector-amplifier. One is thus limited to relatively strong absorptions in the visible and ultra-violet. The resolving time is then limited to ~ 4 μ sec., as determined by the time required for the shock to cross the observing beam.

This could, of course, be reduced by using narrower slits if light sources of sufficient intensity were available. This limitation prevented Carrington and Davidson from making measurements at temperatures greater than 30°C. since the reaction became too fast. The limit of resolution of the impact tube type of experiment is set by the minimum diameter of the impact tubes which can be made and the maximum non-turbulent flow velocity. Impact tubes can be constructed as small as 0.01 cm. while the maximum useful velocity is approximately 2×10^4 cm.sec.$^{-1}$. This gives a time constant of ~ 0.5 μ sec. The relaxation time must be within a factor of 10 of this for an appreciable defect to be observed, and hence the limit of time resolution of this type of experiment is ~ 0.05 μ sec. Relaxation times as long as 10^{-2} sec. may be determined by studying the entropy gain in the nozzle.

One serious limitation on the impact tube method is that it requires large quantities of gas. The shock tube method does not require such large volumes. Because trace impurities may greatly effect the relaxation time the gas used must be quite pure, and with the large volumes involved in the impact tube experiment this restriction presents a difficult though not insoluble problem. There is also the possibility of working out a suitable recycling technique.

The shock tube method can also be used over a somewhat wider range of pressures, temperatures, and concentrations than the impact equipment which has been built to date. Further, the observed pressure defect in the impact tube experiments depends on an integral of the form

$$\int_{t_o}^{\infty} \frac{\Delta F}{T} \left(\frac{du}{dt}\right) dt \quad ,$$

whereas the shock tube method has a decided advantage in that the concentration of the reactants is measured directly as a function of time. To its disadvantage is the relative complexity of the equipment required compared to that utilized in the impact tube experiment.

Further Analysis of CO_2 and N_2O_4

Heat Capacity Lag Data

From the theoretical analysis presented in section VC. two conclusions follow: (a) The available data may be interpreted in terms of a single relaxation time only to a rough approximation; three and possibly more relaxation times are in evidence. (b) A general treatment for the case of plural relaxation times has been outlined. Hence, before continuing with experimental work in which this method is applied to other homogeneous fast gas reactions, the data recorded in this report will be reviewed with the object of deducing values for the several relaxation times. The degree of success which we shall meet will determine whether extensive further development of the (isentropic flow + impact tube) method will be undertaken.

The distribution list may be found at the end of Section I.

APPENDIX I

Consider a system in equilibrium and having <u>one</u> relaxation time. Suppose to this system one applies a step perturbation $h_s(t) = \begin{cases} h_s^\circ & \text{for } t \geqslant 0 \\ o & \text{for } t < 0 \end{cases}$. Now define a parameter $\eta_s(t)$ which is a measure of instantaneous departure from equilibrium. The step perturbation imposes an initial departure from equilibrium of η_s°.

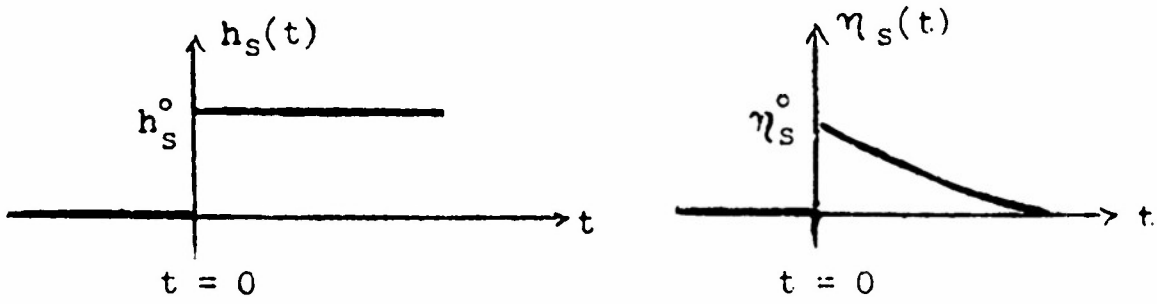

That is the ratio of departure from equilibrium to perturbation, r, is

$$r \equiv \left(\frac{\eta_s^\circ}{h_s^\circ}\right) .$$

The decay curve will then be described by the differential equation

$$\frac{d\eta_s}{dt} = -\frac{\eta_s}{\tau} \quad , \qquad \text{where}$$

τ is the relaxation time of the system. The integrated form of this equation will be

$$\eta_s(t) = \eta_s^\circ \, e^{-t/\tau} .$$

If one now assumes that the departure is additive in terms of the perturbation, <u>i.e.</u>, independent of previous

perturbation history a given perturbation always produces the same departure, the general case may easily be treated. Suppose h(t') has a general form as shown below. It is

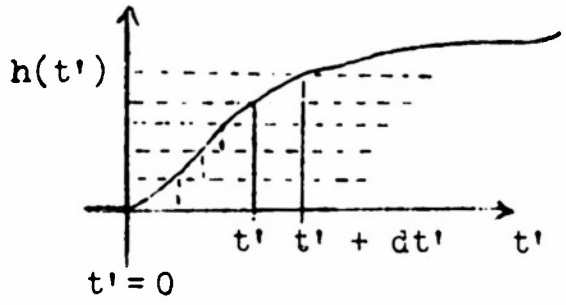

clear that assuming the additive property this may be looked upon as a series of step perturbations spaced in time t'. Over a time interval dt' around t' the additional perturbation will be

$$\left[\frac{\partial h(t')}{\partial t'}\, dt'\right] .$$

This additional perturbation will contribute to the departure from equilibrium at all times subsequent to t' and the contribution will amount to

$$\left[\frac{\partial h(t')}{\partial t'}\, dt'\right] \left(\frac{n_s^\circ}{h_s^\circ}\right) e^{-(t-t')/\tau} .$$

Hence in general one may write

$$\eta(t) = \int_{t=0}^{t=t} \int_{t'=0}^{t'=t} \left[\frac{\partial h(t')}{\partial t'}\, dt'\right] \left(\frac{n_s^\circ}{h_s^\circ}\right) e^{-\frac{(t-t')}{\tau}}\, dt ,$$

where one has summed over all the perturbations. This may be rewritten as

$$\eta(t) = e^{-\frac{t}{\tau}} \int_0^t \left(\frac{\eta_s^o}{h_s^o}\right) \frac{\partial h(t')}{\partial t'} e^{+\frac{t'}{\tau}} dt' \quad .$$

If one now further assumes that r is independent of time the above may be written as

$$\eta(t) = e^{-\frac{t}{\tau}} \left(\frac{\eta_s^o}{h_s^o}\right) \int_0^t \frac{\partial h(t')}{\partial t'} e^{\frac{t'}{\tau}} dt' \quad .$$

For the case where the perturbation, although extended in time, starts with a step function, the last equation assumes the form

$$\eta(t) = e^{-\frac{t}{\tau}} \left[\eta_s^o + \left(\frac{\eta_s^o}{h_s^o}\right) \int_0^t \frac{\partial h(t')}{\partial t'} e^{-\frac{t'}{\tau}} dt'\right] \quad .$$

BIBLIOGRAPHY

Note: In this list the journal names have been abbreviated as in Chemical Abstracts.

1. (a) Kantrowitz, A. i) Thesis (Columbia University, 1946); ii) J. Chem. Phys. 10, 145 (1942); iii) J. Chem. Phys. 14, 150 (1946).
(b) Huber, P. W., and Kantrowitz, A., J. Chem. Phys. 15, 275 (1947). See also ref. 53.

2. Boltzmann, L.
(a) Ann. der Physik und Chemie 141, 473 (1870).
(b) "Wissenschaftlichen Abhandlungen" (Leipzig, 1909) 1, 157.

3. Lorentz, H. A.
(a) Arch. néerl. sci. 16, 1 (1881).
(b) "Abhandlungen über theoretische Physik" (Leipzig, 1907) 1, 73.
(c) Collected Papers (The Hague, 1938) 6, 1.

4. Hertz, H. R., Crelle, J. Math., 92, 156 (1882).

5. Jeans, J. H., Phil. Mag. 6, 279 (1903).

6. Stewart, J. G,, Phil. Mag. 28, 743 (1914); cf. id, Journal of the Institute of Mechanical Engineers, Oct., 1914.

7. Pierce, G. W., Proc. Am. Acad. Arts Sci. 60, 271 (1925).

8. Herzfeld, K., and Rice, F. O., Phys. Rev. 31, 691 (1928).

9. Freedman, E. H., Thesis (Cornell University, 1952).

10. Widom, B., Thesis (Cornell University, 1953).

11. Zener, C., Eleventh Report of Committee on Contact Catalysis, N.R.C. (1935) p. 103, and references quoted therein.

12. Zener, C., Phys. Rev. 38, 277 (1931).

13. Landau, L., and Teller, E., Physik. Z. Sowjetunion 10, 34 (1936).

14. Massey, H. S. W., Reports on Prog. in Phys. 12, 248 (1948-49).

15. Curtis, F. C., and Adler, F. T., J. Chem. Phys. 20, 249 (1952).

16. Herzfeld, K. F., J. Chem. Phys. 20, 388 (1952).

17. Schwartz, R. N., Slawsky, Z. I., and Herzfeld, K. F., J. Chem. Phys. 20, 1591 (1952); cf. Takayanagi, K., Progress of Theoretical Physics, Vol. 8, No. 1, July 1952.

18. Rosen, N., and Zener, C., Phys. Rev. 40, 502 (1932).

19. Eucken, A., and Becker, R., Z. physik. Chem., B, 27, 235 (1934).

20. (a) Laidler, K. J., "Chemical Kinetics" (McGraw-Hill, New York, 1950) Ch. 13.
(b) Glasstone, S., Laidler, K. J., and Eyring, H., "The Theory of Rate Processes" (McGraw-Hill, New York, 1941) pp. 289-295.

21. Franck, J., and Eucken, A., Z. physik. Chem., B, 20, 460 (1933).

22. Eyring, H., Gershinowitz, H., and Sun, C. E., J. Chem. Phys. 3, 786 (1935).

23. Castellan, G. W., and Hulburt, H. M., J. Chem. Phys. 18, 312 (1950).

24. For a study of this type using iodine vapor see: Roessler, F., Z. Physik 96, 251 (1935).

25. Rosen, N., J. Chem. Phys. 1, 319 (1933).

26. Rice, O. K., J. Chem. Phys. 1, 625 (1933).

27. Bauer, E.
(a) Phys. Rev. 84, 315 (1951).
(b) Phys. Rev. 85, 277 (1952).

28. Messiah, A. M. L., Phys. Rev. 84, 204 (1951).

29. Richards, W. T., Revs. Modern Phys. 11, 36 (1939).

30. Kittel, C., Reports on Progress in Physics 11, 205 (1946-47).

31. Markham, J. J., Beyer, R. T., and Lindsay, R. B., Revs. Modern Phys. 23, 353 (1951).

32. Lambert, J. D., and Rowlinson, J. S., Proc. Roy. Soc. 204A, 424 (1950).

33. Zartman, I. F., J. Acoust. Soc. Am. 21, 171 (1949).

34. In a few cases such as the excitation of oxygen by water vapor triple collisions appear to be a possibility.
(a) Kneser, H. O., J. Acoust. Soc. Am. 5, 122 (1933).
(b) Kneser, H. O., Physik. Zeits. 35, 983 (1934).
(c) Kneser, H. O., and Knudsen, V. O., Ann. d. Physik 21, 682 (1935).

35. Ref. 1(a) iii), p. 163.

36. (a) Ref. 29, p. 49.
(b) Ref. 30.

37. (a) Eucken, A., and Becker, R., Zeits. f. physik. Chemie 20B, 467 (1933); ibid., 27B, 219-62 (1934).
(b) Eucken, A., and Jaacks, H., ibid., 30B, 85-112 (1935).
(c) Eucken, A., and Numann, E., ibid., 36B, 163-183 (1937).

38. Ref. 37(c), p. 174, Tabelle 3.

39. Ref. 1(a) iii), p. 163 and graph on p. 162.

40. Smiley, E. F., Winkler, E. H., and Slawsky, Z. I., J. Chem. Phys. 20, 923 (1952).

41. Gorelik, G., Compt. rend. acad. sci. U.R.S.S. 54, 779-780 (1946).

42. Slobodskaya, P. V., Izvest. Akad. Nauk S.S.S.R., Ser. Fiz., 12, 656-61 (1948).

43. Cottrell, T. L., Trans. Faraday Soc. 46, 1025 (1950).

44. Griffith, W. C.
(a) Thesis (Harvard University, 1947).
(b) Jour. App. Phys. 21, 1319 (1950).

45. Keutel, F., "Ueber die specifische Wärme von Gasen", Inaugural-Dissertation, Frederich-Wilhelms-Universität zu Berlin (Berlin, 1910).

46. Einstein, A., Sitzber. preuss. Akad. Wiss. Physik.-math. Klasse 330 (1920).

47. Gibbs, J. W., Trans. Connecticut Acad. 3, 108, 343 (1875-6-7-8); Am. J. Sci., Ser. 3, 18 (1879).

48. Strother, C. O., and Richards, W. T., J. Chem. Phys. 4, 566 (1936).

49. Grüneisen, E., and Goens, E., Ann. d. Physik. 72, 193 (1923).
See table 7 of this work. This calculation was made in accordance with the theory of Einstein (ref. 46), correcting for an obvious slip as to sign in Einstein's work. Kistiakowsky and Richards (ref. 56), apparently not correcting for the wrong sign, give a larger theoretical lowering of about 5.1%.

50. Natanson, E. and L., Wied. Ann. 24, 454 (1885); Ibid., 27, 606 (1886).

51. Selle, H., Z. physik. Chem. 104, 1 (1923).

52. Argo, W. L., J. Phys. Chem. 18, 438 (1914).

53. Richards, W. T., and Reid, J. A.
(a) J. Chem. Phys. 1, 114 (1933).
(b) J. Am. Chem. Soc. 54, 3014 (1932).
(c) J. Chem. Phys. 2, 193, 206 (1934).

54. Olson, A. R., and Teeter, C. E. Jr., Nature 124, 444 (1929).

55. Teeter, C. E. Jr.
(a) J. Chem. Phys. 1, 251 (1933).
(b) J. Am. Chem. Soc. 54, 4111 (1932).

56. Kistiakowsky, G. B., and Richards, W. T., J. Am. Chem. Soc. 52, 4661 (1930).

57. Kneser, H. O., and Gauler, O., Physik. Z. 37, 677 (1936).

58. Luck, D. G. C., Phys. Rev. 40, 440 (1932).

59. Damköhler, G., Z. Elektrochem. 48, 62, 116 (1942).
cf., Bourgin, D. G., Phys. Rev. 50, 355 (1936) for kinetic theory transcript of these same notions.

60. Dirac, P. A. M., Proc. Cambridge Phil. Soc. 22, 132 (1924).

61. Brass, P. D., and Tolman, R. C., J. Am. Chem. Soc. 54, 1003 (1932).

62. Carrington, T., and Davidson, N.
(a) J. Chem. Phys. 19, 1313 (1951).
(b) Division of Phy. and Inorg. Chem., A.C.S., Abstracts of Papers Presented at Atlantic City, N.J., Sept. 14 to Sept. 19, 1952, 46P-107.
(c) Carrington, T., Thesis (University of California, 1951).

63. Bauer, S. H., "L. Farkas Memorial Volume" (Research Council of Israel, Special Publication No. 1, Jerusalem, 1952).

64. See ref. 1(b) for extension to rotational relaxation measurements.

65. (a) Manes, M., Hofer, L. J. E., and Weller, S., J. Chem. Phys. 18, 1355 (1950).
(b) Private communication to Prof. S. H. Bauer.

66. Landau, L., Physik. Zeits. Sowjetunion 1, 89 (1934).

67. Bethe, H. A., and Teller, E., Report X-117, Ball. Res. Lab., Aberdeen Proving Ground.

68. Southwell, R. V., "Relaxation Methods in Engineering Science" (Clarendon Press, Oxford, 1940).

69. Gilkerson, W. R., Jones, M. M., and Gallup, G. A., J. Chem. Phys. 20, 1182 (1952).

70. See p. 282 of reference 1(b) for complete details of method followed.

71. Carbon dioxide heat capacities taken from: "Selected Values of Properties of Hydrocarbons", Am. Pet Inst. Research Proj. 44, Table Oy.

72. (a) Bergmann, L., "Der Ultraschall" (S. Herzel, Zurich, 1949) p. 376.
(b) Walker, R. A., J. Chem. Phys. 19, 494 (1951).

73. Computed following method of E. H. Kennard, "Kinetic Theory of Gases" (McGraw-Hill Book Co., Inc., New York, 1938, Tables), pp. 26 and 149.

74. Herzberg, G., "Infrared and Raman Spectra of Polyatomic Molecules" (D. Van Nostrand Co., Inc., New York, 1945) p. 284.

75. (a) Giauque, W. F., and Kemp, J. D., J. Chem. Phys. 6, 40 (1938).
(b) Sutherland, G. B. B. M., Proc. Roy. Soc. London A141, 342 (1933).
(c) Ref. 74, p. 184.

76. Verhoek, F. H., and Daniels, F., J. Am. Chem. Soc. 53, 1186, 1250 (1931).

77. See for instance: Emrich, R. J., Mack, J. E., and Shunk, R. A., Abstracts of papers presented at meeting of American Physical Society, Cambridge, Mass., January 1953, U1.